

“Hypoxia-dependent mechanisms in the pulmonary circulation - Role of dimethylarginine dimethylaminohydrolase 1 (DDAH-1) in acute, sustained and chronic hypoxia”

Inaugural Dissertation
Submitted to the Faculty of Medicine
in partial fulfilment of the requirements
for the degree of Doctor in Human Biology (Dr. biol. hom.)
of the Faculty of Medicine
of the Justus Liebig University Giessen

by

Adel Gaber Mohammed Bakr

Al-Azhar University
Elminia (Egypt)

Giessen 2011

From the Department of Internal Medicine
Director: Prof. Dr. Werner Seeger
of the Faculty of Medicine of the Justus Liebig University Giessen

First Supervisor and Committee Member: Prof. Dr. Norbert Weissmann

Second Supervisor and Committee Member: Prof. Dr. Rainer Schulz

Date of Doctoral Defense: 14.06.2011

CONTENT

LIST OF ABBREVIATIONS..... IV

LIST OF TABLES..... VII

LIST OF FIGURES..... VIII

1. INTRODUCTION..... 1

 1.1 Pulmonary circulation..... 1

 1.1.1 The discovery of the pulmonary circulation..... 1

 1.1.2 Physiology of the pulmonary circulation..... 2

 1.1.3 Pulmonary circulation and hypoxia..... 2

 1.1.3.1 Hypoxic pulmonary vasoconstriction (HPV)..... 3

 1.1.3.1.1 Principle..... 3

 1.1.3.1.2 Anatomic site of HPV..... 3

 1.1.3.1.3 Mechanism(s) of HPV..... 3

 1.1.3.2 Effects of chronic hypoxia..... 5

 1.2 Pulmonary hypertension (PH)..... 7

 1.2.1 Definition..... 7

 1.2.2 Classification..... 7

 1.2.3 Epidemiology..... 9

 1.2.4 Clinical symptoms..... 9

 1.2.5 Physical signs..... 10

 1.2.6 Pathogenesis..... 10

 1.2.7 Disease management..... 11

 1.2.7.1 General recommendations..... 11

 1.2.7.2 Medical treatment..... 12

 1.2.7.2.1 Pulmonary vasodilator therapies..... 12

 1.2.7.2.2 Interventional and surgical therapies..... 13

 1.3 Endothelium..... 13

 1.3.1 Endothelium-derived factors and their role in HPV and PH..... 14

 1.3.1.1 Endothelin (ET)..... 14

 1.3.1.2 Prostacyclin..... 15

 1.3.1.3 Nitric oxide..... 15

 1.3.1.3.1 Nitric oxide synthases..... 16

 1.3.1.3.1.1 NOS inhibitors..... 16

 1.3.1.3.2 Dimethylarginine dimethylaminohydrolase (DDAH)..... 18

1.3.1.3.3 Guanylate cyclases.....	18
2. AIM OF THE STUDY.....	20
3. MATERIALS.....	21
3.1 Chemicals, solutions and drugs.....	21
3.2 Consumables.....	22
3.3 Set-up for animal experiments.....	23
3.4 Software.....	23
3.5 Materials for histology.....	23
3.6 Antibodies.....	25
3.7 System and software for morphometry.....	25
4. METHODS.....	26
4.1 Animals.....	26
4.2 Acute and sustained (3 h) hypoxic experiments.....	26
4.2.1 Isolated, ventilated and perfused mouse lungs.....	26
4.2.2 Isolation, perfusion and ventilation of mouse lungs.....	26
4.2.3 Colorimetric determination of cGMP by Cayman’s cGMP-Kit (ELISA).....	29
4.2.4 Colorimetric determination of ADMA by using ADMA-Kit (ELISA).....	32
4.2.5 Measurement of NO metabolites in perfusate.....	34
4.3 Chronic hypoxic experiments.....	35
4.3.1 In vivo hemodynamic measurements.....	35
4.3.2 Vascular morphometry.....	36
4.3.3 Heart ratio.....	39
4.4 Statistical analysis.....	39
5. RESULTS.....	40
5.1 Acute and sustained hypoxic experiments.....	40
5.1.1 PAP of isolated lungs of WT & DDAH1 ^{tg} mice during acute and sustained hypoxic ventilation.....	41
5.1.2 PAP of isolated lungs of WT & DDAH1 ^{tg} mice during normoxic ventilation.....	42
5.1.3.1 Effect of L-NNA on pulmonary vasoconstriction induced by acute & sustained HOX in WT and DDAH1 ^{tg} mice.....	43
5.1.3.2 Effect of L-NNA on PAP of isolated lungs of WT & DDAH1 ^{tg} mice during normoxic ventilation.....	46
5.1.4.1 Effect of ODQ on pulmonary vasoconstriction induced by acute & sustained HOX in WT and DDAH1 ^{tg} mice.....	48

5.1.4.2 Effect of ODQ on PAP of isolated lungs of WT & DDAH1 ^{tg} mice during normoxic ventilation.....	51
5.1.5 Weight of mice used in acute and sustained hypoxic & normoxic experiments...	53
5.1.6 Weight changes of isolated mouse lungs.....	54
5.1.7 NO release into the perfusate of isolated lungs of WT and DDAH1 ^{tg} mice.....	57
5.1.8 cGMP concentrations in the perfusate of isolated lungs of WT and DDAH1 ^{tg} mice.....	58
5.1.9 ADMA concentrations in the perfusate of isolated lungs of WT and DDAH1 ^{tg} mice.....	59
5.2 Chronic hypoxic experiments.....	60
5.2.1 RVSP in WT and DDAH1 ^{tg} mice.....	60
5.2.2 Hematocrit values (%) in WT and DDAH1 ^{tg} mice.....	61
5.2.3 Right heart hypertrophy.....	62
5.2.4 Weight of mice used in chronic hypoxic experiments.....	63
5.2.5 Degree of muscularization.....	64
6. DISCUSSION.....	68
6.1 Effects of DDAH1 on acute hypoxic response.....	68
6.2 Effects of DDAH1 on sustained phase of HPV.....	69
6.3 Chronic hypoxic exposure.....	73
7. SUMMARY.....	76
8. ZUSAMMENFASSUNG.....	77
9. REFERENCES.....	79
10. APPENDIX.....	92
10.1 Statement/Erklärung an Eides Statt.....	92
10.2 Acknowledgments	93
10.3 Curriculum vitae.....	94

LIST OF ABBREVIATIONS

ADMA	Asymmetric ω - N ^G , N ^G -dimethylarginine
ATP	Adenosine triphosphate
BALF	Broncho-alveolar lavage fluid
BID	Two times a day
BMPR2	Bone morphogenetic protein receptor type 2
BSA	Bovine serum albumin
[Ca ²⁺] _i	Intracellular calcium concentration
cAMP	Cyclic 3', 5'-adenosine monophosphate
cGMP	Cyclic 3', 5'-guanosine monophosphate
CTEPH	Chronic thromboembolic pulmonary hypertension
DAB	3, 3'- Diaminobenzidine
DDAH	Dimethylarginine dimethylaminohydrolase
DMA	Dimethylamine
DMSO	Dimethyl sulfoxide
DNA	Deoxyribonucleic acid
dtn	Determinant
EDRF	Endothelium derived relaxing factor
ELISA	Enzyme linked immunosorbent assay
eNOS	Endothelial nitric oxide synthase
ET	Endothelin
ET _A	Endothelin A receptor
ET _B	Endothelin B receptor
FDA	Food and Drug Administration
Fig.	Figure
FMN	Flavin mononucleotide
FPAH	Familial pulmonary arterial hypertension
G	Gauge
g	Gram
h	Hour
H ₂ O ₂	Hydrogen peroxide
HE	Hematoxylin and eosin
HIV	Human immunodeficiency virus
HOX	Hypoxia
HPV	Hypoxic pulmonary vasoconstriction
Ig	Immunoglobulin
IPAH	Idiopathic pulmonary arterial hypertension
IV	Intravenous
kg	Kilogram
l	Liter
L-Arg	L-arginine
L-NMMA	N ^G -monomethylarginine
L-NNA	N _ω -Nitro-L-arginine
LV	Left ventricle
M	Molar (mol/l)
mg	Milligram
min	Minute
ml	Milliliter
mM	Millimolar
M.O.M.	Mouse on mouse
μg	Microgram

μ l	Microliter
μ m	Micrometer
μ M	Micromolar
n	Number of experiments
NADPH	Nicotinamide adenine di-nucleotide phosphate (reduced)
ng	Nanogram
nM	Nanomolar
nm	Nanometer
nNOS	Neural nitric oxide synthase
NO	Nitric oxide
NOA	Nitric oxide analyzer
NOS	Nitric oxide synthase
NYHA	New York Heart Association
OD	Optical density
ODQ	1H-[1, 2, 4]oxadiazolo[4, 3-a]quinoxalin-1-one
PAH	Pulmonary arterial hypertension
PAP	Pulmonary arterial pressure
PASMCs	Pulmonary arterial smooth muscle cells
PBS	Phosphate-buffered saline
PCH	Pulmonary capillary hemangiomatosis
PDE5	Phosphodiesterase type 5
PEEP	Positive end-expiratory pressure
PH	Pulmonary hypertension
pH	Negative log of hydrogen ion concentration
PKC	Proteinkinase C
PKG	Proteinkinase G
PO_2	Partial pressure of oxygen
PRMT	Protein arginine methyltransferase
PVOD	Pulmonary veno-occlusive disease
QID	Four times a day
ROK	RhoA/Rho kinase
ROS	Reactive oxygen species
R. T. U.	ready to use
RV	Right ventricle
RVSP	Right ventricular systolic pressure
S	Septum
SAH	S-adenosyl homocysteine
SAM	S-adenosyl methionine
SD	Standard deviation
SDMA	Symmetric ω - N^G , N^G -dimethylarginine
SEM	Standard error of the mean
sGC	Soluble guanylyl cyclase
SMA	Smooth muscle actin
SPH	Secondary pulmonary hypertension
SQ	Subcutaneous
tg	Overexpression
TID	Three times a day
TMB	Tetramethylbenzidine
TRP	Transient receptor potential
UK	United Kingdom
VIP	Very intense purple

vWF	vonWillebrand factor
v.s.	Versus
WHO	World Health Organization
WT	Wild-type
y+	Cationic amino acid

LIST OF TABLES

Table 1: Updated Clinical Classification of Pulmonary Hypertension (Dana Point, 2008).... 8

Table 2: Functional Assessment of Patients with Pulmonary Hypertension..... 9

Table 3: FDA-approved medications for PAH..... 12

Table 4: Materials supplied from Cayman Chemical Company for cGMP measurement..... 29

Table 5: Sample plate format for cGMP measurement..... 31

Table 6: Contents of the kit used in ADMA measurement..... 32

Table 7: Sample plate format for ADMA measurement..... 34

Table 8: Protocol for double antibody immunostaining against α -actin and vWF factor..... 36

LIST OF FIGURES

Figure 1: Consequences of pulmonary artery endothelial cell dysfunction on pulmonary artery smooth muscle cell tone and proliferation.....	11
Figure 2: Synthesis of methylarginine compounds.....	17
Figure 3: Isolated, perfused and ventilated mouse lung.....	27
Figure 4: Schematic representation of the experimental set-up of the isolated, perfused and ventilated mouse lung.....	28
Figure 5: Representative recording of PAP, weight changes (referred to the start of the experiment after the steady state period) and LVP during acute and sustained hypoxia of isolated lungs of WT mice.....	40
Figure 6: PAP of isolated lungs of WT and DDAH1 ^{tg} mice during acute and sustained hypoxic ventilation.....	41
Figure 7: PAP of isolated lungs of WT and DDAH1 ^{tg} mice during normoxic ventilation.....	42
Figure 8: Effect of L-NNA on PAP of isolated lungs of WT mice.....	43
Figure 9: Effect of L-NNA on PAP of isolated lungs of DDAH1 ^{tg} mice.....	44
Figure 10: Effect of L-NNA on PAP of isolated lungs of DDAH1 ^{tg} mice compared to WT mice.....	45
Figure 11 A, B, C: Effect of L-NNA on PAP of isolated lungs of WT & DDAH1 ^{tg} mice during normoxic ventilation.....	46
Figure 12: Effect of ODQ on PAP of isolated lungs of WT mice.....	48
Figure 13: Effect of ODQ on PAP of isolated lungs of DDAH1 ^{tg} mice.....	49
Figure 14: Effect of ODQ on PAP of isolated lungs of DDAH1 ^{tg} mice compared to WT mice.....	50
Figure 15 A, B, C: Effect of ODQ on PAP of isolated lungs of WT & DDAH1 ^{tg} mice during normoxic ventilation.....	51
Figure 16: Weight of mice used in acute and sustained hypoxic experiments, as well as normoxic experiments.....	53
Figure 17 A, B, C, D, E, F: Weight changes of isolated mouse lungs.....	54
Figure 18: NO concentrations in the perfusate of isolated lung experiments of WT and DDAH1 ^{tg} mice.....	57
Figure 19: cGMP concentrations in the perfusate of isolated lung experiments of WT and DDAH1 ^{tg} mice.....	58
Figure 20: ADMA concentrations in the perfusate of isolated lung experiments of WT and DDAH1 ^{tg} mice.....	59

Figure 21: RVSP in WT and DDAH1 ^{tg} mice.....	60
Figure 22: Hematocrit values in WT and DDAH1 ^{tg} mice.....	61
Figure 23: Values of RV/(LV+S) ratio in WT and DDAH1 ^{tg} mice.....	62
Figure 24: Weight of mice used in chronic hypoxic experiments.....	63
Figure 25: Degree of muscularization of pulmonary arterial vessels (diameter 20-70 μm)....	65
Figure 26: Degree of muscularization of pulmonary arterial vessels (diameter 70-150 μm)...	65
Figure 27: Degree of muscularization of pulmonary arterial vessels (diameter >150 μm)....	66
Figure 28: Degree of muscularization of total pulmonary arterial vessels.....	66
Figure 29: Morphometrical analysis in WT and DDAH1 ^{tg} mice.....	67
Figure 30: Effects of DDAH1 overexpression on alterations of the pulmonary vasculature induced by acute, sustained and chronic hypoxia.....	75

1. INTRODUCTION

1.1 Pulmonary circulation

1.1.1 The discovery of the pulmonary circulation

The first description of the pulmonary circulation was provided by Galen in the 2nd century, who said that the blood reaching the right side of the heart went through invisible pores in the septum to the left side of the heart where it mixed with air to create spirit and then was distributed to the body. According to Galen's views, the venous system was completely separate from the arterial system, except when they came in contact by the invisible pores ¹. However, Ibn Al-Nafis in the 13th century stated that the blood had to arrive from the right side of the heart at the left side without any direct pathway between them. He thought that the thick septum of the heart was not perforated and did not have invisible pores as Galen said. He further hypothesized that the blood from the right side of the heart had to flow through the pulmonary artery to the lungs, spread through its substances, mix with air, and pass through the pulmonary vein to reach the left side of the heart. In the description of the anatomy of the lungs, Ibn Al-Nafis said the lungs were composed of three parts, the bronchi, the branches of the pulmonary vein, and the branches of the pulmonary artery, all of them connected by loose porous flesh. Then he added, the function of the pulmonary artery was to transport the blood to the lung. Therefore what leaked through the pores of the branches of this vessel into the alveoli of the lungs could mix with air. The mixing process occurred in the left cavity of the heart ². Later, in 1553, Michael Servetus wrote in his book "Christianismi Restitutio" that air mixed with blood was sent from the lung to the heart through the arterial vein and therefore, the mixture was made in the lungs. In 1543, Andreas Vesalius explained in his book "De Fabrica", the pulmonary circulation in a manner similar to previous Ibn Al-Nafis' description. An interesting observation is that in the first edition of the book, Vesalius agreed with Galen that the blood soaked through the septum from the right into the left ventricle. Then in the second edition (1555), he deleted the above statement and wrote instead: "I do not know how the blood pass through the septum from the right to the left ventricle" ³. Then William Harvey, in 1628, demonstrated in animal experiments the movement of blood from the right ventricle to the lung and he observed the blood returning to the left side of the heart via the pulmonary vein and therefore he concluded that there were no pores in the interventricular septum.

1.1.2 Physiology of the pulmonary circulation

The main function of the pulmonary circulation is to deliver oxygen to the blood and free it of carbon dioxide. This aim is achieved when the blood flows through the lungs. The walls of pulmonary arteries and veins are significantly thinner than the walls of corresponding vessels in the rest of the body. Therefore, the pressure in this part of the system is only about one-sixth as that in the systemic circulation. In the pulmonary circulation, the roles of arteries and veins are the opposite of what they are in the systemic circulation: Blood in the arteries has less oxygen, while blood in the veins is oxygen-rich. The circuit starts with the pulmonary artery, which extends from the right ventricle and carries blood with low oxygen content to the lungs. In the lungs, it branches into two arteries, one for each lung, and then into arterioles and capillaries. The gas exchange between the inhaled air and the blood takes place in the pulmonary capillaries. Their walls act as filters by allowing molecules of gas but not molecules of fluid to pass through. The total surface area of the capillaries in the lungs ranges from 500 to 1.000 square feet. The carbon dioxide is removed from the blood in the pulmonary arteries across capillary walls and leaves the body through the mouth and nose. The blood that has picked up oxygen returns to the heart through four pulmonary veins into the left atrium.

1.1.3 Pulmonary circulation and hypoxia

More than 100 years ago, Bradford and Dean in the UK had described the effects of hypoxia on the pulmonary circulation⁴. However, scientific interest in this field only started with the discovery of hypoxic pulmonary vasoconstriction (HPV) in the cat by von Euler and Liljestrand in 1946, and in man a year later in Andre Coumand's laboratory⁵. Despite the extensive research in this field for more than 50 years, we still do not completely understand the mechanism of HPV or why the response of the pulmonary vasculature to hypoxia is diametrically opposite to that of the systemic circulation. As lung and systemic vessels have different functions, lung vessels collecting oxygen while systemic vessels distributing it, most systemic vessels of adult organisms dilate during hypoxia, pulmonary vessels, however, constrict. In the isolated, buffer-perfused lung, HPV is activated when partial pressure of oxygen (PO_2) becomes <100 mmHg⁶.

1.1.3.1 Hypoxic pulmonary vasoconstriction (HPV)

1.1.3.1.1 Principle

HPV is a physiological self-regulatory response to alveolar hypoxia that distributes pulmonary capillary blood flow to areas of high oxygen availability. This principle, also known as the von Euler-Liljestrand mechanism, thereby optimises gas exchange at the blood-air interface ⁷.

1.1.3.1.2 Anatomic site of HPV

It was initially proposed, that the main site of vasoconstriction is located at the primary site of gas exchange, the alveoli. Angiographic visualization of the pulmonary vasculature during acute hypoxia demonstrated a decrease in diameter of small pulmonary arteries, but an increase in caliber of the larger proximal vessels, suggesting that the small arteries or precapillary pulmonary arteries are the major site for acute hypoxic pulmonary response and that the site of oxygen sensing is not exclusively located in the alveolar capillaries ⁸. In 1966, Kato and Staub provided a histologic confirmation that the major site of hypoxic vasoconstriction is the small muscular pulmonary arteries at the level of the terminal respiratory bronchioles using the rapid freezing technique of hypoxic lung segments ⁹. Nagasaka et al. (1984) determined the microvascular profile in the feline lung during normoxia and hypoxia in a variety of experiments using the technique of micropuncture of subpleural vessels and they discovered that the predominant site of hypoxic vasoconstriction is within the arterial segment (30-50 μm) ¹⁰. From all these experiments, it was concluded that the major site of hypoxic vasoconstriction locates in the small pulmonary arteries (30-50 μm), with only minor increase in vascular resistance arising from the capillary bed and the venous system. Several studies, including micropuncture experiments ¹⁰, and isolated perfused lung experiments ¹¹, demonstrated small changes in venous pressure during hypoxia compared to the arterial segment. Therefore, the pulmonary veins probably make a small contribution to the increase in vascular resistance during hypoxic vasoconstriction. Even if they constrict (which is possible) they do not necessarily contribute to peripheral vascular resistance.

1.1.3.1.3 Mechanism(s) of HPV

The exact mechanism(s) by which a decrease in oxygen pressure is sensed and translated into vasoconstriction in the pulmonary circulation is still not completely elucidated.

Vasoconstriction is achieved by myosin light chain phosphorylation. When intracellular calcium concentration ($[Ca^{2+}]_i$) increases, it binds to calmodulin and this complex activates myosin light chain kinase causing phosphorylation of the light chain of myosin. Then myosin binds to actin filaments causing contraction. This reaction is adenosine triphosphate dependent. The duration of contraction is modulated by the activity of myosin light chain phosphatase (MLCP) which dephosphorylates the light chain of myosin leading to relaxation. Inhibition of the activity of MLCP prevents the dephosphorylation of myosin light chain and allows for sustained calcium-independent contraction. MLCP activity is regulated partially by RhoA/Rho kinase pathway. Activation of RhoA/Rho kinase leads to inactivation of MLCP even when $[Ca^{2+}]_i$ decreases. Sustained activation of RhoA/Rho kinase pathway is central to the calcium sensitization that maintains vascular tone¹². Both, MLCP by an intracellular calcium increase, as well as calcium sensitization, have been made responsible for HPV¹³. The intracellular calcium increase might be achieved by release of calcium from intracellular stores and by influx of extracellular calcium through L-type calcium channels and non-specific cation channels¹⁴. Hypoxia does not cause vasoconstriction in absence of extracellular calcium, demonstrating that influx of calcium is critical¹⁵. However, L-type channel blockers do not completely inhibit hypoxia induced vasoconstriction suggesting that calcium enters through other pathways¹⁶.

Recently, a subtype of the transient receptor potential (TRP) channels has been shown to be essential for acute HPV. Acute hypoxia induces PSMCs depolarization by inactivation of voltage-gated potassium channels on the cell membrane, that might lead to the influx of extracellular Ca^{2+} through the voltage-dependent Ca^{2+} channels¹⁵. The mechanism by which the TRP channels are activated remains to be elucidated. Concerning the initial signal for activation of calcium and potassium channels there are currently several hypotheses, including an increase or decrease of reactive oxygen species originating from mitochondria or NADPH oxidases, changes in redox state due to decreased oxygen levels or an AMP-kinase dependent mechanism. During sustained HPV Rho-kinase might be activated by ROS¹⁷ or vasoconstrictor signals, including those mediated by G protein-coupled receptors and receptor tyrosine kinases¹⁸.

Several reports have shown that hypoxia can cause contraction of isolated PSMCs¹⁹ and this would appear to suggest that HPV is a function of the smooth muscle and does not involve the endothelium. However, whereas some reports have described HPV in isolated pulmonary arteries following disruption of the endothelium²⁰, other studies have shown that the endothelium is definitely required, certainly for sustained vasoconstriction²¹⁻²³. Most

reports, especially those on isolated cells, tend to describe processes that occur during the first 10-15 min. However, isolated pulmonary arteries show a biphasic response to hypoxia when observed over longer periods^{24, 25}. Also, the biphasic response to sustained hypoxia has been described in isolated lungs²⁶. This biphasic response consists of a rapid, transient increase in vascular tone over about 5-10 min (phase 1), which then eventually falls, but does not reach the baseline. This is followed by a more slowly developing sustained increase in tone (phase 2), which reaches a plateau after about 40 min. Whereas the phase 1 constriction is relatively unaffected by removal of the endothelium, phase 2 is abolished, the endothelium does not affect $[Ca^{2+}]_i$ during the sustained phase, but releases factor(s) that sensitize the contractile apparatus of the SMCs to calcium^{23, 27}. Acute HPV is mediated by increase of calcium ion concentration in PASMC, while sustained HPV was shown to rely on a calcium sensitization of the myofilaments, possibly via phosphorylation by Rho-kinase^{25, 28, 29}. It would seem that the second sustained phase of constriction in isolated arteries is more relevant to physiological HPV than the transient first phase.

1.1.3.2 Effects of chronic hypoxia

The effects of chronic hypoxia occur when the alveolar oxygen tension remains below the threshold for pulmonary vasoconstriction of approximately 75 mmHg. This degree of chronic hypoxia is obviously seen at high altitude and also can occur in other conditions like chronic bronchitis, emphysema and hypoventilatory states. It was found, that the most prominent effects of chronic hypoxia besides vasoconstriction are structural changes in the terminal portions of the pulmonary arterial tree³⁰ and polycythaemia³¹ which contribute to the maintenance of chronic hypoxic pulmonary hypertension. The most striking effect of alveolar hypoxia is muscularization of pulmonary arterioles < 70 μ m. Most pulmonary arterial vessels of this diameter normally contain only a single elastic lamina without any smooth muscle. The smooth muscles of these arterioles are distally extended causing the small pulmonary arterioles to develop a distinct media with smooth muscle sandwiched between an inner and an outer elastic lamina. It still remains unclear how these pulmonary arterioles come to be muscularized. It is unlikely to be the result of work hypertrophy because these vessels have no muscle in normal subjects and hypoxic vasoconstriction occurs in vessels proximal to these arterioles. Once pulmonary arterioles become muscularized they can constrict in response to hypoxia and vasoconstriction moves to a more peripheral site in the pulmonary vascular tree³².

Additionally, chronic hypoxic exposure increases intimal thickness by causing hypertrophy and hyperplasia in both endothelial and subendothelial layers. Endothelial cell hypertrophy is associated with an increased number and size of cell organelles, including ribosomes, rough endoplasmic reticulum, and golgi apparatus.

The vascular alterations resulting in hypoxia-induced PH are caused by several mechanisms. Chronic hypoxia increases the sensitivity of the contractile apparatus to Ca^{2+} to mediate vasoconstriction. Myofilament Ca^{2+} sensitization through the activation of RhoA/Rho kinase (ROK) and consequent inhibition of MLCP is considered the main pathway in the vascular smooth muscle contraction during sustained HPV, as described above, but also during chronic hypoxia³³. The effect of chronic hypoxia via ROK was confirmed by using Y-27632, a ROK inhibitor, where the mean PAP and total pulmonary resistance in chronic hypoxia-induced PH were drastically reduced³⁴.

Hypoxia has been shown to increase the production of reactive oxygen species (ROS) such as superoxide anion and hydrogen peroxide in rat PASMCs^{35, 36} and endothelial cells³⁷. ROS are important modulators of vascular tone and act as second messengers to activate a variety of intracellular signalling cascades including RhoA/ROK³⁸. A detailed description of endothelial pathways regulating hypoxia-induced PH is given in the chapter 1.3.1.

Another effect of chronic hypoxia, subsequently to muscularization of pulmonary arterioles and pulmonary hypertension, is cardiac hypertrophy and failure of the right heart. Cardiac hypertrophy is an increase in the mass of the contractile and ancillary proteins of the heart above normal. The heart responds to pressure overload by hypertrophy in the form of wall thickening and a reduced cavity size. In its initial stages, the hypertrophied ventricle is able to compensate in the face of increased workload, however in the later stages, the systolic and diastolic properties become impaired and consequently fail to compensate leading to heart failure. In the hypertrophied heart, the heart cells start to die and this myocyte necrosis is associated with fibroblast proliferation and expansion of the extracellular matrix. Heart failure can be defined as the inability of the heart to provide the metabolising tissues with enough nutrients³⁹.

1.2 Pulmonary hypertension (PH)

1.2.1 Definition

PH is defined as a group of diseases summarized in Table 1 according to the most recent PH World Symposium at Dana Point and is characterized by a progressive increase of pulmonary vascular resistance leading to right ventricular failure and premature death.

1.2.2 Classification

Classification of PH is necessary to facilitate the diagnosis and for determination of the lines of treatment. The first classification was proposed in 1973 at an international conference on primary PH endorsed by the World Health Organization (WHO) Symposium which classified PH into two categories depending on the known causes. Primary Pulmonary Hypertension (PPH) was classified as a separate entity of unknown cause and Secondary Pulmonary Hypertension (SPH) with identifiable causes⁴⁰. The updated classification from the second World Symposium on Pulmonary Arterial Hypertension (PAH) in Evian, France, 1998, focused on the clinical presentation, pathophysiological mechanisms, and therapeutic options⁴¹. This was a simple classification aimed to provide a useful guide for the clinician in evaluating PH patients and developing treatment plans. In 2003, the third World Symposium on PAH held in Venice, Italy, proposed some modifications to the Evian classification⁴². In this modification, the term “primary pulmonary hypertension” was replaced with “idiopathic pulmonary arterial hypertension (IPAH)”. In addition, the pulmonary capillary hemangiomatosis and pulmonary veno-occlusive disease were reclassified and risk factors were updated. Moreover, the guidelines for the classification of congenital systemic-to-pulmonary shunts were also included. The most recent classification was proposed during the fourth World Symposium on PH held in 2008 in Dana Point, California, which is listed in Table 1⁴³.

According to this classification, PH can be associated with lung disease and/or hypoxia (group 3), which shows validity of the experimental model of hypoxia-induced PH for occurrence of disease in human. However, as current guidelines for diagnosis and treatment are only applicable for PAH (group 1), it is referred to in the following chapters as this subgroup of PH. Furthermore, the New York Heart Association (NYHA) functional classification for heart diseases established a new functional classification (Table 2)⁴⁴. The NYHA classification was successful for comparison of the patients regarding the clinical severity of the disease state.

1. Pulmonary arterial hypertension (PAH)

1.1 Idiopathic PAH

1.2 Heritable

1.2.1 Bone morphogenetic protein receptor type 2 (BMP2)

1.2.2 Activin receptor-like kinase type 1 (ALK1), endoglin (with or without hereditary hemorrhagic telangiectasia)

1.2.3 Unknown

1.3 Drug- and toxin-induced

1.4 Associated with

1.4.1 Connective tissue diseases 1.4.2 Human immunodeficiency virus (HIV) infection

1.4.3 Portal hypertension 1.4.4 Congenital heart diseases

1.4.5 Schistosomiasis 1.4.6 Chronic hemolytic anemia

1.5 Persistent pulmonary hypertension of the newborn

Pulmonary veno-occlusive disease (PVOD) and/or pulmonary capillary hemangiomatosis (PCH)

2. Pulmonary hypertension owing to left heart disease

2.1 Systolic dysfunction 2.2 Diastolic dysfunction 2.3 Valvular disease

3. Pulmonary hypertension owing to lung diseases and/or hypoxia

3.1 Chronic obstructive pulmonary disease 3.2 Interstitial lung disease

3.3 Other pulmonary diseases with mixed restrictive and obstructive pattern

3.4 Sleep-disordered breathing 3.5 Alveolar hypoventilation disorders

3.6 Chronic exposure to high altitude 3.7 Developmental abnormalities

4. Chronic thromboembolic pulmonary hypertension (CTEPH)**5. Pulmonary hypertension with unclear multifactorial mechanisms**

5.1 Hematologic disorders: myeloproliferative disorders, splenectomy

5.2 Systemic disorders: sarcoidosis, pulmonary Langerhans cell histiocytosis: lymphangioliomyomatosis, neurofibromatosis, vasculitis

5.3 Metabolic disorders: glycogen storage disease, Gaucher disease, thyroid disorders

5.4 Others: tumoral obstruction, fibrosing mediastinitis, chronic renal failure on dialysis

Table 1: Updated Clinical Classification of Pulmonary Hypertension (Dana Point, 2008).

PAH: pulmonary arterial hypertension; BMP2: bone morphogenetic protein receptor type 2;

ALK1: activin receptor-like kinase type 1; HIV: human immunodeficiency virus; PVOD:

pulmonary veno-occlusive disease; PCH: pulmonary capillary hemangiomatosis; CTEPH:

chronic thromboembolic pulmonary hypertension. From Simonneau et al. *J. Am. Coll. Cardiol.* 2009; 54:S43-S54.

Class I Patients with pulmonary hypertension but without resulting limitation of physical activity. Ordinary physical activity does not cause dyspnea or fatigue, chest pain or near syncope.

Class II Patients with pulmonary hypertension resulting in a marked limitation of physical activity. They are comfortable at rest. Ordinary physical activity causes dyspnea or fatigue, chest pain or near syncope.

Class III Patients with pulmonary hypertension resulting in marked limitation of physical activity. They are comfortable at rest. Less than ordinary activity causes dyspnea or fatigue, chest pain or near syncope.

Class IV Patients with pulmonary hypertension. They are unable to carry out any physical activity without symptoms. These patients manifest signs of right heart failure. Dyspnea and/or fatigue may even be present at rest. Discomfort is increased by any physical activity.

Table 2: Functional Assessment of Patients with Pulmonary Hypertension. From Rich et al. Executive summary from the second World Symposium on Primary Pulmonary Hypertension, Evian, France, September 6–10, 1998: World Health Organization.

1.2.3 Epidemiology

IPAH has an estimated incidence of 1 to 2 cases per 1 million population⁴⁴. It is 2 to 3 times more frequent in women than in men^{45, 46} presenting most commonly in the third decade of life in women and in the fourth decade in men. Most cases of IPAH are sporadic; however, heritable PAH occurs in about 6% to 12% of patients with IPAH^{47, 48}. Heritable PAH is inherited in an autosomal dominant fashion, with incomplete penetrance (as low as 10% to 20%)⁴⁵. Thus, most individuals who inherit the mutation have an estimated risk of approximately 10% of developing the disease⁴⁹.

1.2.4 Clinical symptoms

PAH may be asymptomatic in its early stages. The most common symptoms are exertional dyspnea, fatigue, and syncope and reflect an inability to increase cardiac output during activity. A small percentage of patients may report typical angina pectoris. The symptoms of

PAH can also include weakness and abdominal distension⁴⁴. Hemoptysis resulting from the rupture of distended pulmonary vessels is a rare but potentially devastating event. Raynaud's phenomenon occurs in approximately 2% of patients with PAH.

1.2.5 Physical signs

Physical signs of PAH become more apparent with the progression of right ventricular dysfunction. The presence of an accentuated pulmonary component of the second heart sound is very common, occurring in 90% of patients with IPAH. Other signs include (1) a right-sided gallop, (2) a palpable right ventricular lift, (3) a mid-systolic ejection murmur across the pulmonary valve, (4) increased jugular venous pressure, (5) tricuspid regurgitation, (6) hepatomegaly and ascites, and (7) peripheral edema. Cyanosis may also indicate the presence of right-to-left shunting, severely decreased cardiac output or impairment in intrapulmonary gas transfer.

1.2.6 Pathogenesis

The pathogenesis of PAH is a complex process. PAH was long held to be a sign of pulmonary vasoconstriction and proliferation of vascular smooth muscle cells; however, mounting evidence implicates dysfunction of the pulmonary vascular endothelium in the pathogenesis of this disease. Changes in the production of a variety of endothelial-derived vasoactive mediators appear to be very critical in the development of PAH. Among these are prostacyclin, endothelin-1, and nitric oxide (Fig. 1). The imbalance of these mediators and their role in HPV and PH will be described later in chapter 1.3 about the endothelium.

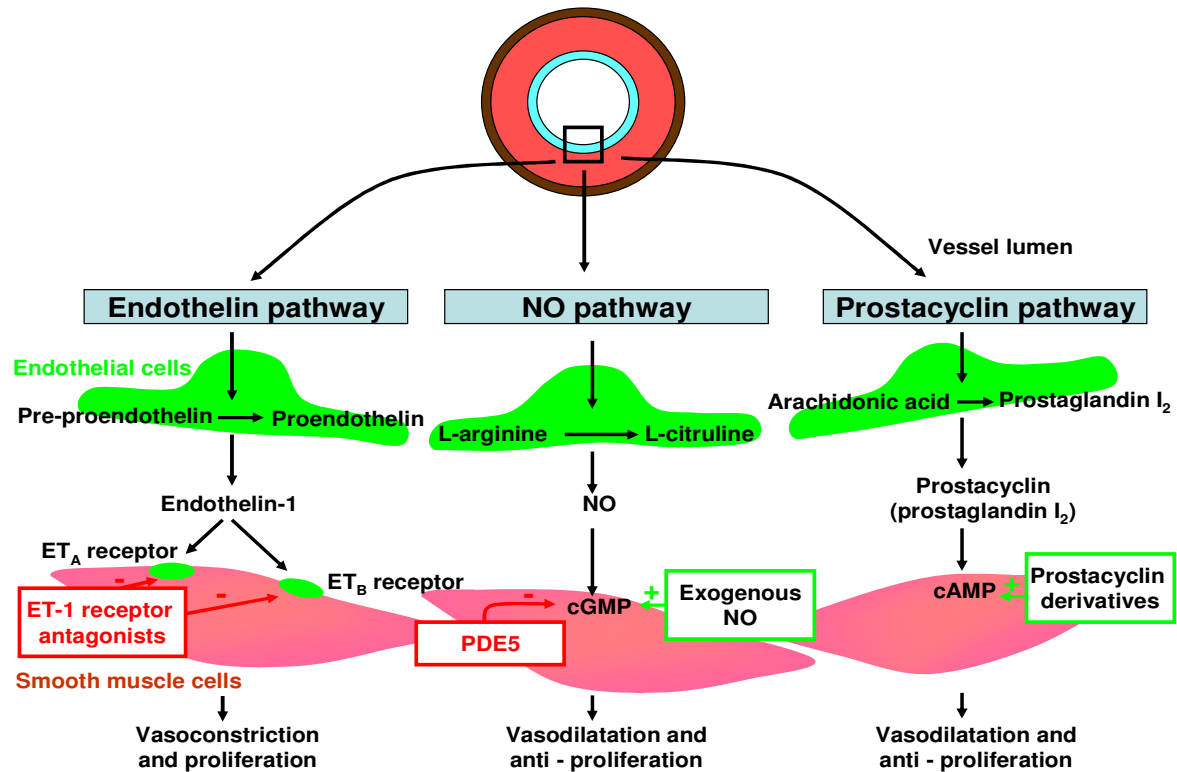


Figure 1: Consequences of pulmonary artery endothelial cell dysfunction on pulmonary artery smooth muscle cell tone and proliferation. NO: nitric oxide; cAMP: cyclic 3', 5'-adenosine monophosphate; cGMP: cyclic 3', 5'-guanosine monophosphate; PDE5: phosphodiesterase type 5; ET: endothelin; ET_A: endothelin A receptor; ET_B: endothelin B receptor. From Humbert et al. J. Am. Coll. Cardiol. 2004; 43: 13S-24S with modifications.

1.2.7 Disease management

1.2.7.1 General recommendations:

- High altitude exposure should be avoided to prevent hypoxemia.
- No smoking (nicotine is a vasoconstrictor).
- Excessive sodium intake should be avoided to prevent salt retention.
- Avoid hard physical activity.
- Avoid hot baths or showers to prevent peripheral vasodilatation.
- Need for supplemental oxygen during air travel.
- All vasoconstrictor medications, appetite and diet pills should be avoided.

1.2.7.2 Medical treatment

1.2.7.2.1 Pulmonary vasodilator therapies

Food and Drug Administration (FDA) approved agents for the treatment of PAH only (group 1, Table 1). Recent pharmacologic treatment for PAH include prostanoids, endothelin receptor antagonists, and phosphodiesterase (PDE) 5 inhibitors (Table 3)⁵⁰.

Drug class	Drug	Dose, Route
Prostanoids	Epoprostenol	Start 2 ng/kg/min, IV and titrate to clinical effect
	Treprostinil	0.625 - 40 ng/kg/min, IV/SQ 18 - 54 µg inhalations, QID
	Iloprost	2.5 - 5 µg nebulized inhaled solution to maximum of nine doses daily
Endothelin-1 receptor antagonists	Bosentan	62.5 - 125 mg BID, oral
	Ambrisentan	5 - 10 mg/day, oral
Phosphodiesterase Inhibitors	Sildenafil	20 mg TID, oral
	Tadalafil	40 mg/day, oral

Table 3: FDA-approved medications for PAH. IV: intravenous; SQ: subcutaneous; QID: four times a day; BID: two times a day; TID: three times a day; ng: nanogram; µg: microgram; mg: milligram; min: minute; kg: kilogram. From Falk et al. Vasc. Health Risk Manag. 2010; 6: 273-280 with modifications.

- **Prostanoids:** Epoprostenol is the most important drug in the treatment of PAH. It remains the treatment of choice for advanced disease. This potent, short-acting vasodilator and inhibitor of platelet aggregation is produced by vascular endothelium. A continuous intravenous infusion of epoprostenol improved exercise capacity, quality of life, hemodynamics and long-term survival in patients with functional class III or IV (Table 2)⁵¹.

Treprostinil is a prostacyclin analogue with a half life of 3 hours (h), which is a major advantage over epoprostenol. It can be given subcutaneously or intravenously. Iloprost is another prostacyclin analogue with a half life of 20-25 min. It can be administered by inhalation.

- **Endothelin-1 receptor antagonists:** Bosentan is a non-selective endothelin receptor antagonist. Its use in patients with PAH has been associated with an improvement in

hemodynamic parameters and a decreased risk of clinical worsening^{52, 53}. Sitaxsentan and Ambrisentan are new selective ET_A receptor antagonists, but they cause hepatotoxicity (as Bosentan) as a main side effect.

- Phosphodiesterase 5 inhibitors: Cyclic guanosine monophosphate (cGMP) augmentation by nitric oxide leads to pulmonary vasodilatation (see 1.3.1.3). cGMP is rapidly degraded by PDEs. Sildenafil is a potent inhibitor of PDE5, it augments the pulmonary vascular response to endogenous NO. Its clinical use in patients with PAH has been associated with improvements in function and hemodynamics⁵⁴⁻⁵⁷. Therefore, sildenafil may be efficacious in the treatment of PAH with acceptable side effects which include headache, nasal congestion, and visual disturbance. Tadalafil is another PDE5 inhibitor used in treatment of PAH. It has a longer half life (17.5 h) when compared to sildenafil (4 h), thus allowing once-daily dosing. PDE5 inhibitors have recently become attractive as the first line of choice in the treatment of milder forms of PAH.

1.2.7.2.2 Interventional and surgical therapies: Despite advancement in the medical treatment of PAH, prognosis is still poor and patients may stabilize only for few years followed by deterioration again. Therefore further therapy may be necessary.

- Atrial septostomy/stenting or septectomy

This involves the creation of right to left interatrial shunt in the catheter lab (atrial septostomy/stenting) or surgically (atrial septectomy) to decompress the right heart failure. The time of interventions is very important because these surgical treatments have high mortality and morbidity rates, if performed in patients who are severely ill on inotropic support in intensive care units⁵⁸. However, due to its bad prognosis, it is normally used as a rescue method when medical therapy is not available.

- Lung transplantation

Lung transplantation is the surgery to replace a person's diseased lung with a healthy one from a deceased donor. Lung transplantation is an option in some patients that are not responsive to other medical managements. This procedure may be useful for people who have PAH caused by severe lung disease. Shortage of donors is the main limiting factor in this process. After lung transplantation, survival rates decrease by time.

1.3 Endothelium

The endothelium has semipermeable properties and regulates the transfer of small and large molecules. Endothelial cells are dynamic and have both metabolic and synthetic functions.

They exert significant autocrine, paracrine and endocrine actions and influence smooth muscle cells, platelets and peripheral leucocytes⁵⁹.

1.3.1 Endothelium-derived factors and their role in HPV and PH

Alveolar hypoxia may potentially activate vascular endothelial cells to elicit basic alterations in their local production of vasodilative and vasoconstrictive mediators. Imbalances of the following mediators in the pulmonary vasculature participate in the development of vasoconstriction and pulmonary hypertension⁶⁰.

1.3.1.1 Endothelin (ET)

The vasoconstrictor ET is produced by endothelial cells, with marked effects on vascular tone. There are three types of ET, but vascular endothelial cells produce only ET-1⁶¹. ET-1 is a 21-amino acid peptide. ET-1 has been found in lung tissue and pulmonary endothelial cells⁶² and pulmonary blood vessels possess ET-1 receptors⁶³. ET-1 is a potent vasoconstrictor peptide, and hypoxia has been demonstrated to increase ET-1 gene expression⁶⁴.

ET-1 increases intracellular calcium through multiple mechanisms directed by binding to G protein coupled receptors. These receptors stimulate phospholipase C activity leading to two important intracellular signalling messengers, inositol triphosphate and diacylglycerol. Binding of inositol triphosphate to sarcoplasmic reticulum triggers calcium release into the cytoplasm: diacylglycerol along with calcium activates protein kinase C which phosphorylates specific target proteins important in contraction and proliferation. ET-1 exerts vasoconstrictor actions through stimulation of ET_A receptors in vascular smooth muscle and vasodilator actions through stimulation of ET_B receptors in endothelial cells^{65, 66}. There is strong evidence that endothelium-derived ET-1 is a major player in the vasodilator/vasoconstrictor imbalance characteristic of PAH. Levels of lung and circulating ET-1 are increased in animals and patients with pulmonary hypertension of various etiologies⁶⁷. ET-1 may participate in HPV in isolated lung preparations, because HPV was markedly attenuated by either selective ET_A or nonselective ET receptor antagonists^{68, 69}. Thus, HPV may be intrinsic for the SMC, but requires ET-1 for the full in vivo expression of the hypoxic vascular response. The basal level of endogenous ET-1 might amplify the depolarizing effect of hypoxia in vivo^{70, 71}. In chronic hypoxic rats ET-1 fulfills the priming role by sensitising the contractile apparatus through stimulation of Rho-kinase. The permissive role of ET-1 in HPV may also be played through suppression of K_{ATP}-channels⁷².

1.3.1.2 Prostacyclin

Prostacyclin was described as endothelium-derived relaxing factor in 1979. Prostacyclin binds to a G protein coupled receptor, thereby increasing concentration of cyclic adenosine monophosphate (cAMP) that activates protein kinase A and lowers intracellular calcium concentration. The effect of prostacyclin is also connected to NO effects. It facilitates NO release from endothelial cells and in turn NO potentiates prostacyclin effects in smooth muscle by inhibition of phosphodiesterases, which degrade cAMP⁷³. PH induced by chronic exposure to hypoxia can be inhibited in mice that overexpress the prostacyclin synthase gene⁷⁴. Furthermore, the comparative studies with wild-type (WT) mice and prostacyclin receptor knock-out mice showed that after exposure of the animals to chronic hypoxia, prostacyclin receptor knock-out mice developed a greater degree of pulmonary hypertension and pulmonary arterial media thickening than WT mice⁷⁵.

1.3.1.3 Nitric oxide

NO is a relatively stable gas, with the ability to easily diffuse through the cell membrane. NO is one of the major endothelium-derived vasoactive mediators. It is synthesized from L-arginine and oxygen by a family of three NO synthases (NOSs), all of which are expressed in the lung. Endothelial NOS (eNOS) appears to play an important role in maintaining low pulmonary vascular tone⁷⁶.

NO stimulates soluble guanylyl cyclase (sGC) to synthesize cGMP that, in turn, activates cGMP-dependent protein kinase (PKG) which leads to the inhibition of calcium influx and decreased calcium calmodulin stimulation of myosin light chains. This, in turn, reduces the phosphorylation of myosin light chains, lowering smooth muscle tension, resulting in vasodilation⁷⁷.

The actions of cGMP are limited via its catabolism by PDEs. In addition, NO can elicit effects via cGMP-independent mechanisms including interactions with heme-containing molecules (in addition to sGC) and proteins containing reactive thiol groups. NO plays an important role in many physiological processes and is important in regulation of the vascular system, neurotransmission and various homeostatic events⁷⁸. Synthesis of NO involves incorporation of molecular oxygen, and hypoxia might therefore be expected to reduce basal NO production. Hypoxia also can inhibit uptake of L-arginine, the NO precursor, by pulmonary arterial endothelial cells and may suppress the expression and the activity of NO synthase⁷⁹. It has been suggested, that this inhibition of NO production may be effectively causing HPV⁸⁰. However, although NO is the most important vasodilator that specifically suppresses HPV,

inhibition of NO synthase has no effect on normoxic tone and results in enhancement of HPV, findings which are thought to contradict the conclusion that reduced production of NO is the initiating mechanism of HPV^{81, 82}. With regard to chronic hypoxia, the vascular responses have partially been attributed to decreased concentration of NO⁸³. Chronic exposure to hypoxia reduces the production of both prostacyclin and NO, both substances that are antiproliferative⁸⁴. Thus, a reduction in their production could contribute to proliferation of SMC or fibroblasts. NO can induce reversible inactivation of the protein kinase C (PKC) pathway, an intracellular pathway associated with cell proliferation⁷⁹.

1.3.1.3.1 Nitric oxide synthases

Three isoforms of NOS characterized by different genes, different localization, regulation, catalytic properties and inhibitor sensitivity have been identified. These isoforms include nNOS (also known as Type I, NOS-I and NOS-1) predominating in neuronal tissue, iNOS (also known as Type II, NOS-II and NOS-2) which is inducible in a wide range of cells and tissues and eNOS (also known as Type III, NOS-III and NOS-3) being found in vascular endothelial cells. These isoforms have been also differentiated on the basis of their constitutive (eNOS and nNOS) versus inducible (iNOS) expression, and their calcium-dependence (eNOS and nNOS) or -independence (iNOS).

The most important isoform expressed in the pulmonary vasculature is eNOS. It was demonstrated in perfused lungs, that HPV in eNOS-deficient mice approximately doubled that in WT mouse lungs. However, there was a slight increase in HPV in iNOS-deficient lungs, and HPV in nNOS-deficient lungs was equal to that observed in WT mice. Therefore, in isolated perfused lungs eNOS is the main source of the NO that modulates the responses to hypoxia⁷⁶. The expression of all three isoforms has been reported to be increased^{85, 86}, whereas in another study only the levels of eNOS protein were increased in rats with hypoxic pulmonary hypertension⁸⁷.

1.3.1.3.1.1 NOS inhibitors

- **N_ω-Nitro-L-arginine (L-NNA)** is an L-arginine analogue which causes inhibition of NO biosynthesis in vitro and in vivo. L-NNA increases arterial pressure in rats⁸⁸. In addition, L-NNA causes coronary vasoconstriction, especially of the large coronary arteries⁸⁹. L-NNA elevated both pulmonary and systemic vascular tone during hypoxia⁹⁰. Several reports have

shown that administration of L-NNA to isolated lungs causes a marked vasoconstriction in rats with chronic hypoxic pulmonary hypertension^{91,92}.

- **Methylarginine compounds** are the most important endogenous NOS inhibitors. The methylation of protein arginine residues is catalyzed by a family of intracellular enzymes termed protein arginine methyltransferases (PRMTs). In mammalian cells, these enzymes have been classified into type I and type II, depending on their specific catalytic activity. Both types of PRMTs catalyze the formation of mono-methylarginine (MMA) from L-arginine. In the second step, type I PRMT form asymmetric ω -N^G, N^G-dimethylarginine (ADMA). However, type II PRMT produce symmetric ω -N^G, N^G-dimethylarginine (SDMA) (Fig. 2)⁹³.

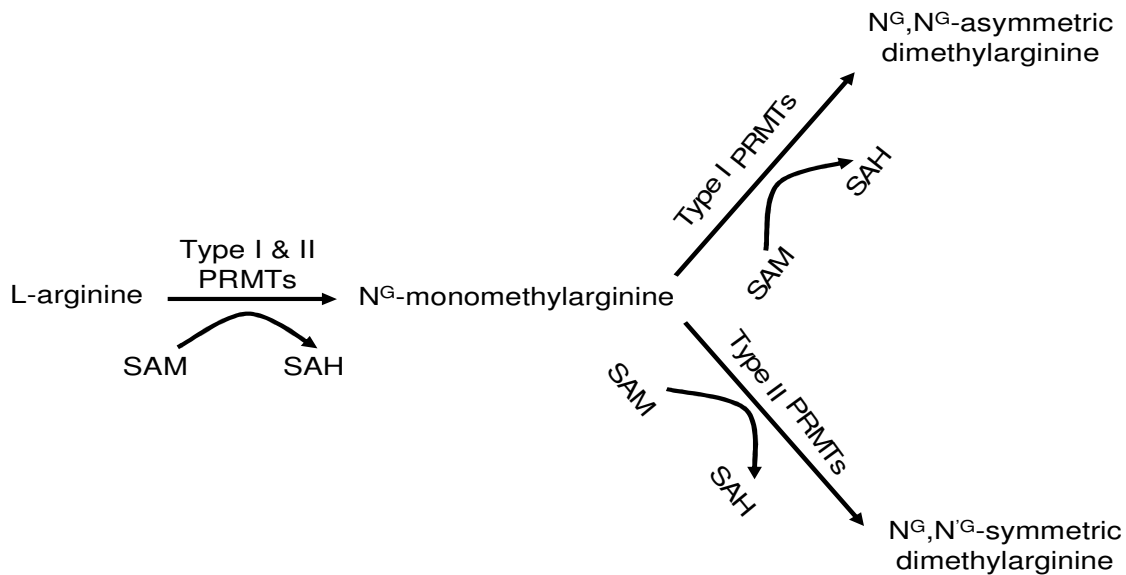


Figure 2: Synthesis of methylarginine compounds. SAM: S-adenosylmethionine; SAH: S-adenosylhomocysteine; PRMT: protein arginine methyltransferases. From Bedford et al. Mol. Cell 2005; 18: 263-272 with modifications.

After proteolytic degradation of methylated intracellular proteins, free MMA, SDMA, or ADMA can be released from cells. Released ADMA can be taken up by other cells via the cationic amino acid (γ +) transporters, which are widely expressed in mammalian cells⁹⁴.

ADMA has been detected in urine, plasma, cerebrospinal and broncho-alveolar lavage fluid (BALF), and various types of tissues⁹⁵. Free methylarginines are cleared from the body by renal excretion and hepatic metabolism. ADMA may control pulmonary cell functions

through inhibition of NOS and subsequently altered NO generation. Furthermore, the lung generates a significant amount of ADMA which may contribute to interstitial and plasma ADMA levels ⁹⁶. The activity of the NOS enzymes can be competitively inhibited by L-NMMA and ADMA. Both of these inhibitors are naturally occurring, but the concentration of ADMA in the human circulation is approximately 10 times greater than that of L-NMMA. In contrast, SDMA does not directly inhibit NOS function but is a potent inhibitor of the γ -transporter that mediates the intracellular uptake of arginine ⁹⁴. In addition, elevated plasma ADMA concentrations are associated with multiple pathological conditions, including renal failure ⁹⁷, hypertension ⁹⁸, and hypercholesterolemia ⁹⁹. Furthermore, some studies demonstrated that plasma ADMA concentrations are increased in patients with severe pulmonary hypertension ¹⁰⁰ suggesting that NOS inhibition by ADMA may contribute to the disease. It was demonstrated that chronic hypoxia-induced PH is associated with increased levels of pulmonary concentrations of ADMA ¹⁰¹.

1.3.1.3.2 Dimethylarginine dimethylaminohydrolase (DDAH)

There are two DDAH isoforms, DDAH1 and DDAH2 ¹⁰². Both of them are responsible for degradation of MMA and ADMA to citrulline and mono- or dimethylamines, respectively. DDAH activity controls endogenous ADMA concentrations and thus NOS activity. It was reported that the distribution of DDAH1 is similar to neuronal NOS, whereas the distribution of DDAH2 is similar to endothelial NOS, suggesting that DDAH1 and DDAH2 are expressed mainly in neuronal tissue and vascular endothelium, respectively ¹⁰³. However, some studies reported that DDAH1 is highly expressed in vascular endothelial cells in hearts ¹⁰⁴, which is consistent with another report showing strong DDAH1 expression in renal vascular endothelial cells ¹⁰⁵. In transgenic mice with DDAH1 overexpression, ADMA levels should be reduced leading to increased NOS activity and consequently increased NO production and pulmonary vasodilation. It was reported, that the activity of DDAH enzyme in the lungs was decreased in chronic hypoxia-induced PH. This might be at least a result of the corresponding decrease in the protein expression of the DDAH1 isoform. Hypoxic exposure inhibits the expression of the DDAH1 isoform, thus increasing ADMA levels ¹⁰¹.

1.3.1.3.3 Guanylate cyclases

It was established in 1970 that guanylyl cyclase activity was found in both soluble (sGC) and particulate (pGC) fractions of most cells. sGC is a heterodimer composed of $\alpha 1\beta 1$ and $\alpha 2\beta 2$ -isoforms, and is able to synthesize cGMP from GTP. The $\alpha 1\beta 1$ is thought to be the

predominant heterodimer in the vasculature responsible for smooth muscle relaxation ¹⁰⁶. However, the $\alpha 2\beta 2$ heterodimer is prominent in synaptic membranes and may play a role in synaptic transmission ¹⁰⁷. sGC is expressed in the cytoplasm of almost all mammalian cells and mediates a variety of important physiological functions, such as inhibition of platelet aggregation, relaxation of smooth muscle, vasodilatation, neuronal signal transduction, and immunomodulation ¹⁰⁸. It was reported, that sGC- $\alpha 1$ is essential for the pulmonary vasodilator response to inhaled NO during HPV and limits pulmonary vascular remodeling and RV hypertrophy associated with chronic hypoxia-induced pulmonary hypertension ¹⁰⁹. Metabolism of H_2O_2 leads to activation of guanylate cyclase and increased production of cGMP and vasodilatation. There is evidence that suggests that hypoxia may reduce H_2O_2 -stimulated production of cGMP in PASMCs. According to this hypothesis, hypoxia might decrease H_2O_2 production and subsequently decrease guanylate cyclase/cGMP induced pulmonary vasodilatation ¹¹⁰. It is also possible that hypoxia increases H_2O_2 level which oxidizes sGC and decrease cGMP. Some compounds like Bay41-2272 stimulate sGC and therefore can be used as systemic pulmonary vasodilator ¹¹¹. It was also demonstrated that Bay41-2272, the sGC stimulator, and Bay58-2667, the sGC activator, reverse pulmonary hypertension in chronically hypoxic mice. Thus, sGC is considered an effective vasodilator in the treatment of hypoxia-induced pulmonary vascular diseases ¹¹². In contrast, sGC is inhibited by 1H-[1, 2, 4]oxadiazolo[4, 3-a]quinoxalin-1-one (ODQ) which causes oxidation of the prosthetic heme group of sGC, markedly reducing or inhibiting the pulmonary vasodilator effect of NO. ODQ has been used to examine the specificity of sGC activation induced by NO donors such as nitroglycerin ¹¹³.

2. AIM OF THE STUDY

Hypoxia has long been known to elicit pulmonary vasoconstriction and pulmonary hypertension, but the mechanisms of hypoxic pulmonary vasoconstriction and hypoxia-induced pulmonary hypertension are still unclear. It has been proposed, that the endothelium plays an important role in the regulation of acute, and in particular sustained and chronic effects of hypoxia on pulmonary vasculature. Therefore, the aim of the current study was to investigate the role of dimethylarginine dimethylaminohydrolase 1 (DDAH-1), expressed in the endothelium, on the effects of acute, sustained and chronic hypoxia on pulmonary vasculature. NO is the most effective pulmonary vasodilator and is well known to influence hypoxia-induced alterations of lung vessels. It is synthesized from L-arginine by NO synthases which are strongly inhibited by ADMA, which is degraded by DDAH.

Therefore this study aimed to:

- 1- a) Compare the effect of acute and sustained hypoxia on PAP of isolated lungs of DDAH1^{tg} and WT mice.
b) Elucidate the mechanism of DDAH1 induced effects on pulmonary vasculature.
- 2- Compare the development of PH in DDAH1^{tg} and WT mice exposed to 3 weeks of chronic hypoxia by a) measurement of right ventricular systolic pressure, b) morphometrical analysis and c) determination of right/left heart ratio.

3. MATERIALS

3.1 Chemicals, solutions and drugs

- Anti foam 204, Sigma-Aldrich, Steinheim, Germany
- Aqua B.Braun Ecotainer®, Braun, Melsungen, Germany
- Chlorhydric acid 1N, Merck, Darmstadt, Germany
- 1H-[1, 2, 4]oxadiazolo[4, 3-a]quinoxalin-1-one, Sigma-Aldrich, Steinheim, Germany
- Heparin Liquemin N 25000®, Roche, Basel, Swiss
- Ketamine hydrochloride 100 mg/ml, Pfizer Pharma GmbH, Karlsruhe, Germany
- Krebs-Henseleit electrolyte solution, Serag-Wiessner KG, Naila, Germany
- N_ω-Nitro-L-arginine, Sigma-Aldrich, Steinheim, Germany
- Oncotic agent HAES®, Fresenius Kabi, Bad Homburg, Germany
- Potassium chloride, Fluka Biochemika, Buchs, Switzerland
- Potassium dihydrogen phosphate, Merk, Darmstadt, Germany
- Rompun 2% (xylazine hydrochloride), Bayer, Leverkusen, Germany
- Sodium bicarbonate 8.4%, Serag-Wiessner KG, Naila, Germany
- Sodium chloride, Fluka Biochemika, Buchs, Switzerland
- Sodium hydroxide 1N, Merck, Darmstadt, Germany
- Sodium nitrite, Sigma-Aldrich, Steinheim, Germany
- Sterile isotonic saline solution (0.9% NaCl), Braun, Melsungen, Germany
- UltraPure® DNase/RNase-Free Distilled Water, Invitrogen, Karlsruhe, Germany
- Vanadium chloride, Sigma-Aldrich, Steinheim, Germany
- Composition of Krebs-Henseleit solution

Sodium chloride	120 mM
Potassium chloride	4.3 mM
Potassium dihydrogen phosphate	1.1 mM
Calcium chloride-dihydrate	2.4 mM
Magnesium chloride-hexahydrate	1.3 mM
Glucose	13.32 mM
Hydroxyethylamylopectin (molecular weight 200.000):	5% (wt/vol.)

Krebs-Henseleit electrolyte solution was used as a perfusion buffer. 24 mM of sodium bicarbonate was added to the perfusion buffer in order to adjust pH at 7.35 - 7.45.

3.2 Consumables

- BD Microlance needles 21G and 26G, Becton Dickinson, Heidelberg, Germany
- Cannula for left heart catheterisation support 22G and 20G, Braun, Melsungen, Germany
- Cannula for pulmonary artery catheterisation support 22G and 20G, Braun, Melsungen, Germany
- Combi-Stopper, Intermedica GmbH, Klein-Winternheim, Mainz, Germany
- Combitips Plus 1 and 10 ml, Eppendorf Biopur®, Eppendorf AG, Hamburg, Germany
- Combitrans Monitoring-Set, Braun, Melsungen, Germany
- Disposable feather scalpel, Feather Safety Razor Company, Osaka, Japan
- Disposable micropipettes intraMARK 50 µl, Blaubrand Brand GmbH, Wertheim-Bettingen, Germany
- Filter papers, Whatman Schleicher & Schuell GmbH, Dassel, Germany
- Gauze balls size 6, Fuhrman Verbandstoffe GmbH, Munich, Germany
- Hematocrit sealing compound, Blaubrand Brand GmbH, Wertheim-Bettingen, Germany
- Heparinized microcapillary tubes, Hämacont, Heilbronn, Germany
- Napkins, Tork, Mannheim, Germany
- Pipette 10, 100 and 1000 µl, Eppendorf AG, Hamburg, Germany
- Pipette tips, blue, yellow and white, Eppendorf AG, Hamburg, Germany
- Single use gloves Transaflex®, Ansell, Surbiton Surrey, UK
- Single use syringes Inject Luer® 1, 10 and 20 ml, Braun, Melsungen, Germany
- Sterile gauze 5 x 4 cm Purzellin®, Lohmann und Rauscher, Rengsdorf, Germany
- Surgical instruments, Martin Medizintechnik, Tuttlingen, Germany
- Surgical threads non-absorbable ETHIBOND EXCEL® size 5-0, Ethicon GmbH, Norderstedt, Germany
- Threads Nr. 12, Coats GmbH, Kenzingen, Germany
- Tracheal cannula from BD Microlance 15 or 20G shortened to 1.5 cm, Becton Dickinson, Heidelberg, Germany
- Tygon® lab tubing 3603, Cole-Parmer Instruments Company, Vernon Hills, Illinois, USA

3.3 Set-up for animal experiments

- Blood analyser ABL 330, Radiometer, Copenhagen, Denmark
- Frigomix1495, Braun, Melsungen, Germany
- Magnetic stirrer Ret-Basic, IKA Labortechnik, Staufen, Germany
- Microliter centrifuge cooled Mikro 200R, Andreas Hettich GmbH & Co KG, Tuttlingen, Germany
- Microliter centrifuge cooled Mikro 210, Andreas Hettich GmbH & Co KG, Tuttlingen, Germany
- Microplate Reader ELx 808IU, BIO-TEK® Instruments, Inc. Winooski, Vermont, USA
- Microplate Washer, SLT-Lab Instruments, Achterwehr, Germany
- Nitric Oxide Analyzer (NOA) Sievers 280, Foehr Medical Instruments (FMI) GmbH, Seeheim, Germany
- Peristaltic pump REGLO Digital MS-4/12, Ismatech Labortechnik-Analytik, Glattbrugg, Switzerland
- Piston pump Minivent Type 845, Hugo Sachs Elektronik Harvard Apparatus GmbH, March-Hugstetten, Germany
- Research Grade Isometric Force Transducer, Harvard Apparatus, Holliston, USA
- Shaker, Keutz Labortechnik, Reiskirchen, Germany
- Thermomix UB, Braun, Melsungen, Germany
- Transbridge BM4, World Precision Instruments, Berlin, Germany
- Vortexer MS1 Minishaker, IKA Labortechnik, Staufen, Germany

3.4 Software

- Data Acquisition Software LABTECH NOTEBOOK version 10.1, LABTECH, Andover, USA
- NoaWin 32 Software, DeMeTec (development of measurement and medical technologies), Langgöns, Germany

3.5 Materials for histology

- Acetone, Sigma-Aldrich, Steinheim, Germany
- 100 ml Automated microtom RM 2165, Leica Microsystems, Nussloch, Germany
- Biotin-Blocking kit, Vector/Linaris, Wertheim-Bettingen, Germany

- Cooling plate EG 1150C, Leica Microsystems, Nussloch, Germany
- 3, 3'- Diaminobenzidine (DAB) substrat kit, Vector/Linaris, Wertheim-Bettingen, Germany
- Disodium hydrogen phosphat-dihydrat pro analysis, Merck, Darmstadt, Germany
- Digital Camera Microscope DC 300F, Leica Microsystems, Nussloch, Germany
- Ethanol 70%, 96% and 99.6%, Fischer, Saarbrücken, Germany
- Flattening bath for paraffin sections HI 1210, Leica Microsystems, Nussloch, Germany
- Flattening table HI 1220, Leica Microsystems, Nussloch, Germany
- Formaldehyde alcohol free 37%, Fischer, Saarbrücken, Germany
- Histological glass slides Superfrost Plus®, R. Langenbrinck, Emmendingen, Germany
- Horseradish peroxidase streptavidin, Alexis Biochemicals, Grünberg, Germany
- Hydrogen peroxide 30% pro analysis, Merck, Darmstadt, Germany
- Isopropanol 99.8%, Sigma-Aldrich, Steinheim, Germany
- Laser capture micro dissection, Leica Microsystems, Nussloch, Germany
- Methanol reinst, Sigma-Aldrich, Steinheim, Germany
- Methyl green counter stain, Vector/Linaris, Wertheim-Bettingen, Germany
- Microtom blades S35, Feather Safety Razor Company, Osaka, Japan
- Mounting medium Pertex®, Medite GmbH, Burgdorf, Germany
- Normal Horse Serum, Alexis Biochemicals, Grünberg, Germany
- Parafilm, American National Can Menasha, Wisconsin, USA
- Paraffin embedding medium Paraplast Plus®, Sigma-Aldrich, Steinheim, Germany
- Pikric acid, Fluka Biochemika, Buchs, Switzerland
- Potassium dihydrogen phosphat pro analysis, Merck, Darmstadt, Germany
- Silicon, Sigma-Aldrich, Steinheim, Germany
- Sodium chloride pro analysis, Fischer, Saarbrücken, Germany
- Streptavidin blocking kit, Vector/Linaris, Wertheim-Bettingen, Germany
- Stereo light microscope DMLA, Leica Microsystems, Nussloch, Germany
- Tissue-embedding machine EG 1140H, Leica Microsystems, Nussloch, Germany
- Tissue-processing automated machine TP 1050, Leica Microsystems, Nussloch, Germany
- Trypsin Digest All 2®, Zytomed, Berlin, Germany
- Universal-embedding cassettes, Leica Microsystems, Nussloch, Germany

- Vector VIP Substrat Kit, Vector/Linaris, Wertheim-Bettingen, Germany
- Xylol, Fischer, Saarbrücken, Germany

3.6 Antibodies

- Anti-alpha-smooth muscle actin, Sigma-Aldrich, Steinheim, Germany
- Anti-von Willebrand factor, Dako Cytomation, Hamburg, Germany
- Secondary antibody (anti rabbit IgG antibody peroxidase-conjugated), Vector/Linaris, Wertheim-Bettingen, Germany

3.7 System and software for morphometry

- Computer Q 550 IW, Leica Microsystems, Nussloch, Germany
- Software Qwin V3, Leica Microsystems, Nussloch, Germany
- Macro for degree of muscularization, Leica Microsystems, Nussloch, Germany

4. METHODS

4.1 Animals

Adult WT mice (C57BL/6J) were purchased from Charles River (Sulzfeld, Germany). DDAH1 overexpressing mice were provided by John Cooke (Stanford University School of Medicine, Stanford, CA, USA). Animals had access to food and water ad libidum. All mice used in all experiments were 8 to 12 weeks of age, and weighed 20 to 28 g each. Animals were kept under pathogen free conditions and handled in accordance with the European Community recommendations for experimentation. All animal experiments were approved by the local authorities (Regierungspräsidium Giessen).

4.2 Acute and sustained (3 h) hypoxic experiments

4.2.1 Isolated, ventilated and perfused mouse lungs

Isolated, perfused and ventilated mouse lungs have long been used by investigators interested in the physiological, biochemical, pharmacological and metabolic aspects of this complex organ¹¹⁴. This technique has also been adapted to study the effects of different substances and drugs and the expected mechanisms by which they act. In addition, cells in the isolated perfused mouse lung are maintained in their “normal” anatomical and physiological associations and local physiological regulations in the organ. We took advantage of isolated mouse lungs as this model allows:

- 1- Use of different genetically altered animals in order to identify the role of specific genes in our measurements.
- 2- Use of several drugs to determine the dose and also to investigate the mechanism(s) by which they act.

4.2.2 Isolation, perfusion and ventilation of mouse lungs

In all experiments, lungs were totally separated from the remainder of the body. Mice were deeply anesthetized intraperitoneally with pentobarbital sodium (100 mg/kg body weight) and anticoagulated with heparin (1000 U/kg body weight) by intravenous injection. A median incision was done ventrally in the center of the neck, and the trachea was exposed by blunt dissection and partially transected. Animals were then intubated via a tracheostoma and were ventilated with room air (tidal volume 250 μ l; respiratory rate 90 breaths/min; positive end-

expiratory pressure = 2 cm H₂O) with a specific piston pump (Minivent Type 845, Hugo Sachs Elektronik Harvard Apparatus GmbH, March-Hugstetten, Germany).

After midsternal thoracotomy the ribs were spread, the heart was incised at the apex and then the right ventricle was incised, and a fluid-filled perfusion catheter was immediately placed into the pulmonary artery and secured with a ligature. Immediately after insertion of the catheter, perfusion with a perfusion pump (REGLO Digital MS-4/12, Ismatech Labortechnik-Analytik, Glattbrugg, Switzerland) with sterile Krebs-Henseleit solution (Serag-Wiessner KG, Naila, Germany) was started, the temperature of the system was 4°C at the beginning of the perfusion then gradually increased till 37.5°C. In parallel with the onset of artificial perfusion, ventilation was changed from room air to a pre-mixed normoxic normocapnic gas mixture with 21% O₂, 5.3% CO₂, balanced with N₂ (Air Liquid, Deutschland GmbH, Ludwigshafen, Germany).

Next, the trachea, lungs, and heart were excised *en bloc* from the thoracic cage without interruption of ventilation and perfusion and were freely suspended from a force transducer for monitoring of organ weight. A second perfusion catheter with cannula was introduced via the left ventricle into the left atrium (Fig. 3). Meanwhile, the flow was slowly increased from 0.2 to 2 ml/min (total system volume 13 ml). After rinsing the lungs with more than 20 ml of buffer for washing the preparation from blood, the perfusion circuit was closed for recirculation. Left atrial pressure was fixed at 2.0 mmHg. The isolated, perfused lung was placed in a temperature-equilibrated housing chamber and the whole system (perfusate reservoirs, tubing, housing chambers) was heated to 37.5°C¹¹⁵.

For hypoxic ventilation, a gas mixture containing 1% O₂, 5.3% CO₂, balanced with N₂ was used.

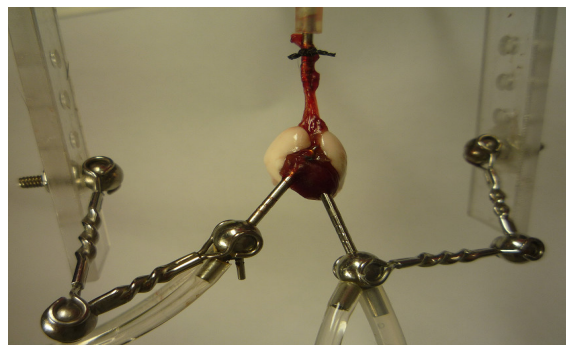


Figure 3: Isolated, perfused and ventilated mouse lung.

About 30 min after the isolation of the lung, steady state period was achieved. When PAP values were stable for 15 min, the experiment was started. Pressures in the pulmonary artery,

the left ventricle and the trachea were registered by means of pressure transducers connected to the perfusion catheters via small diameter tubings and were digitised with an analogue-to-digital converter, thus allowing data sampling with a personal computer (Fig. 4). The transducers were calibrated prior to each experiment.

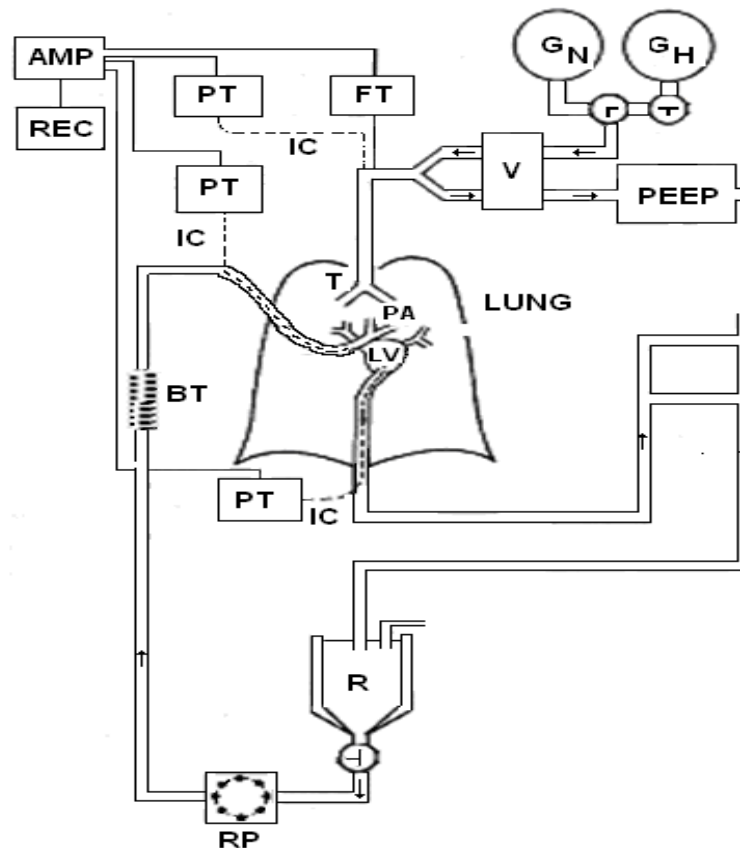


Figure 4: Schematic representation of the experimental set-up of the isolated, perfused and ventilated mouse lung. AMP: amplifier; BT: bubble trap; FT: force transducer; G_N : normoxic gas supply; G_H : hypoxic gas supply; IC: intraluminal catheter; LV: left ventricle; PA: pulmonary artery; PEEP: positive end-expiratory pressure; PT: pressure transducer; R: reservoir; RP: roller pump; REC: recording device; T: trachea; V: ventilator. From Seeger et al. *Methods Enzymol.* 1994; 233:549-584 with modifications.

In acute and sustained hypoxic experiments, after a normoxic ventilation (NOX) period for 15 min, hypoxia (HOX) was applied for 10 min (acute phase), then changed to NOX for 15 min then to 3 h HOX (sustained phase) followed by 15 min NOX, another 10 min HOX and finally 10 min NOX.

4.2.3 Colorimetric determination of cGMP by Cayman's cGMP-Kit (ELISA)

The level of cGMP was measured by Cayman's cGMP-Kit according to Cayman chemical company's (Hamburg, Germany) instructions.

1- Principle: Cayman's cGMP assay is based on the competition between free cGMP in a sample (perfusate) and acetylcholinesterase (AChE) conjugated cGMP (cGMP tracer) for a limited amount of cGMP-specific rabbit antibody binding sites. The concentration of the cGMP tracer is held constant while the concentration of cGMP varies; the amount of cGMP tracer that is able to bind to the rabbit antibody is inversely proportional to the concentration of cGMP in the reaction well. This rabbit antibody-cGMP complex binds to the mouse monoclonal anti-rabbit immunoglobulin G (IgG) that has been previously attached to the well. The plate is washed to remove any unbound reagents and then Ellman's reagent (which contains the substrate for AChE) is added to each well.

The product of this enzymatic reaction has a distinct yellow color and absorbs light strongly at 412 nm. The intensity of this color, determined spectrophotometrically, is proportional to the amount of cGMP tracer bound to the well, which is inversely proportional to the amount of free cGMP present in the well during the incubation. When the concentration of cGMP in the sample is very low, the sensitivity of the reaction can be increased by an acetylation procedure for both, the standard and the experimental samples, because antibody binding is increased, if an acetyl group is present on the 2-hydroxyl group of the cGMP.

The concentration of cGMP was determined in samples of pulmonary venous effluent during different experimental time periods of the isolated lung experiments. Perfusate samples were taken from venous effluent during the experiment at the time points of 10, 20, 35, 45 and 220 min (10 and 35 min were during normoxic ventilation, while the other time points were during hypoxic ventilation) and immediately frozen in liquid nitrogen and stored at -20°C until measurement. The materials provided by the company for performing the assay are listed in Table 4.

Catalog number	Item	96 wells, quantity/size
481022	cGMP EIA antiserum	1 vial/100 dtn
481020	cGMP AChE tracer	1 vial/100 dtn
481024	cGMP EIA standard	1 vial
400060	EIA buffer concentrate (10X)	2 vials/10 ml
400062	Wash buffer concentrate (400X)	1 vial/5 ml

400035	Tween 20	1 vial/3 ml
400004	Mouse anti-rabbit IgG coated plate	1 plate
400012	96-Well cover sheet	1 cover
400050	Ellman's reagent	3 vials/100 dtn
400031	Acetic anhydride	1 vial/2.5 ml
400029	KOH	1 vial
400040	EIA tracer dye	1 vial
400042	EIA antiserum dye	1 vial

2- Table 4: Materials supplied from Cayman Chemical Company for cGMP measurement. cGMP: cyclic 3', 5'-guanosine monophosphate; EIA: enzyme immuno assay; dtn: determinant; AChE: acetylcholinesterase; IgG: immunoglobulin G; KOH: potassium hydroxide.

3- Measurement was performed as follows:

Acetylation procedure: To 500 μ l of sample/standard, 100 μ l of 4 M KOH and 25 μ l acetic anhydride were added in quick succession, shaken for 15 seconds, then 25 μ l of 4 M KOH was added and vortexed again for also 15 seconds. This was repeated for all samples and standard tubes.

Addition of the reagents

The scheme of the plate set-up is given in Table 5.

1- 100 and 50 μ l enzyme immuno assay (EIA) buffer were added to non-specific binding (NSB) and maximum binding (Bo) wells, respectively.

2- 50 μ l from standard/sample were added to their specific wells in a duplicate.

3- 50 μ l from cGMP AChE tracer was added to each well except the total activity (TA) and the blank (Blk) wells.

4- 50 μ l from cGMP EIA antiserum was added to each well except TA, NSB and Blk wells. Then the plate was covered with plastic film, and was incubated for 18 hours at room temperature.

Development of the plate

1- Ellman's reagent was reconstituted immediately before use with 20 ml UltraPure water.

2- Solutions in the wells were discarded and the wells were rinsed five times with wash buffer.

3- 200 μ l of Ellman's reagent was added to each well.

4- 5 μ l of tracer was added to TA well.

5- The plate was covered with plastic film. Optimum development was obtained by using an orbital shaker for 90 min at 4°C.

Reading the plate

1- The bottom of the plate was wiped with clean tissue to remove fingerprint, dirt etc.

2- The plate cover was removed carefully.

3- The plate was read at a wavelength between 405 and 420 nm by using ELx 808IU (BIO-TEK® Instruments, Inc. Winooski, Vermont, USA) connected to a computer which contained software to calculate the concentrations automatically.

	1	2	3	4	5	6	7	8	9	10	11	12
A	Blk	Blk	S1	S1	1	1	9	9	17	17	25	25
B	Blk	Blk	S2	S2	2	2	10	10	18	18	26	26
C	NSB	NSB	S3	S3	3	3	11	11	19	19	27	27
D	NSB	NSB	S4	S4	4	4	12	12	20	20	28	28
E	Bo	Bo	S5	S5	5	5	13	13	21	21	29	29
F	Bo	Bo	S6	S6	6	6	14	14	22	22	30	30
G	Bo	Bo	S7	S7	7	7	15	15	23	23	31	31
H	TA	TA	S8	S8	8	8	16	16	24	24	32	32

Table 5: Sample plate format for cGMP measurement. Blk: blank; NSB: non-specific binding; Bo: maximum binding; TA: total activity; S1-S8: standard 1-8; 1-32: samples.

4- Definitions:

1- Blank: Background absorbance caused by Ellman's reagent.

2- Total activity: Total enzyme activity of AChE-linked tracer.

3- NSB (Non-Specific Binding): Non-immunological binding of the tracer to the well. Even in the absence of specific antibody a very small amount of tracer still binds to the well; the NSB is a measure of this low binding.

4- Bo (maximum binding): Maximum amount of tracer that the antibody can bind in the absence of sample.

5- % B/Bo (% Bound/Maximum Bound): Ratio of the absorbance of a particular sample or standard well to that of the maximum binding well.

6- Dtn: Determinant, one dtn is the amount of reagent used per well.

4.2.4 Colorimetric determination of ADMA by using ADMA-Kit (ELISA)

For determination of ADMA, the ADMA-Kit of DLD Diagnostika GmbH, Hamburg, Germany, was used.

1- Principle: The competitive ADMA-ELISA assay uses the microtiter plate format. ADMA is bound to the solid phase of the microtiter plate. ADMA in a sample (perfusate) is acylated and competes with solid phase bound ADMA for a fixed number of rabbit anti-ADMA antiserum binding sites. When the system is in equilibrium, free antigen and free antigen-antiserum complexes are removed by washing. The antibody bound to the solid phase ADMA is detected by anti-rabbit IgG conjugated with peroxidase. The amount of antibody bound to solid phase ADMA is inversely proportional to the ADMA concentration of the sample. The substrate tetramethylbenzidine (TMB)/peroxidase reaction is monitored at 450 nm. Perfusate samples were taken from venous effluent during the experiment at the time points of 10, 20, 35, 45 and 220 min (10 and 35 min were during normoxic ventilation, while the other time points were during hypoxic ventilation) and immediately frozen in liquid nitrogen and stored at -20°C until measurement. The materials provided by the company for performing the assay are listed in Table 6.

Microtiter-Strips: 8 wells each, break apart precoated with ADMA	12 strips
Standards 1 – 6: in a concentration of 0.0, 0.1, 0.3, 0.6, 1.0, 5.0 $\mu\text{mol/l}$, each 4 ml, ready for use	6 vials
Control 1 & 2: each 4 ml, ready for use	2 vials
Acylation buffer: 3.5 ml, ready for use	1 bottle
Acylation reagent: dissolve content in 2.8 ml solvent before use	2 vials
Antiserum: 5.5 ml, ready for use, rabbit-anti-N-acyl-ADMA	1 vial
Enzyme conjugate: 12 ml, ready for use, goat anti-rabbit-IgG-peroxidase	1 vial
Wash buffer: 20 ml, concentrated, dilute content with distilled water to 500 ml total volume, store at 2 - 8°C .	1 bottle
Substrate: 12 ml TMB solution, ready for use	1 vial
Stop solution: 12 ml, ready for use, contains 0.3 M sulphuric acid	1 vial
Reaction Plate: for acylation	1 piece

Equalizing reagent: dissolve content with 20.5 ml distilled water, dissolve carefully to minimize foam formation	1 vial
Solvent: 6 ml, contains acetone/DMSO	1 vial

2- Table 6: Contents of the kit used in ADMA measurement. ADMA: asymmetric ω -N^G, N^G-dimethylarginine; IgG: immunoglobulin G; TMB: tetramethylbenzidine; DMSO: dimethyl sulfoxide.

3- Measurement was performed as follows:

- **Preparation of samples (acylation):** The wells of the reaction plate for the acylation can be used only once.

1- 20 μ l standard 1 - 6, each 20 μ l control 1 & 2 and each 20 μ l samples were added into the respective wells of the reaction plate.

2- 25 μ l acylation buffer was added into all wells.

3- 200 μ l equalizing reagent was pipetted into all wells, mixing the reaction plate for 10 seconds.

4- 50 μ l prepared acylation reagent was added to wells, mixed immediately, then the reaction plate was incubated for 90 min at room temperature (approx. 20°C) on an orbital shaker without covering the wells or the plate. Afterwards, all reagents were transferred to room temperature and mixed carefully.

- **Sample incubation:** Each 50 μ l prepared standards, 50 μ l prepared controls and 50 μ l prepared samples was added to the respective wells of the coated microtiter strips in a duplicate design, then 50 μ l antiserum was pipetted into all wells and shaken shortly on an orbital shaker. The plate was covered with adhesive foil and incubated for 15 – 20 h at 4°C.

- **Washing:** The solution contents of the wells were discarded and washed thoroughly with each 250 μ l wash buffer (shaken shortly on an orbital shaker). This procedure was repeated 4 times. Residual liquid was removed by tapping the inverted plate on clean absorbent paper.

- **Conjugate incubation & washing:** Each 100 μ l enzyme conjugate was added to each well, and then incubated for 60 min at room temperature on an orbital shaker, and then step 3 was repeated.

- **Substrate incubation:** Each 100 μ l substrate was added into all wells and incubated for 20 to 30 min at room temperature on an orbital shaker.

- **Stopping:** 100 μ l stop solution was pipetted to each well.

- **Reading:** The optical density was determined at 450 nm by using a microplate photometer. The concentrations of the samples were calculated.

	1	2	3	4	5	6	7	8	9	10	11	12
A	S1	S1	1	1	9	9	17	17	25	25	33	33
B	S2	S2	2	2	10	10	18	18	26	26	34	34
C	S3	S3	3	3	11	11	19	19	27	27	35	35
D	S4	S4	4	4	12	12	20	20	28	28	36	36
E	S5	S5	5	5	13	13	21	21	29	29	37	37
F	S6	S6	6	6	14	14	22	22	30	30	38	38
G	C1	C1	7	7	15	15	23	23	31	31	39	39
H	C2	C2	8	8	16	16	24	24	32	32	40	40

Table 7: Sample plate format for ADMA measurement. S1-S6: standard 1-6; C1, C2: control 1 & 2; 1-40: samples

4.2.5 Measurement of NO metabolites in perfusate

The metabolic products of NO (nitrite, nitrate and peroxynitrite) were determined in perfusate samples by using Nitric Oxide Analyzer (NOA) “Sievers 280” (FMI GmbH, Seeheim, Germany) according to manufacturer instructions. Perfusate samples were taken from venous effluent during the experiment at the time points of 10, 20, 35, 45 and 220 min (10 and 35 min were during normoxic ventilation, while the other time points were during hypoxic ventilation) and immediately frozen in liquid nitrogen and stored at -20°C until measurement. The principle of NO measurement depends on the reduction of NO metabolic products by vanadium chloride in hydrochloric acid at 95°C (to achieve high conversion efficiency) to NO gas which is provided to the NO analyzer connected to a computer for data transfer and analysis by using “NoaWin 32” software (DeMeTec, Langgöns, Germany). If the samples contain high levels of protein, the reagent will start to foam as samples are injected. An antifoaming 204 agent (a mixture of non-silicone organic defoamers in a polyol dispersion) (100 μl) was therefore added to the purge vessel containing vanadium chloride solution at the beginning of the experiment. To prevent damage to the NOA from hydrochloric acid vapour, a gas bubbler filled with aqueous sodium hydroxide was installed between the purge vessel

and the NOA. A standard solution of 100 mM sodium nitrite was prepared and dilutions of the standard used for constructing the calibration curve. NO concentration can be determined from the peak which appears about 30 seconds after injection of the sample. All samples were measured in a duplicate.

4.3 Chronic hypoxic experiments

Pulmonary hypertension was induced in mice by exposure to hypoxia (10% inspired O₂ fraction) in a normobaric chamber for 21 days. Constant level of hypoxia was maintained with the aid of an autoregulatory control unit (model 4010, O₂ controller, Labotec, Göttingen, Germany) supplying either nitrogen or oxygen. Excess humidity in the system was prevented by condensation in a cooling system. CO₂ was continuously removed by soda lime. Cages were opened for food and water supply and for cleaning. The chamber temperature was maintained at 22-24°C. Control animals were placed in similar condition in a normoxic chamber with normal oxygen environment (21% inspired O₂ fraction).

4.3.1 In vivo hemodynamic measurements

For general anesthesia, mice were given an intraperitoneal injection of a combination of ketamine and xylazine (100 mg/kg, and 15 mg/kg, body weight, respectively). The anesthetic mixture was prepared as a mixture of 20 µl ketamine, 20 µl xylazine and 40 µl NaCl, the required volume to achieve the specific dose was injected and mice were anticoagulated with heparin (1000 U/kg). The anesthetized animals were placed in a heating chamber in order to maintain the body temperature within the physiological range. The trachea was cannulated, and the lungs were ventilated with room air at a tidal volume of 200 µl and at a rate of 120 breaths/min. A positive end expiratory pressure (PEEP) of 1.0 cm H₂O was used throughout the experiment. Through a small opening in the chest a 26-gauge stainless steel needle attached to a filled force transducer was carefully inserted into the right ventricle to measure the right ventricular systolic pressure (RVSP). The transducer was calibrated before every measurement. RVSP was recorded for 20 min and the saved data was printed for analysis. After RVSP measurement, blood was collected directly from the right ventricle for hematocrit measurement. Hematocrit was measured immediately by capillary centrifugation technique. The capillary tube containing the whole blood was spun in an Adams Autocrit Centrifuge for 5 min and hematocrit values were obtained.

4.3.2 Vascular morphometry

After finishing hemodynamic measurements, an incision in left ventricle was made, mouse lungs were first flushed with sterile saline solution at a constant pressure of 22 cm H₂O above the pulmonary artery via the pulmonary artery, in order to get rid of blood, and then fixed by passing phosphate-buffer paraformaldehyde through the pulmonary artery. Saline was infused through the trachea. For vascular morphometry, after 15-25 min, lungs were gently isolated from the chest cavity and allowed to immerse overnight in a fixative solution. Fixed lungs were transferred to 0.1 M PBS (phosphate-buffered saline) on the following day. Afterwards, the lung lobes were individually placed in histological cassettes and dehydrated in an automated dehydration station and then embedded in paraffin blocks. Staining was done on 3 µm lung sections for vascular morphometry.

The degree of muscularization in small pulmonary arteries was investigated in mouse lung paraffin sections after staining with the specific antibodies against α -actin (for smooth muscle) and vonWillebrand factor (vWf) (for endothelial cell). The detailed protocol is given in the following tabular form (Table 8).

Incubation time (min)	Reagent	Remarks
60	Heating slide with paraffin section	58°C
30	Xylol, fresh xylol was used every 10 min	
10	Ethanol 99.6%, after 5 min fresh ethanol 99.6% was used	
5	Ethanol 96%	
5	Ethanol 70%	
15	H ₂ O ₂ - methanol mixture 3%	180 ml methanol + 20 ml H ₂ O ₂ 30% (freshly prepared)
10	H ₂ O, after 5 min fresh H ₂ O was used	
10	PBS, fresh PBS was used every 5 min	
15	Trypsin	(1 ml trypsin + 2 ml diluent)
50	Incubation at 37°C	
15	PBS, fresh PBS was used every 5	

	min	
15	Streptavidin blocking	
5	PBS	
15	Biotin blocking	
5	PBS	
15	10% Bovine serum albumin (BSA)	
10	PBS, fresh PBS was used every 5 min	
60	Mouse IgG blocking reagent, mouse on mouse (M.O.M.) (reagent 1)	100 μ l IgG blocking reagent + 2.5 ml PBS
15	PBS, fresh PBS was used every 5 min	
5	M.O.M. diluent/protein blocking (reagent 2)	7.5 ml PBS + 600 μ l protein concentrate
30	Primary antibody (α -actin)	1:900 dilution with 10% BSA
20	PBS, fresh PBS was used every 5 min	
10	M.O.M. biotinylated IgG reagent (reagent 3)	10 μ l reagent 3 + 2.5 ml M.O.M diluent
20	PBS, fresh PBS was used every 5 min	
30	Horseradish peroxidase streptavidin, R. T. U. (ready to use)	
15	PBS, fresh PBS was used every 5 min	
3 to 4	Vector VIP (very intense purple) substrate kit	5 ml PBS + 150 μ l reagent 1 + 150 μ l reagent 2 + 150 μ l reagent 3 + 150 μ l H ₂ O ₂ solution then the intensity of the purple color was checked microscopically.
5	H ₂ O	

10	PBS, fresh PBS was used every 5 min	
20	10% BSA	
15	PBS, fresh PBS was used every 5 min	
20	Serum block 1	2.5% normal horse serum
30	Primary antibody (vonWillebrand factor (vWF))	1:900 dilution with 10% BSA
20	PBS, fresh PBS was used every 5 min	
30	Secondary antibody (anti rabbit IgG peroxidase)	
20	PBS, fresh PBS was used every 5 min	
1/2	3, 3'- Diaminobenzidine (DAB) substrate kit	5 ml aqua dest + 100 µl buffer pH 7.5 + 200 µl DAB substrate + 100 µl H ₂ O ₂
5	H ₂ O	
3	Counter stain with methyl green	under 60°C in heating plate
1	H ₂ O	
2	Ethanol 96%	
10	Isopropanol, after 5 min fresh isopropanol was used	
15	Xylol, after 5 min fresh xylol was used	
Apply Cover slip fixation with pertex as gluing agent (glass covering)		

Table 8: Protocol for double antibody immunostaining against α -actin and vWF factor. H₂O₂ hydrogen peroxide; PBS: phosphate-buffered saline; IgG: immunoglobulin G; BSA: Bovine serum albumin; DAB: 3, 3'- Diaminobenzidine; min: minute; µl: microliter; ml: milliliter; M.O.M.: mouse on mouse; vWf: vonWillebrand factor; R. T. U.: ready to use; VIP: very intense purple.

Morphometric quantification was carried out microscopically using a Qwin macro program from Leica ¹¹⁶. This program automatically recognized α -actin stained color and categorized vessel into fully muscularized (> 70% vessel circumference), partially muscularized (5%-70% vessel circumference) and non-muscularized (< 5% vessel circumference). One hundred pulmonary arteries (80 vessels for 20-70 micrometer diameter vessels, 15 vessels for 70-150 micrometer vessels and 5 vessels for more than 150 micrometer vessels) were analyzed from each lung lobe in a blinded fashion. The degree of muscularization is given as percentage of total vessel count.

4.3.3 Heart ratio

After RVSP and hematocrit measurements and after lung isolation from the chest cavity, all hearts from mice of the different groups were isolated and dissected under a dissection microscope. The right ventricle (RV) was separated from the left ventricle plus septum (LV+S). After separation, they were placed on glass slides and dried for 1 week at room temperature. The right to left ventricle plus septum weight ratio (RV/LV+S) was calculated, as an index of right ventricular hypertrophy.

4.4 Statistical analysis

All data are expressed as means \pm SEM. Comparison of multiple groups was performed by analysis of variance (ANOVA) with the Student-Newman-Keuls post test. For comparison of two groups a Student's *t*-test was performed. *P* value below 0.05 was considered as statistical significant for all analysis.

5. RESULTS

To investigate the role of DDAH1 on the effects of acute, sustained and chronic hypoxia on pulmonary vasculature, mice overexpressing the enzyme DDAH1, which is responsible for degradation of ADMA, were employed.

5.1 Acute and sustained hypoxic experiments

Lungs were exposed to normoxic ventilation (21% O₂) for 15 min, followed by a period of 10 min exposure to hypoxia (1% O₂) and then to normoxia again for 15 min. After that a 3 hour period of sustained hypoxic ventilation was applied, followed by normoxia for 15 min, and another acute hypoxic challenge (Fig. 5).

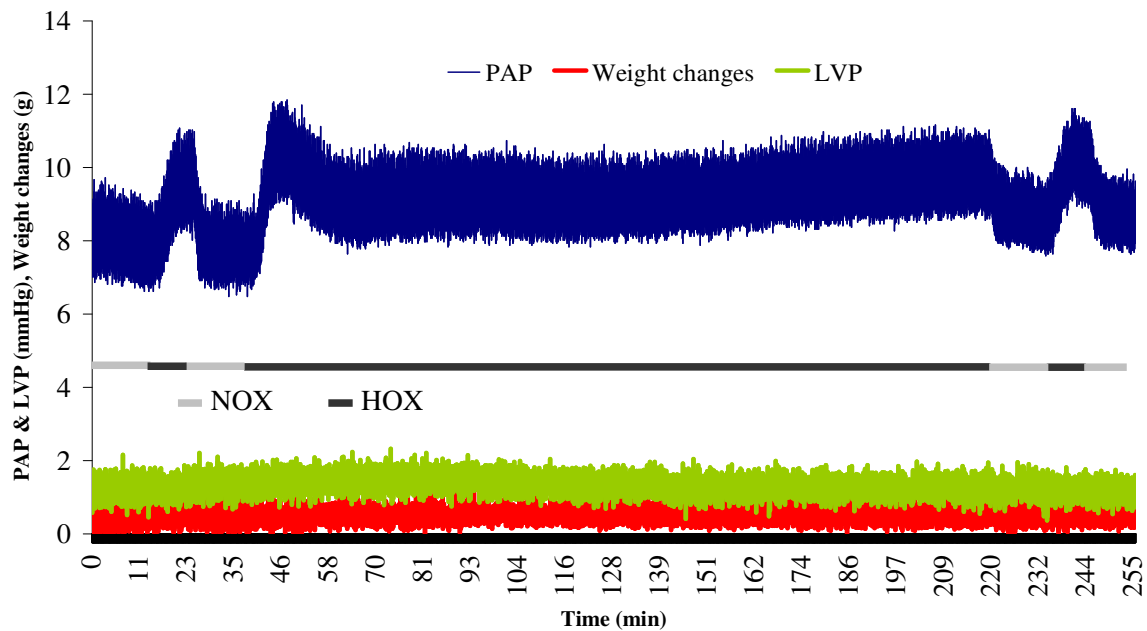


Figure 5: Representative recording of PAP, weight changes (referred to the start of the experiment after the steady state period) and LVP during acute and sustained hypoxia of isolated lungs of WT mice. PAP: pulmonary artery pressure; LVP: left ventricle pressure; NOX: normoxia; HOX: hypoxia; min: minute; g: gram.

5.1.1 PAP of isolated lungs of WT & DDAH1^{tg} mice during acute and sustained hypoxic ventilation

There were no differences in PAP during the first acute hypoxic ventilation period (lasting 10 min) between WT and DDAH1^{tg} mice. Also the kinetics of the response was the same. However, during sustained hypoxic ventilation (lasting 3 hours), there were differences in the strength of HPV between WT and DDAH1^{tg} mice. Upon starting sustained hypoxic ventilation, PAP had the tendency to be decreased in DDAH1^{tg} compared to WT mice. This decrease became statistically significant at min 125 and lasted till the end of the experiments (Fig. 6).

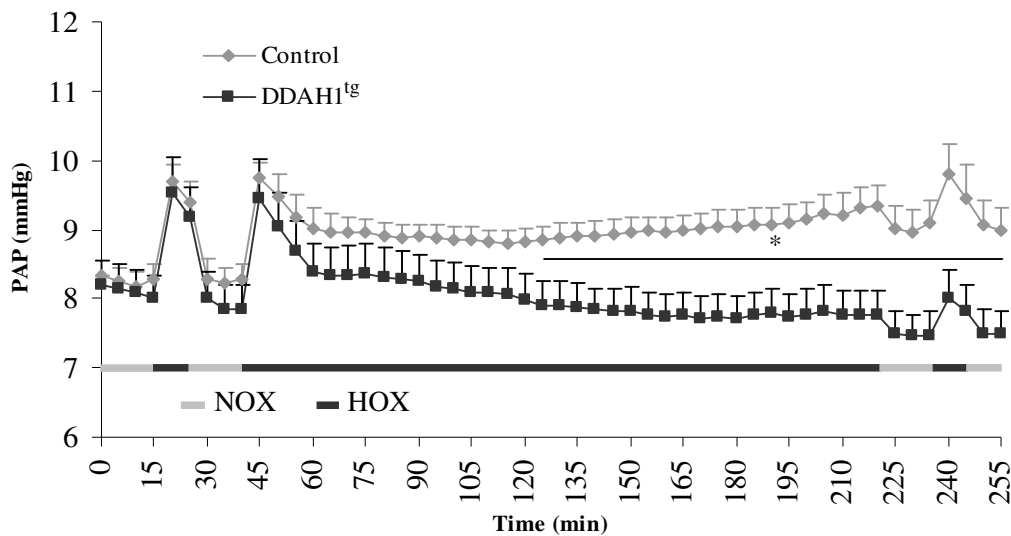


Figure 6: PAP of isolated lungs of WT and DDAH1^{tg} mice during acute and sustained hypoxic ventilation. PAP of isolated lungs of DDAH1^{tg} mice was significantly decreased at min 125 till end of the experiments. Data are expressed as mean \pm SEM (n=9 for control group, n=10 for DDAH1^{tg} group); PAP: pulmonary artery pressure; WT: wild-type; DDAH1^{tg}: dimethylarginine dimethylaminohydrolase 1 overexpressed; min: minute; NOX: normoxia; HOX: hypoxia; * P <0.05 compared to WT mice.

5.1.2 PAP of isolated lungs of WT & DDAH1^{tg} mice during normoxic ventilation

The experiments revealed no significant differences in PAP between WT and DDAH1^{tg} mice in the course of 255 min of normoxic ventilation (Fig. 7).

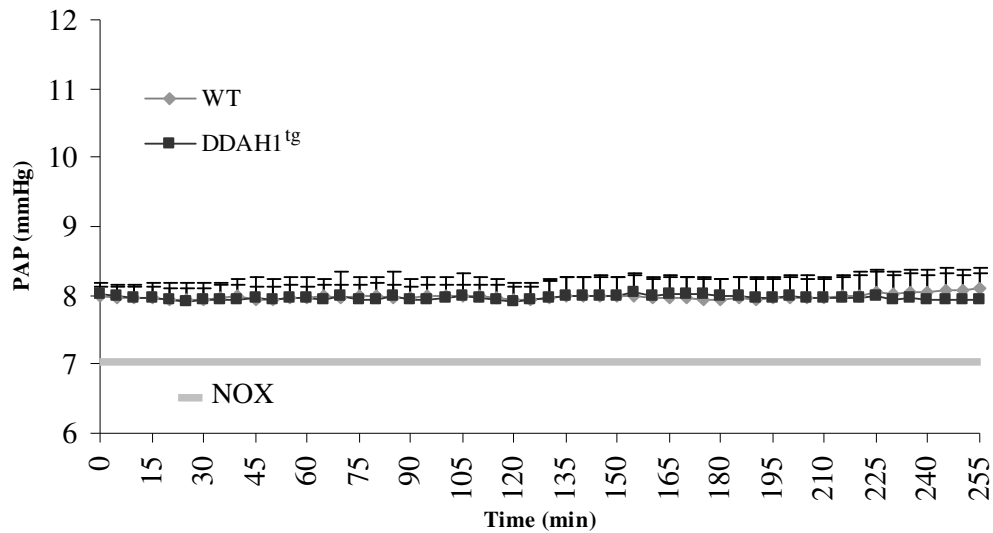


Figure 7: PAP of isolated lungs of WT and DDAH1^{tg} mice during normoxic ventilation. Data are expressed as mean \pm SEM (n=3 mice for each group); PAP: pulmonary artery pressure; WT: wild-type; DDAH1^{tg}: dimethylarginine dimethylaminohydrolase 1 overexpressed; min: minute; NOX: normoxia.

5.1.3.1 Effect of L-NNA on pulmonary vasoconstriction induced by acute & sustained HOX in WT and DDAH1^{tg} mice

Administration of L-NNA in isolated lungs of WT mice 5 min before the first acute hypoxic ventilation maneuver at a dose of 400 μ M resulted in a significant increase in PAP at the time period starting from min 55 to min 125 compared to the untreated WT mice (Fig. 8).

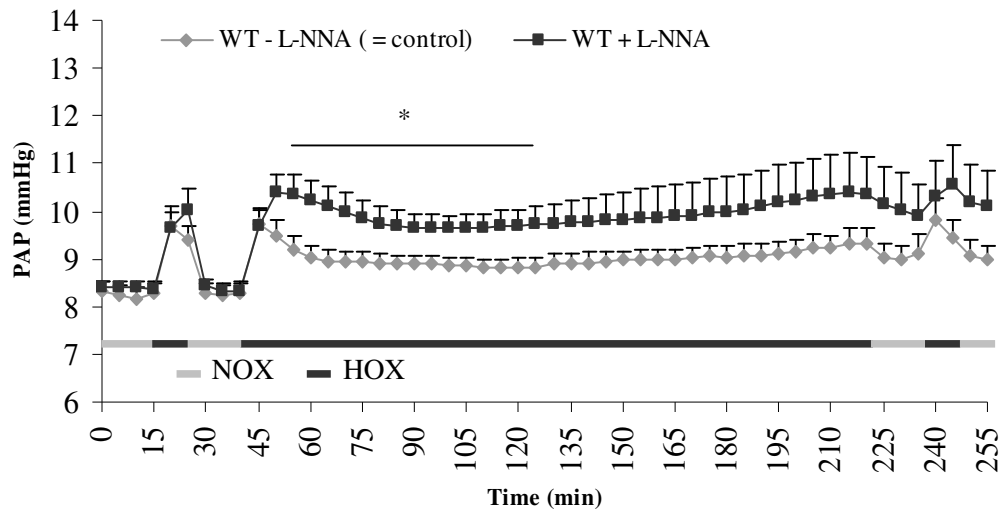


Figure 8: Effect of L-NNA on PAP of isolated lungs of WT mice. PAP was significantly increased from min 55 to min 125 in the L-NNA treated group compared to the control group. Data are expressed as mean \pm SEM (n=9 for control group, n=7 for L-NNA group); PAP: pulmonary artery pressure; L-NNA: N^o-Nitro-L-arginine; WT: wild-type; min: minute; NOX: normoxia; HOX: hypoxia; * P <0.05 compared to control group.

Administration of L-NNA in isolated lungs of DDAH1^{tg} mice 5 min before the first acute hypoxic ventilation maneuver at a dose of 400 μ M caused a significant elevation of PAP starting early after starting sustained hypoxic ventilation (min 50) till the end of experiments (Fig. 9).

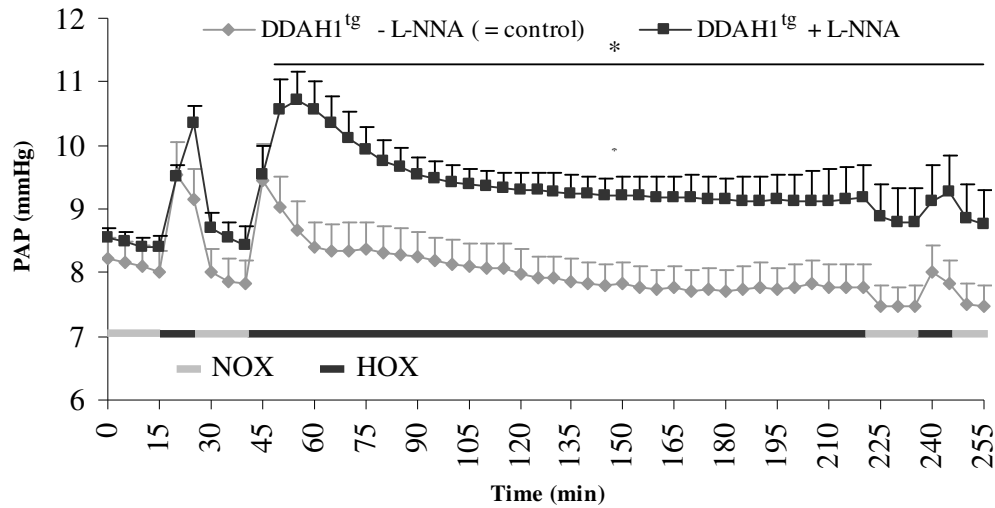


Figure 9: Effect of L-NNA on PAP of isolated lungs of DDAH1^{tg} mice. PAP was significantly increased from min 50 till the end of experiments in presence of L-NNA compared to the control group. Data are expressed as mean \pm SEM (n=10 for control group, n=7 for L-NNA treated group); PAP: pulmonary artery pressure; L-NNA: N_o-Nitro-L-arginine; DDAH1^{tg}: dimethylarginine dimethylaminohydrolase 1 overexpressed; min: minute; NOX: normoxia; HOX: hypoxia; * P <0.05 compared to control group.

When comparing directly the effect of DDAH1 overexpression on HPV in DDAH1^{tg} mice to WT mice in presence of L-NNA, it was found that PAP showed no significant differences in WT treated mice compared to DDAH1^{tg} treated mice (Fig. 10).

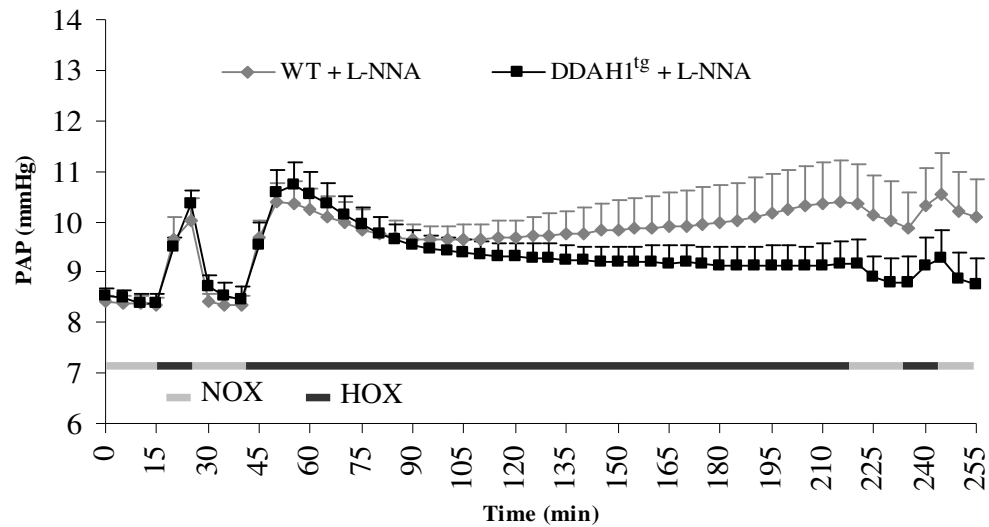
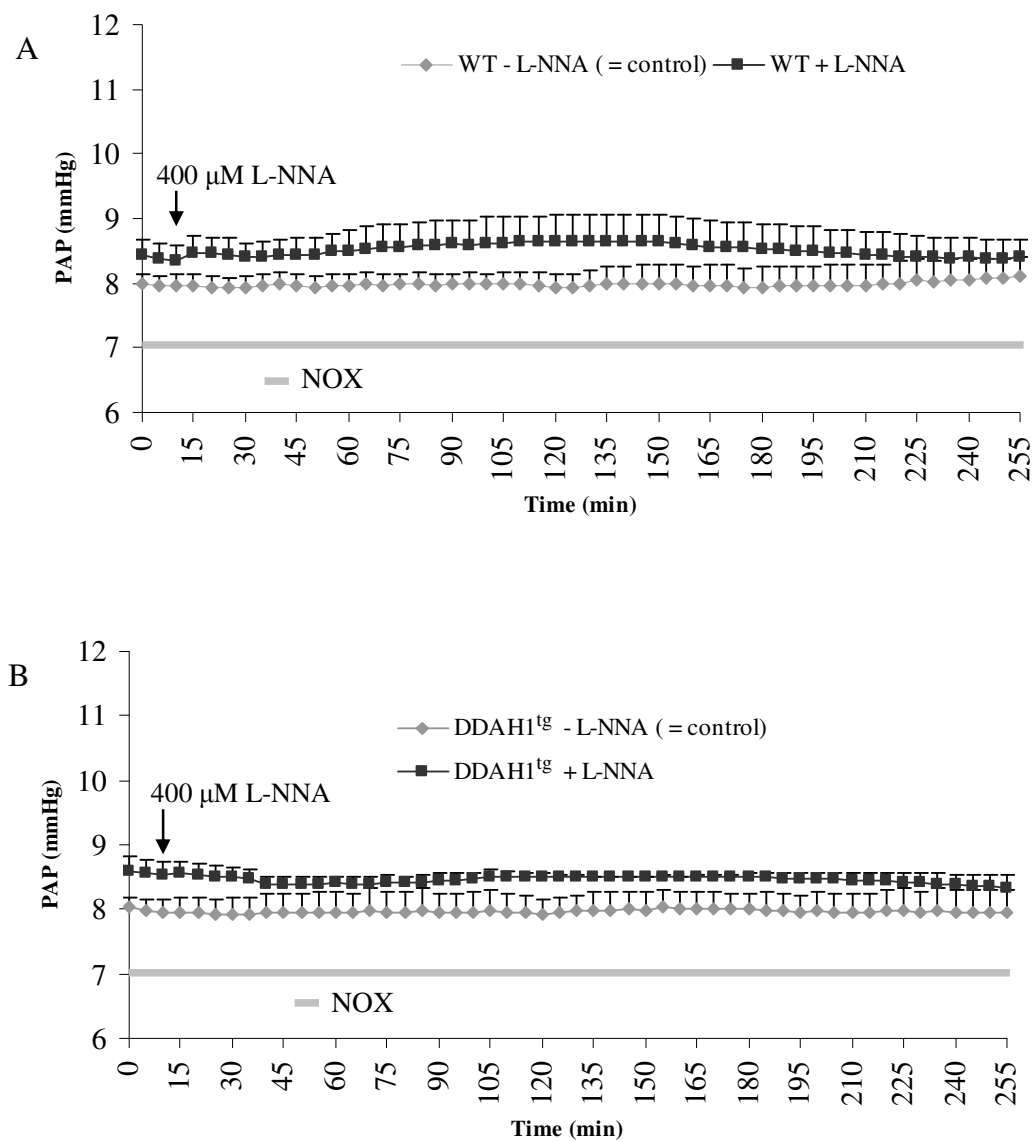


Figure 10: Effect of L-NNA on PAP of isolated lungs of DDAH1^{tg} mice compared to WT mice. Data are expressed as mean \pm SEM (n=7 for each group); PAP: pulmonary artery pressure; L-NNA: N_ω-Nitro-L-arginine; WT: wild-type; DDAH1^{tg}: dimethylarginine dimethylaminohydrolase 1 overexpressed; min: minute; NOX: normoxia; HOX: hypoxia.

5.1.3.2 Effect of L-NNA on PAP of isolated lungs of WT & DDAH1^{tg} mice during normoxic ventilation

Administration of L-NNA in isolated lungs of WT and DDAH1^{tg} mice 10 min after reaching steady state resulted in no significant difference of PAP in the course of 255 min of normoxic ventilation (Fig. 11) when comparing WT mice and WT mice + L-NNA (A), comparing DDAH1^{tg} mice and DDAH1^{tg} mice + L-NNA (B) and comparing WT mice + L-NNA and DDAH1^{tg} mice + L-NNA (C).



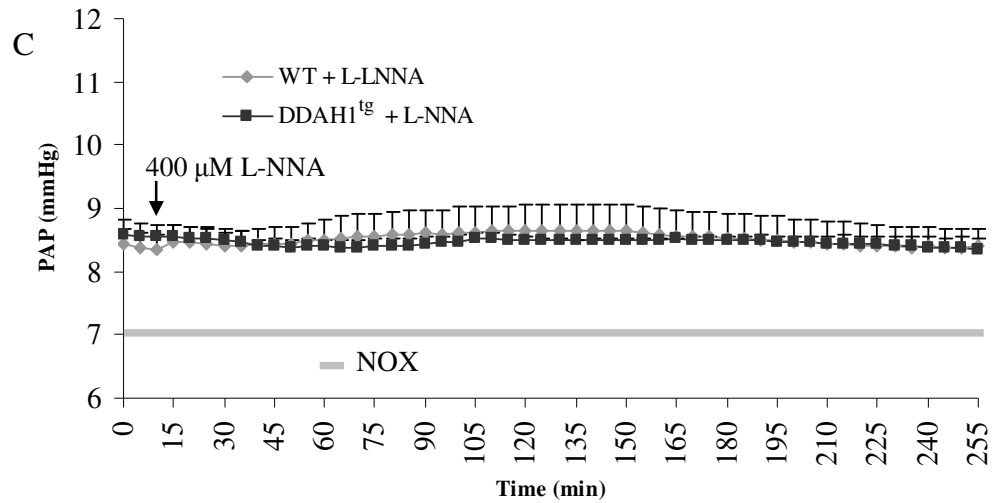


Figure 11 A, B, C: Effect of L-NNA on PAP of isolated lungs of WT & DDAH1^{tg} mice during normoxic ventilation. Data are expressed as mean \pm SEM (n=3 for each group); PAP: pulmonary artery pressure; WT: wild-type; DDAH1^{tg}: dimethylarginine dimethylaminohydrolase 1 overexpressed; L-NNA: N_ω-Nitro-L-arginine; min: minute; NOX: normoxia; μ M: micromolar.

5.1.4.1 Effect of ODQ on pulmonary vasoconstriction induced by acute & sustained HOX in WT and DDAH1^{tg} mice

Administration of ODQ in isolated lungs of WT mice 5 min before the first acute hypoxic ventilation at a dose of 10 μ M caused a significant increase in PAP in the time period from min 165 to min 220 compared to the untreated WT mice (Fig. 12).

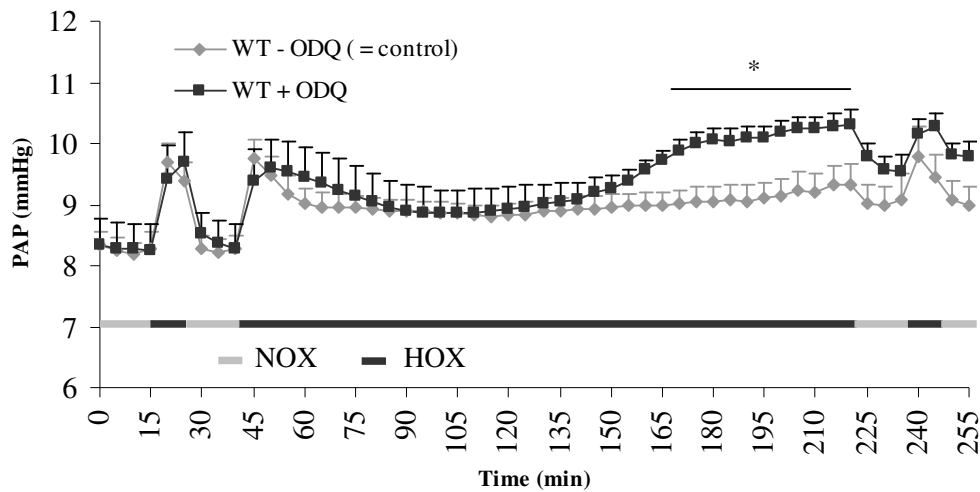


Figure 12: Effect of ODQ on PAP of isolated lungs of WT mice. PAP was significantly increased from min 165 to min 220 in the ODQ treated group compared to the control group. Data are expressed as mean \pm SEM (n=9 for control group, n=6 for ODQ group); PAP: pulmonary artery pressure; WT: wild-type; ODQ: 1H-[1, 2, 4]oxadiazolo[4, 3-a]quinoxalin-1-one; min: minute; NOX: normoxia; HOX: hypoxia; * P <0.05 compared to control group.

Administration of ODQ in isolated lungs of DDAH1^{tg} mice 5 min before the first acute hypoxic ventilation at a dose of 10 μ M caused a significant increase in PAP at the time period starting from min 55 till the end of experiments compared to the untreated control DDAH1^{tg} mice (Fig. 13).

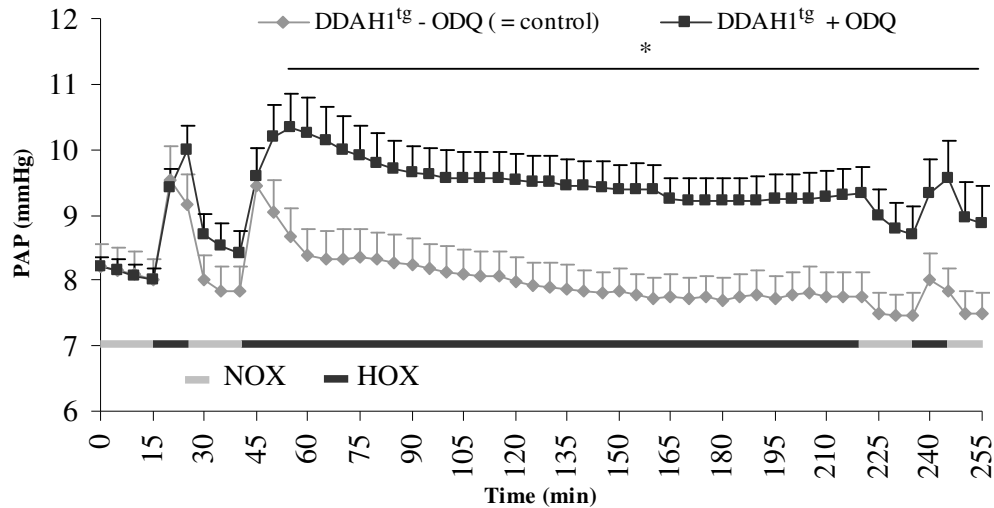


Figure 13: Effect of ODQ on PAP of isolated lungs of DDAH1^{tg} mice. PAP was significantly increased from min 55 till the end of experiments in presence of ODQ compared to the control group. Data are expressed as mean \pm SEM (n=10 for control group, n=5 for ODQ group); PAP: pulmonary artery pressure; DDAH1^{tg}: dimethylarginine dimethylaminohydrolase 1 overexpressed; ODQ: 1H-[1, 2, 4]oxadiazolo[4, 3-a]quinoxalin-1-one; min: minute; NOX: normoxia; HOX: hypoxia; * P <0.05 compared to control group.

When comparing directly the effect of DDAH1 overexpression on HPV in DDAH1^{tg} mice to WT mice in presence of ODQ, it was found that PAP was significantly decreased in the time period from min 200 to min 220 in DDAH1^{tg} treated mice compared to WT treated mice (Fig. 14).

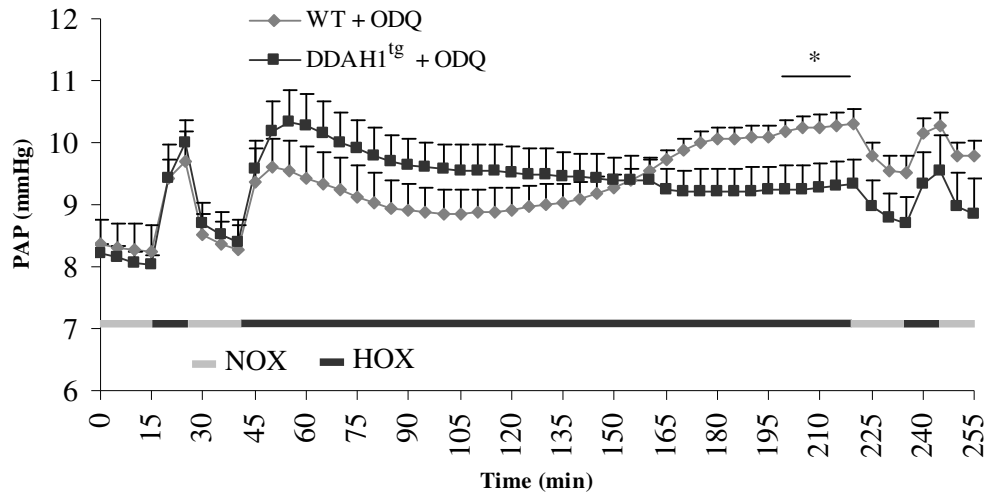
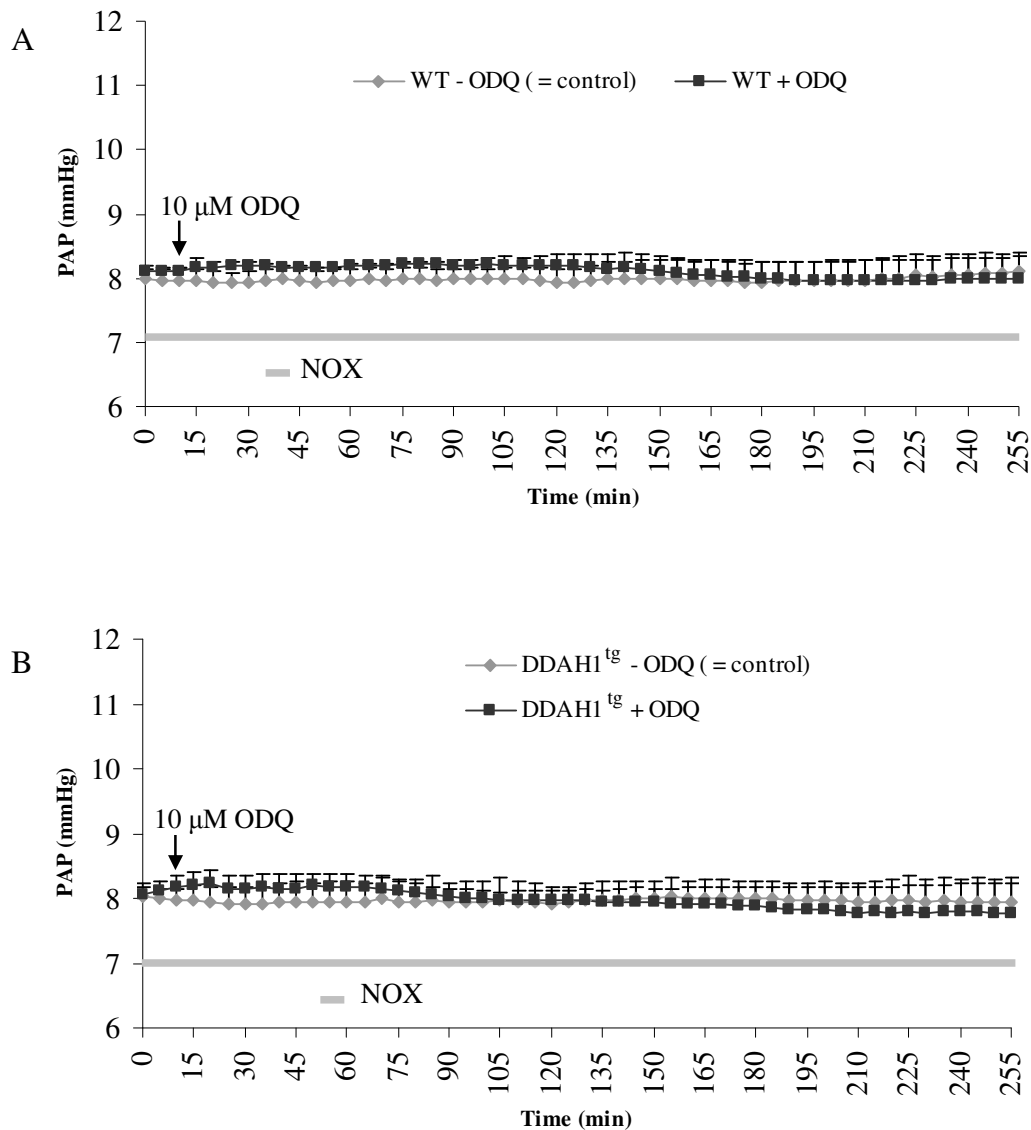


Figure 14: Effect of ODQ on PAP of isolated lungs of DDAH1^{tg} mice compared to WT mice. PAP was significantly decreased in the time period from min 200 to min 220 in DDAH1^{tg} treated mice compared to WT treated mice. Data are expressed as mean \pm SEM (n=6 for WT + ODQ group, n=5 for DDAH1^{tg} + ODQ group); PAP: pulmonary artery pressure; WT: wild-type; DDAH1^{tg}: dimethylarginine dimethylaminohydrolase 1 overexpressed; ODQ: 1H-[1, 2, 4]oxadiazolo[4, 3-a]quinoxalin-1-one; min: minute NOX: normoxia; HOX: hypoxia; * P <0.05 compared to WT treated mice.

5.1.4.2 Effect of ODQ on PAP of isolated lungs of WT & DDAH1^{tg} mice during normoxic ventilation

Administration of ODQ in isolated lungs of WT and DDAH1^{tg} mice 10 min after reaching steady state resulted in no significant difference in PAP in the course of 255 min of normoxic ventilation (Fig. 15) when comparing WT mice and WT mice + ODQ (A), comparing DDAH1^{tg} mice and DDAH1^{tg} mice + ODQ (B) and comparing WT mice + ODQ and DDAH1^{tg} mice + ODQ (C).



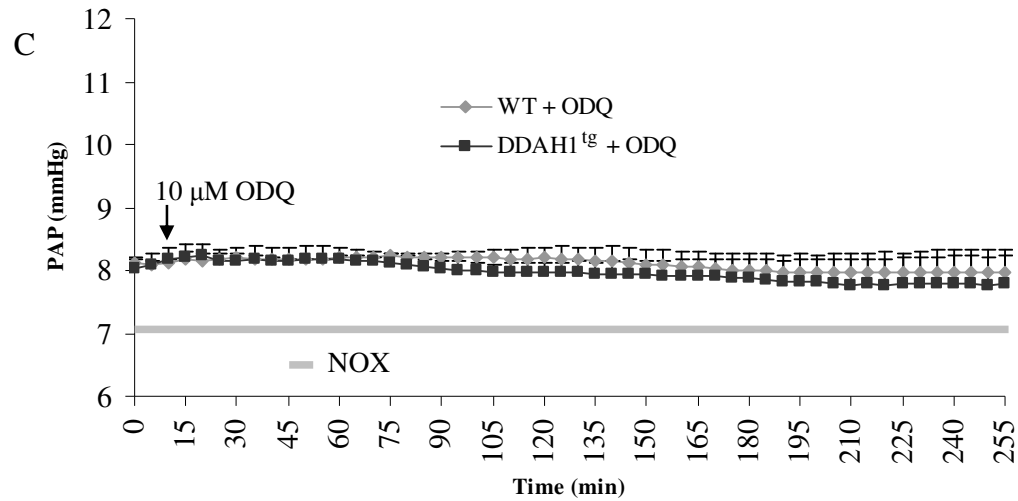


Figure 15 A, B, C: Effect of ODQ on PAP of isolated lungs of WT & DDAH1^{tg} mice during normoxic ventilation. Data are expressed as mean \pm SEM (n=3 for each group); PAP: pulmonary artery pressure; WT: wild-type; DDAH1^{tg}: dimethylarginine dimethylaminohydrolase 1 overexpressed; ODQ: 1H-[1, 2, 4]oxadiazolo[4, 3-a]quinoxalin-1-one; min: minute; NOX: normoxia; μ M: micromolar.

5.1.5 Weight of mice used in acute and sustained hypoxic & normoxic experiments

There were no significant differences between the weights of mice that were used in the isolated lung experiments. Therefore PAP variation in the experiments can not be based on weight changes (Fig. 16).

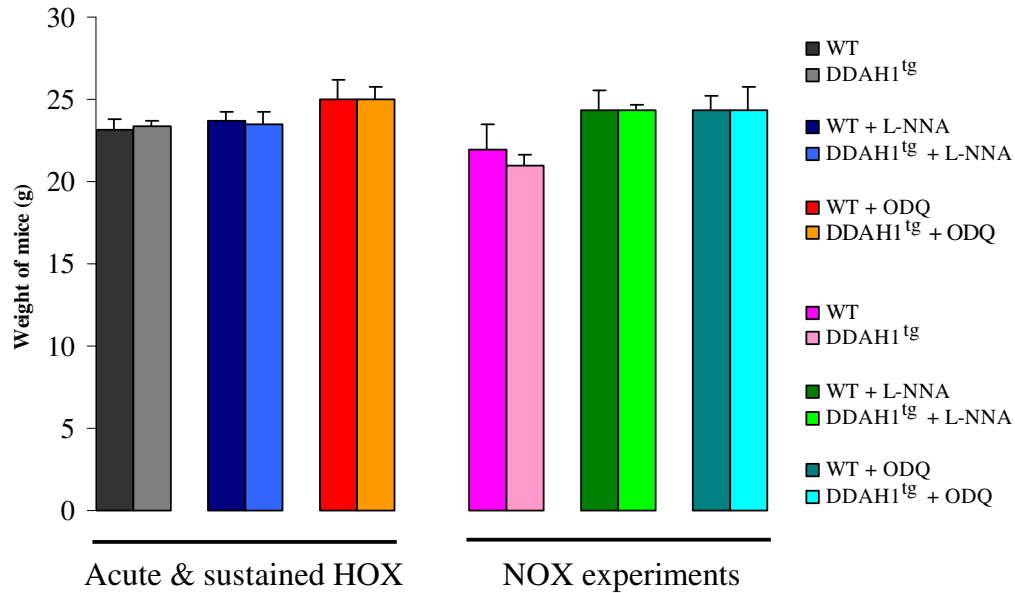
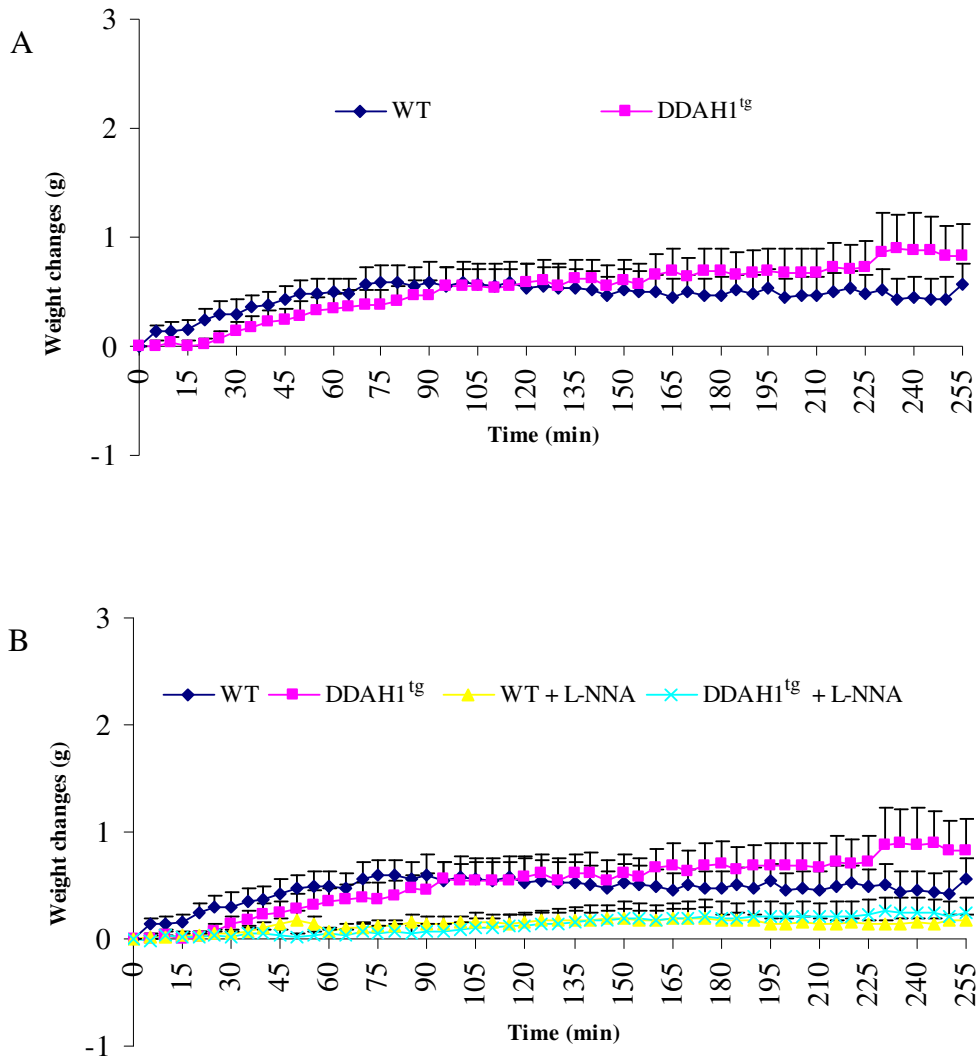
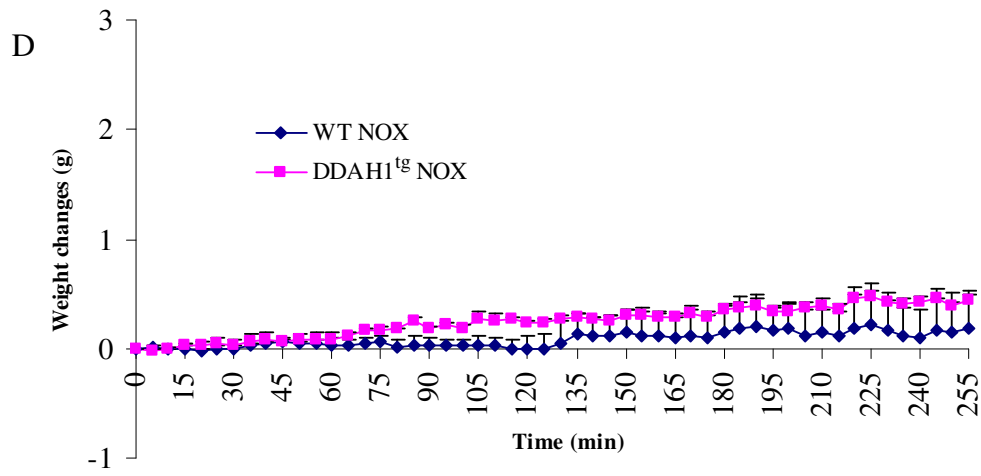
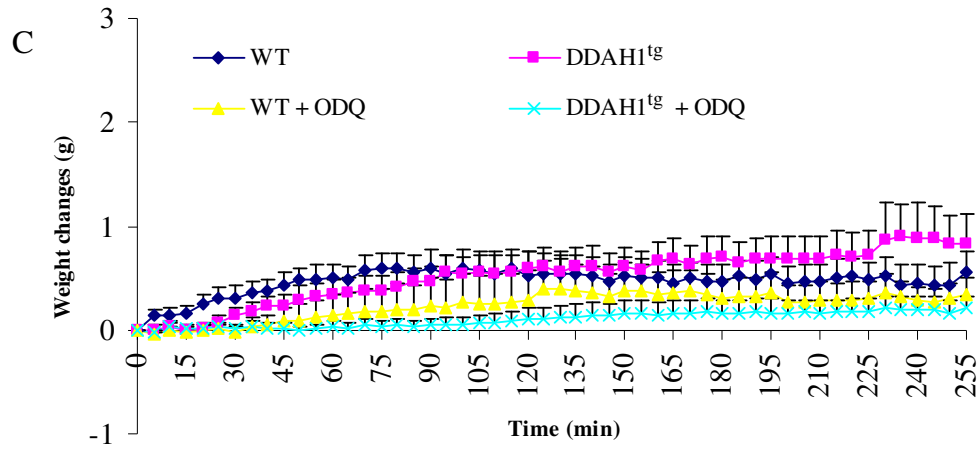


Figure 16: Weight of mice used in acute and sustained hypoxic experiments, as well as normoxic experiments. Data are expressed as mean \pm SEM (n=9 for WT HOX group, n=10 for DDAH1^{tg} HOX group, n=6 for WT + ODQ group, n=5 for DDAH1^{tg} + ODQ group, n= 7 for WT + L-NNA group, n=7 for DDAH1^{tg} + L-NNA group, n=3 for each NOX group); WT: wild-type; DDAH1^{tg}: dimethylarginine dimethylaminohydrolase 1 overexpressed; ODQ: 1H-[1, 2, 4]oxadiazolo[4, 3-a]quinoxalin-1-one; L-NNA: N_ω-Nitro-L-arginine; NOX: normoxia; HOX: hypoxia; g: gram.

5.1.6 Weight changes of isolated mouse lungs

There was no difference in the weight changes (referred to the start of the experiment after the steady state period) of isolated lungs during the time course of the experiments (Fig. 17), when comparing WT mice, DDAH1^{tg} mice during acute and sustained hypoxic experiments (A), comparing WT mice, WT mice + L-NNA, DDAH1^{tg} mice and DDAH1^{tg} mice + L-NNA during hypoxia (B), comparing WT mice, WT mice + ODQ, DDAH1^{tg} mice and DDAH1^{tg} mice + ODQ during hypoxia (C) comparing WT mice and DDAH1^{tg} mice during normoxia (D), comparing WT mice, WT mice + L-NNA, DDAH1^{tg} mice and DDAH1^{tg} mice + L-NNA during normoxia (E) and comparing WT mice, WT mice + ODQ, DDAH1^{tg} mice and DDAH1^{tg} mice + ODQ during normoxic experiments (F).





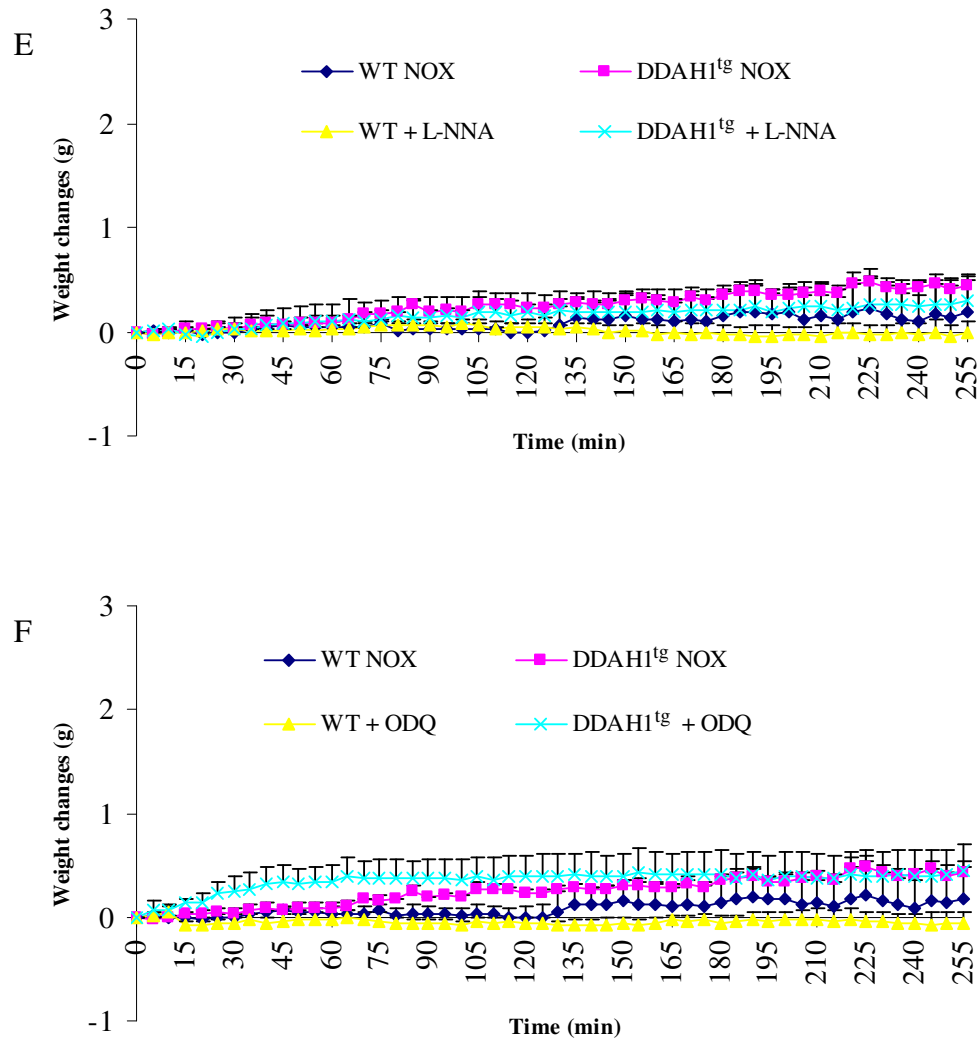


Figure 17 A, B, C, D, E, F: Weight changes of isolated mouse lungs. Data are expressed as mean \pm SEM (n=9 for WT HOX group, n=10 for DDAH1^{tg} HOX group, n=6 for WT + ODQ group, n=5 for DDAH1^{tg} + ODQ group, n=7 for WT + L-NNA group, n=7 for DDAH1^{tg} + L-NNA group, n=3 for each NOX group); WT: wild-type; DDAH1^{tg}: dimethylarginine dimethylaminohydrolase 1 overexpressed; ODQ: 1H-[1, 2, 4]oxadiazolo[4, 3-a]quinoxalin-1-one; L-NNA: N_ω-Nitro-L-arginine; min: minute; NOX: normoxia; HOX: hypoxia; g: gram.

5.1.7 NO release into the perfusate of isolated lungs of WT and DDAH1^{tg} mice

There were no significant differences in NO metabolite levels between WT and DDAH1^{tg} mice at min 10, 20, 35, and 45. However, at min 220 the level of NO metabolites was significantly increased in DDAH1^{tg} mice compared to WT mice (Fig. 18). There were also no significant differences in the NO metabolite levels during the time course of the experiment in WT mice, however, in DDAH1^{tg} mice NO metabolite levels were increased at 220 min HOX compared to the other time points.

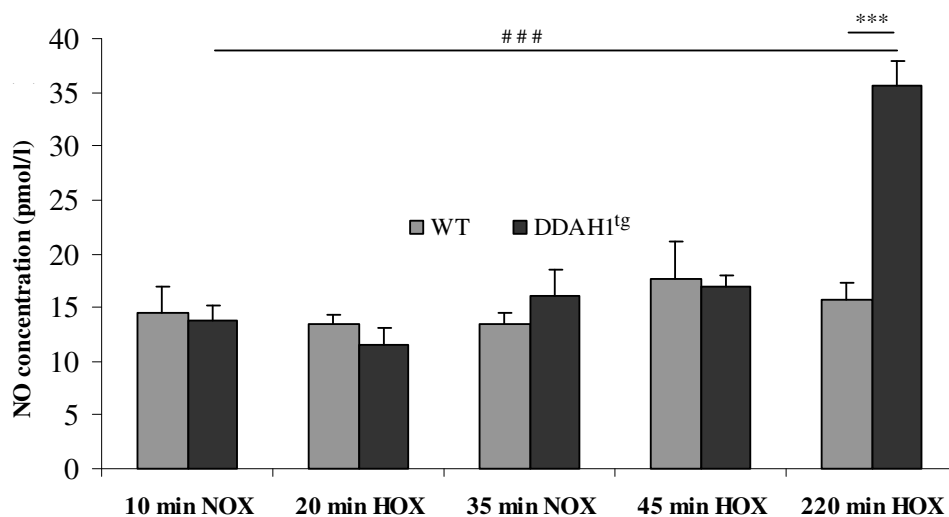


Figure 18: NO concentrations in the perfusate of isolated lung experiments of WT and DDAH1^{tg} mice. NO levels were significantly increased in DDAH1^{tg} mice at min 220 compared to WT mice. Furthermore, in DDAH1^{tg} mice NO levels were significantly increased at 220 min HOX compared to the other time points. Data are expressed as mean \pm SEM (n=4 mice for WT group, n=8 for DDAH1^{tg} group); WT: wild-type; DDAH1^{tg}: dimethylarginine dimethylaminohydrolase 1 overexpressed; HOX: hypoxia; NOX: normoxia; min: minute; *** P <0.001 compared to WT mice, ### P <0.001 compared to DDAH1^{tg} mice at the other time points.

5.1.8 cGMP concentrations in the perfusate of isolated lungs of WT and DDAH1^{tg} mice

As found in measurements of NO metabolites, cGMP levels in the perfusate of isolated lung were significantly increased at min 220 in DDAH1^{tg} compared to WT mouse lungs, but no significant differences at the other time points between both mice types could be detected (Fig. 19). Also cGMP levels were not significantly changed in the time course of the experiment in WT mice, but DDAH1^{tg} mice showed a significant increase at 220 min HOX compared to the other time points.

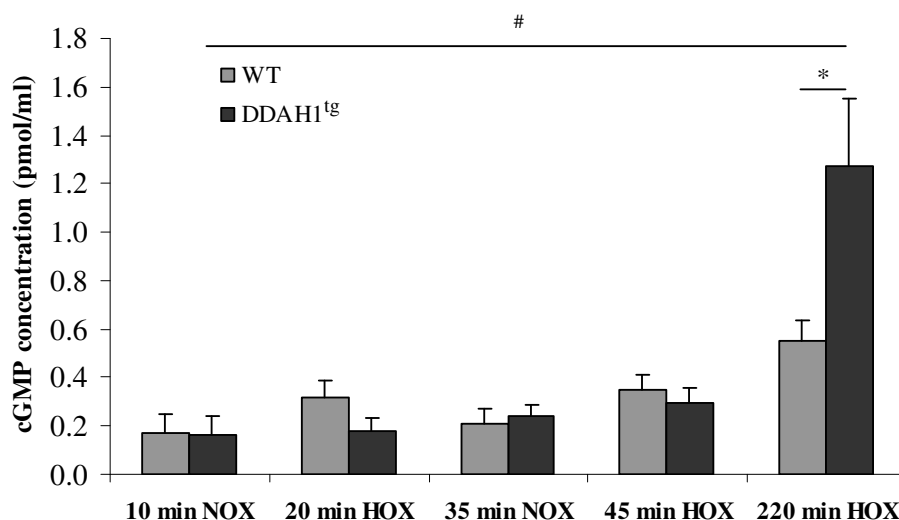


Figure 19: cGMP concentrations in the perfusate of isolated lung experiments of WT and DDAH1^{tg} mice. cGMP levels in the perfusate were significantly increased at min 220 in DDAH1^{tg} compared to WT mouse lungs. In addition, DDAH1^{tg} mice showed a significant increase at 220 min HOX compared to the other time points. Data are expressed as mean \pm SEM (n=5 mice for each group); WT: wild-type; DDAH1^{tg}: dimethylarginine dimethylaminohydrolase 1 overexpressed; HOX: hypoxia; NOX: normoxia; min: minute; * P <0.05 compared to WT mice, # P <0.05 compared to DDAH1^{tg} mice at the other time points.

5.1.9 ADMA concentrations in the perfusate of isolated lungs of WT and DDAH1^{tg} mice

ADMA levels in lung perfusate of DDAH1^{tg} mice were significantly decreased at min 20, 45, and 220 compared to WT mice (Fig. 20). Additionally there was a significant increase in ADMA levels at 220 min HOX in WT and DDAH1^{tg} mice compared to the other time points.

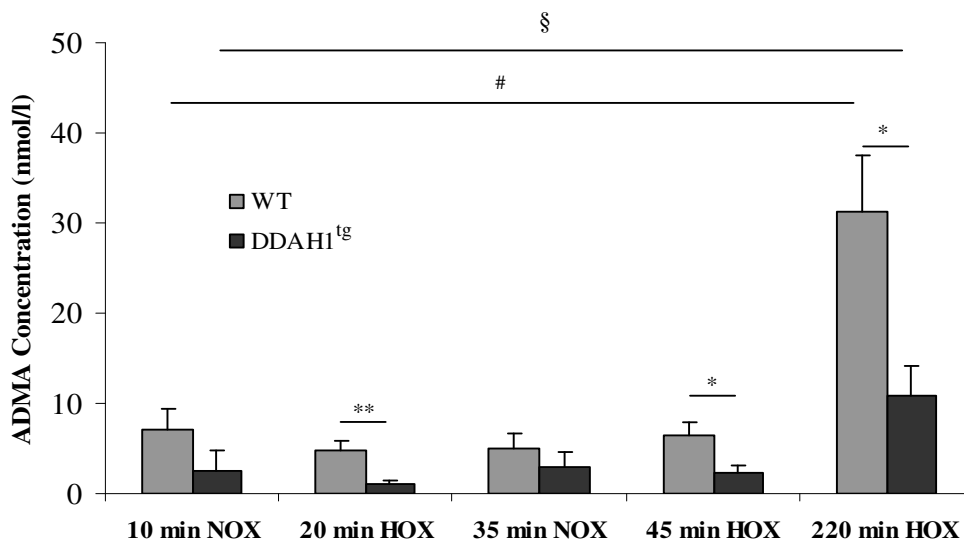


Figure 20: ADMA concentrations in the perfusate of isolated lung experiments of WT and DDAH1^{tg} mice. There was a significant decrease in ADMA levels in lung perfusate of DDAH1^{tg} at min 20, 45, and 220 compared to WT mice. Furthermore, there was a significant increase in ADMA levels at 220 min HOX in WT and DDAH1^{tg} mice compared to the other time points. Data are expressed as mean \pm SEM (n=8 mice for each group); WT: wild-type; DDAH1^{tg}: dimethylarginine dimethylaminohydrolase 1 overexpressed; HOX: hypoxia; NOX: normoxia; min: minute; * P <0.05, ** P <0.005 compared to WT mice, § P <0.05 compared to DDAH1^{tg} mice at the other time points, # P <0.05 compared to WT mice at the other time points.

5.2 Chronic hypoxic experiments

In the following experiments WT and DDAH1^{tg} mice were exposed to 3 weeks of hypoxia. For quantification of PH, RVSP, hematocrit and heart hypertrophy were determined. Furthermore, morphometrical changes of the pulmonary arterial vessels were investigated.

5.2.1 RVSP in WT and DDAH1^{tg} mice

There was a significant elevation in WT and DDAH1^{tg} mice exposed to 3 weeks hypoxia compared to their respective normoxic control groups with regard to RVSP (Fig. 21). RVSP showed no significant difference on exposure to chronic hypoxia in DDAH1^{tg} compared to WT mice, there was no significant difference between both normoxic groups as well.

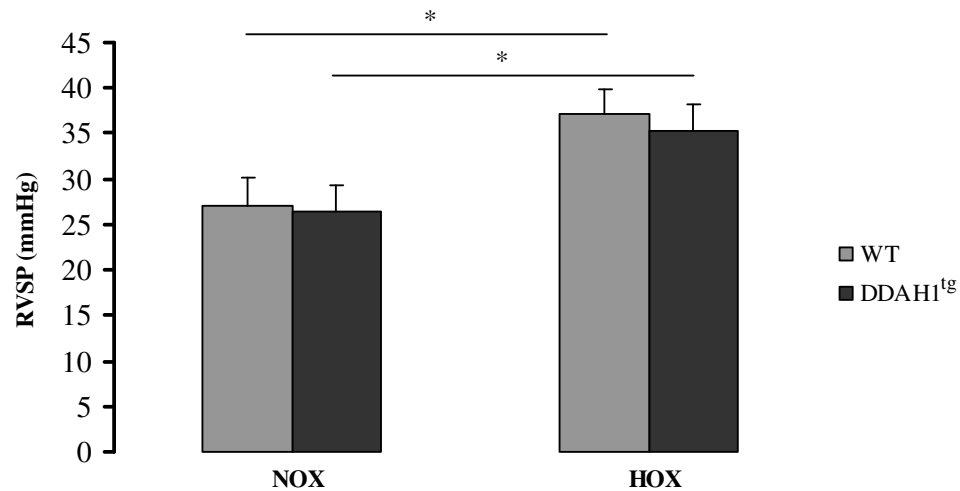


Figure 21: RVSP in WT and DDAH1^{tg} mice. RVSP was significantly increased in hypoxic groups compared to their respective normoxic controls. Data are expressed as mean \pm SEM (n=10 for each group); RVSP: right ventricular systolic pressure; WT: wild-type; DDAH1^{tg}: dimethylarginine dimethylaminohydrolase 1 overexpressed; HOX: hypoxia; NOX: normoxia; * P <0.05 compared to respective normoxic control group.

5.2.2 Hematocrit values (%) in WT and DDAH1^{tg} mice

Hematocrit was significantly increased in hypoxic groups compared to their respective normoxic control in WT and DDAH1^{tg} mice. Hematocrit showed no significant difference on exposure to chronic hypoxia in DDAH1^{tg} compared to WT mice, and there was no significant difference between both normoxic groups (Fig. 22).

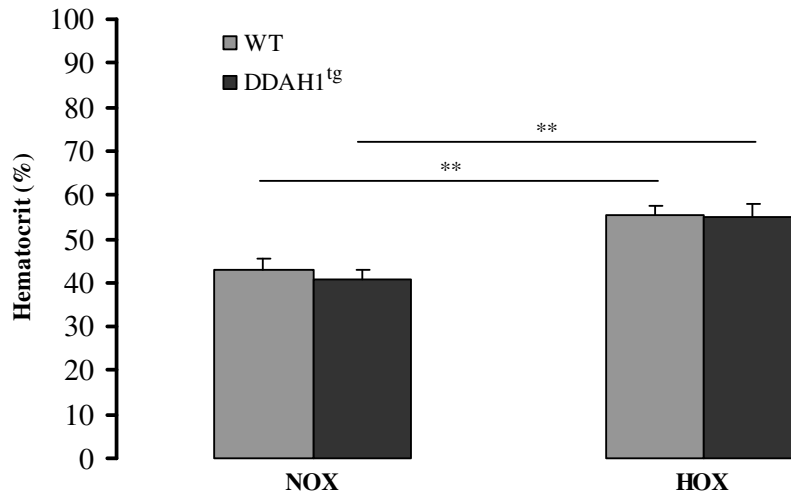


Figure 22: Hematocrit values in WT and DDAH1^{tg} mice. Hematocrit value (%) was significantly increased in the hypoxic groups compared to their respective normoxic controls in WT and DDAH1^{tg} mice. Data are expressed as mean \pm SEM (n=10 for each group); WT: wild-type; DDAH1^{tg}: dimethylarginine dimethylaminohydrolase 1 overexpressed; HOX: hypoxia; NOX: normoxia; ** P <0.005 compared to respective normoxic control group.

5.2.3 Right heart hypertrophy

Hypertrophy of the right ventricle of the heart was quantified as the ratio of the RV/(LV+S). This ratio was significantly increased after hypoxic exposure in WT and DDAH1^{tg} mice compared to their respective normoxically ventilated controls. RV/(LV+S) showed no significant difference on exposure to chronic hypoxia in DDAH1^{tg} compared to WT mice, furthermore, there was no significant difference between both normoxic groups (Fig. 23).

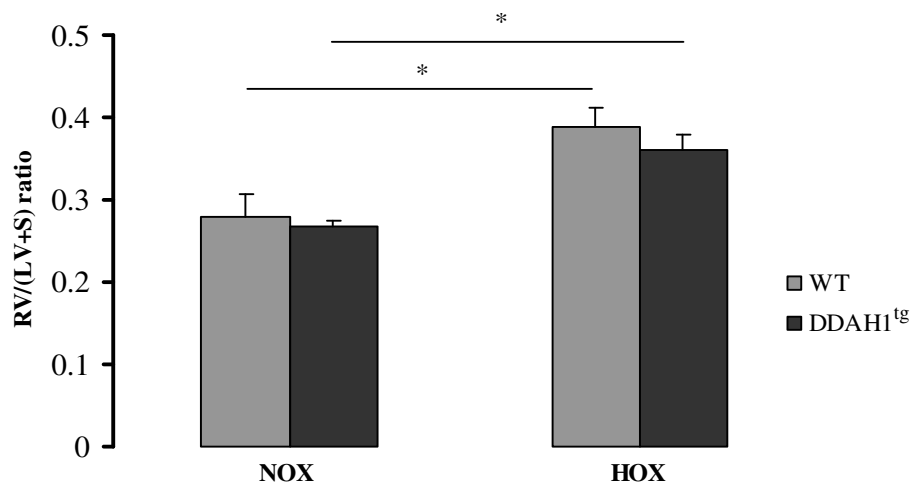


Figure 23: Values of RV/(LV+S) ratio in WT and DDAH1^{tg} mice. The ratio of RV/(LV+S) was significantly increased in hypoxic groups compared to their respective normoxic controls. Data are expressed as mean \pm SEM (n=10 for each group); WT: wild-type; DDAH1^{tg}: dimethylarginine dimethylaminohydrolase 1 overexpressed; RV: right ventricle; LV: left ventricle; S: septum; HOX: hypoxia; NOX: normoxia; * P <0.05 compared to respective normoxic control group.

5.2.4 Weight of mice used in chronic hypoxic experiments

As shown in Fig. 24, weight of mice was significantly decreased in the hypoxic groups compared to their respective normoxic controls in WT and DDAH1^{tg} mice.

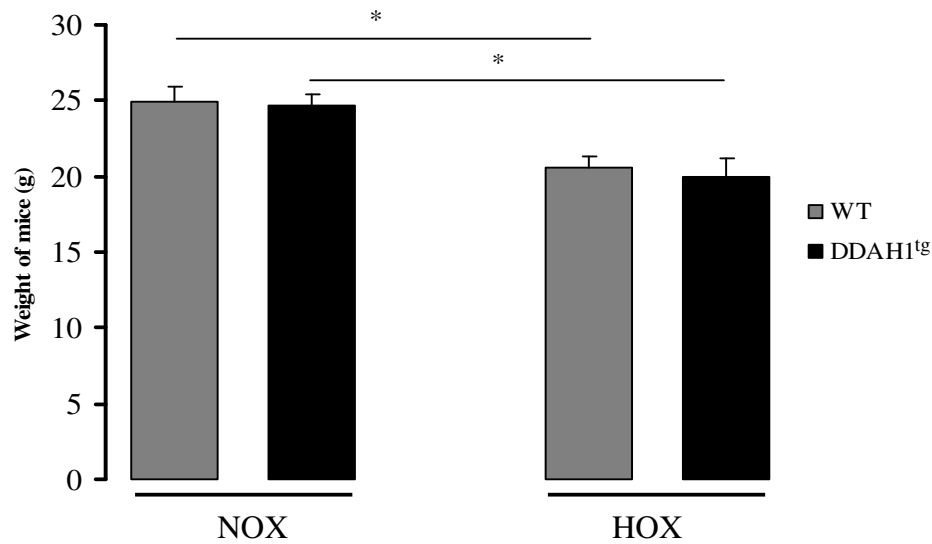


Figure 24: Weight of mice used in chronic hypoxic experiments. Weight of mice was significantly decreased in the hypoxic groups compared to their respective normoxic controls in WT and DDAH1^{tg} mice. Data are expressed as mean \pm SEM (n=10 for each group); WT: wild-type; DDAH1^{tg}: dimethylarginine dimethylaminohydrolase 1 overexpressed; NOX: normoxia; HOX: hypoxia; g: gram; * P <0.05 compared to respective normoxic control group.

5.2.5 Degree of muscularization

Exposure to 3 weeks hypoxia caused alterations in the muscularization of pulmonary arteries of different size in the different mouse strains:

- In small-sized (diameter 20-70 μm) pulmonary arteries, the portion of fully muscularized arteries in WT and DDAH1^{tg} mice exposed to hypoxia was significantly increased compared to their respective normoxic groups. In parallel, the portion of non-muscularized pulmonary arteries in WT and DDAH1^{tg} mice exposed to hypoxia was significantly decreased compared to their respective normoxic groups (Fig. 25).

- In medium-sized (diameter 70-150 μm) pulmonary arteries, the portion of fully muscularized arteries in WT and DDAH1^{tg} mice exposed to hypoxia was significantly increased when compared to their respective normoxic groups. In parallel, the portion of partially and non-muscularized pulmonary arteries was significantly decreased in WT and DDAH1^{tg} mice exposed to hypoxia compared to their respective normoxic groups (Fig. 26).

- In large-sized (diameter >150 μm) pulmonary arteries, the portion of fully muscularized arteries in WT and DDAH1^{tg} exposed to hypoxia was significantly increased compared to their respective normoxic groups. In parallel, the portion of non-muscularized pulmonary arteries had the tendency to be decreased in WT and DDAH1^{tg} mice exposed to hypoxia compared to their respective NOX groups (Fig. 27).

- In all pulmonary arteries, it was found that the portion of fully muscularized arteries in WT and DDAH1^{tg} mice exposed to hypoxia was still significantly increased compared to their respective normoxic groups. Also, the portion of non-muscularized pulmonary arteries was still significantly decreased in WT and DDAH1^{tg} mice exposed to hypoxia compared to their respective NOX groups. Furthermore, the portion of partially muscularized arteries in WT mice exposed to hypoxia was significantly decreased when compared to its normoxic group (Fig. 28).

- The degree of muscularization of pulmonary arteries was determined in histological sections stained with an antibody against α -smooth muscle actin. Representative samples of sections of the different groups are given in Fig. 29. There was no muscularization in small arteries (diameter 20-70 μm) during normoxia in both WT mice (A) and DDAH1^{tg} mice (B). However, after exposure to 3 weeks of hypoxia, pulmonary arteries became muscularized in DDAH1^{tg} mice (D) and WT mice (C).

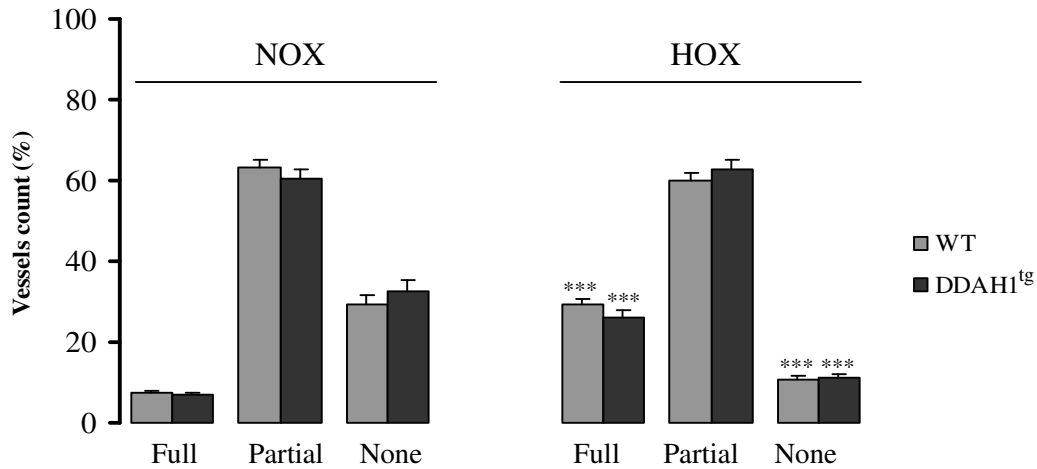


Figure 25: Degree of muscularization of pulmonary arterial vessels (diameter 20-70 μm). Data are expressed as mean \pm SEM (n=10 for each group); WT: wild-type; DDAH1^{tg}: dimethylarginine dimethylaminohydrolase 1 overexpressed; HOX: hypoxia; NOX: normoxia; *** $P < 0.001$ compared to the respective normoxic control group.

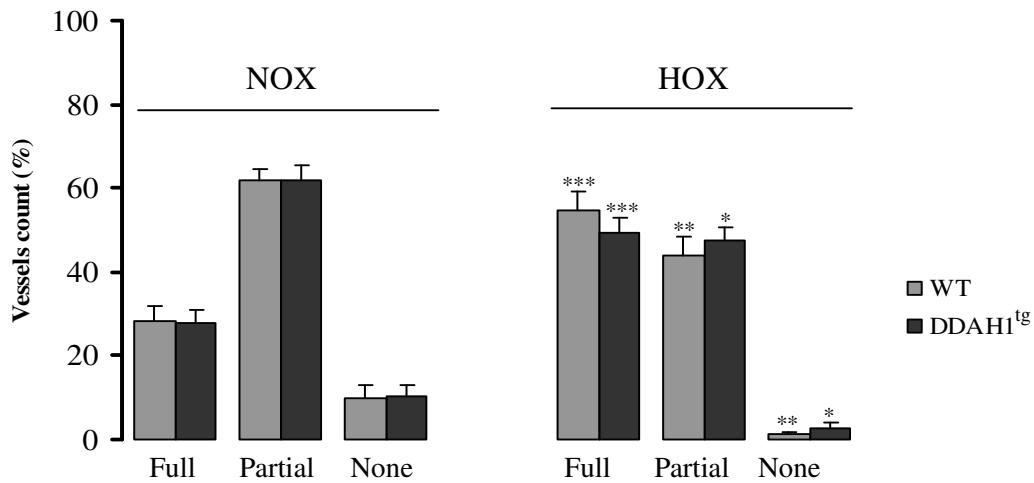


Figure 26: Degree of muscularization of pulmonary arterial vessels (diameter 70-150 μm). Data are expressed as mean \pm SEM (n=10 for each group); WT: wild-type; DDAH1^{tg}: dimethylarginine dimethylaminohydrolase 1 overexpressed; HOX: hypoxia; NOX: normoxia; * $P < 0.05$, ** $P < 0.005$, *** $P < 0.001$ compared to the respective normoxic control group.

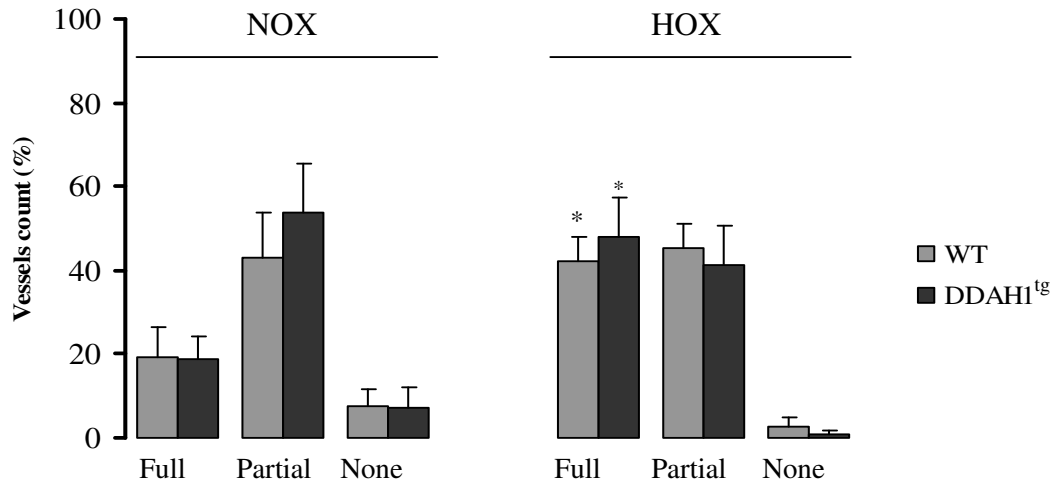


Figure 27: Degree of muscularization of pulmonary arterial vessels (diameter >150 μm). Data are expressed as mean ± SEM (n=10 for each group); WT: wild-type; DDAH1^{tg}: dimethylarginine dimethylaminohydrolase 1 overexpressed; HOX: hypoxia; NOX: normoxia; * $P < 0.05$ compared to respective normoxic control group.

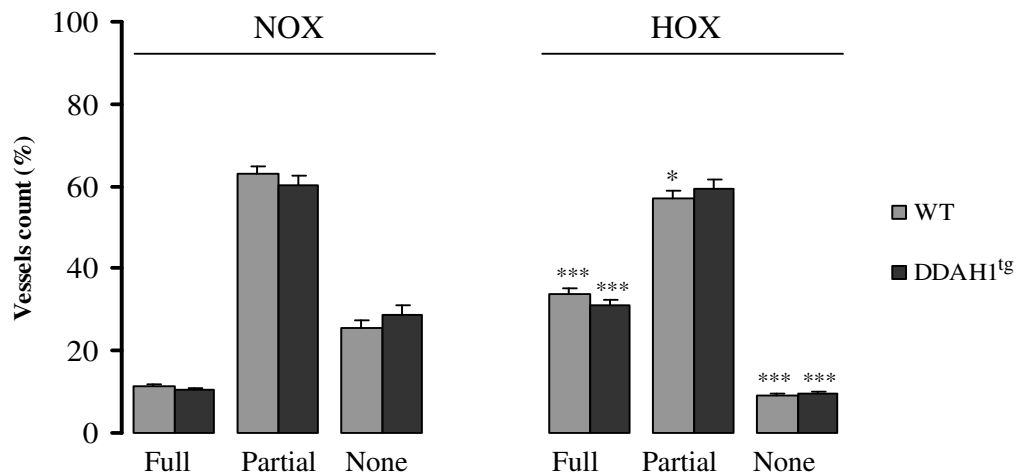


Figure 28: Degree of muscularization of total pulmonary arterial vessels. Data are expressed as mean ± SEM (n=10 for each group); WT: wild-type; DDAH1^{tg}: dimethylarginine dimethylaminohydrolase 1 overexpressed; HOX: hypoxia; NOX: normoxia; * $P < 0.05$, *** $P < 0.001$ compared to respective normoxic control group.

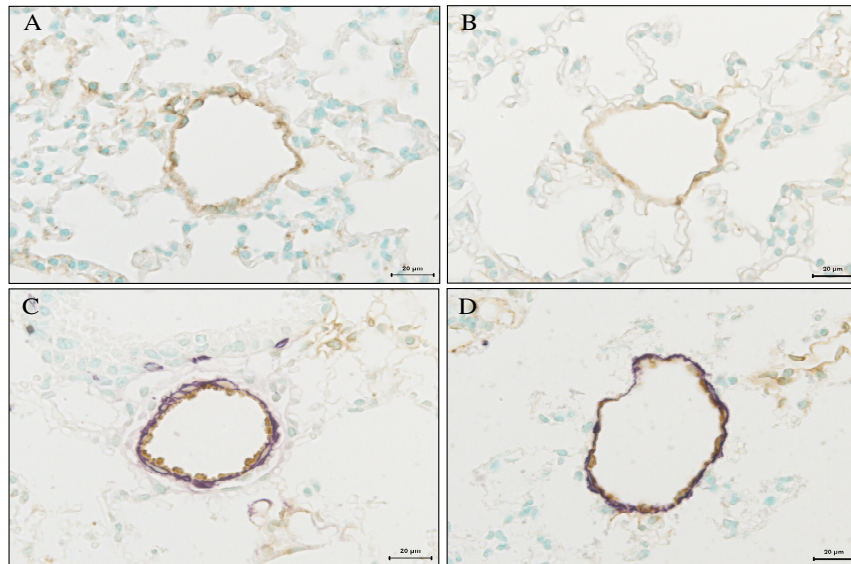


Figure 29: Morphometrical analysis in WT and DDAH1^{tg} mice. The pictures show the degree of muscularization of pulmonary arteries from WT (A) and DDAH1^{tg} mice (B) exposed to normoxia and from WT (C) and DDAH1^{tg} mice (D) exposed to hypoxia for 3 weeks.

6. DISCUSSION

This study showed the impact of DDAH1 overexpression on the acute and sustained phase of HPV, as well as on the effects of chronic hypoxia on the pulmonary vasculature. DDAH1 degrades ADMA, which is the most important endogenous NOS inhibitor and has been suggested to serve as a biomarker of endothelial dysfunction in many diseases such as PAH. This study showed that:

- 1) Acute HPV is not affected by DDAH1 gene overexpression. Similarly perfusate levels of NO and cGMP are not altered in acute hypoxia, however, perfusate ADMA levels were decreased in perfused lungs from DDAH1^{tg} mice without effect on NO, cGMP or vascular tone.
- 2) Sustained HPV is decreased in DDAH1^{tg} mice. Inhibitor studies revealed, that the attenuation is mediated by the NO-cGMP pathway, fitting to increased perfusate levels of NO and cGMP and decreased levels of ADMA in DDAH1^{tg} mice compared to WT mice after 3 h of hypoxic ventilation.
- 3) Chronic hypoxia-induced PH was not altered in DDAH1^{tg} mice.

6.1 Effects of DDAH1 on acute hypoxic response

During acute HPV this study showed no differences in the level of PAP between DDAH1^{tg} and WT mice. Also, administration of L-NNA, which is a NOS inhibitor, at a dose of 400 μ M, or ODQ, which is a sGC inhibitor, at a dose of 10 μ M, in isolated lungs had no effect on HPV in both WT and DDAH1^{tg} during this phase. This is in contrast to another investigation, showing that gene deletion of eNOS results in augmentation of HPV ⁷⁶. The lower level of hypoxia (0% O₂ in ventilated air) used in this study might be one reason for the discrepancy. Supportive for the finding of this thesis is the fact, that the acute hypoxic response in the eNOS knock-out mice was only influenced to a minor degree. In different species NO might be more potent during acute HPV, as inhibition of NO production in rabbits resulted in a large enhancement of HPV ¹¹⁷. Furthermore, the finding that the NO-cGMP pathway mediated vasodilation does not decrease acute HPV is supported by a study showing that sGC- α 1 deficiency does not change the response to acute hypoxia in lungs of anesthetized mice ¹⁰⁹. Additionally it had been shown, that acute HPV is only influenced to a minor degree by the endothelium in isolated pulmonary arteries ¹¹⁸.

The insensitivity of acute HPV to DDAH1 gene overexpression is also supported by the findings of the investigations regarding vasoactive substances in the perfusate. During

normoxia and acute hypoxia, NO and cGMP levels in the perfusate of isolated lungs were unchanged when comparing DDAH1^{tg} and WT mice. However, the level of ADMA was decreased in DDAH1^{tg} mice compared to WT mice. As DDAH1 degrades ADMA this effect could be expected. However, it remains unclear, why the decreased ADMA levels have no impact on the concentration of NO. This could be explained by other vasoactive mediator pathways that counterregulate NO concentration under this condition, e.g. increased NO synthase activity or compensatory downregulation of DDAH2.

In summary, this study provides evidence that DDAH1 gene overexpression does not affect acute HPV. Furthermore, acute HPV in the isolated mouse lung is not regulated by inhibitors of the NO-cGMP pathway

6.2 Effects of DDAH1 on sustained phase of HPV

Application of 3 hours hypoxia in isolated perfused and ventilated mouse lungs resulted in a biphasic vasoconstrictive response. This response consisted of two phases: the first phase was a rapid, transient (5-10 min) increase in PAP which then decreased, but did not reach the basal level. This phase was followed by the second or sustained phase which was a more slowly developing, but sustained increase in PAP.

The three hour hypoxic ventilation period was preceded by an acute hypoxic challenge. This protocol was chosen to confirm reproducible vasoreactivity of the pulmonary vasculature to the hypoxic stimulus in the initial phase of lung perfusion for each individual lung. This allowed assuring vascular reactivity of the explanted organ in the normal range. From previous (unpublished experiments) it is known that the preceding short term hypoxic ventilation does not affect the strength and time course of the subsequent response to sustained (2-3 hours) of hypoxia. This can also be expected from a teleologic point of view as acute HPV is a physiologic response to adapt blood flow to alveolar ventilation in an immediate ("from breath to breath") and fully reversible manner. In line with these characteristics of acute HPV, the vascular response to acute hypoxia was completely reversible in the current investigation as PAP returned to baseline when switching from ten minutes hypoxic ventilation to normoxia. This observation of the present study is also in line with the complete reversibility and high reproducibility of the HPV response during repetitive hypoxic ventilation maneuvers¹¹⁵. Thus, a modulating effect of a preceding acute hypoxic ventilation on the subsequent sustained HPV can be excluded - also as the chosen hypoxic ventilation is, in contrast to e.g. ischemic/hypoxic damage in other organs induces a physiological, reversible response.

The biphasic response to sustained hypoxia has been described before in isolated lungs²⁶, isolated pulmonary arteries²⁴, and even isolated PASM¹¹⁹, however, it was also challenged by other investigators finding only monophasic responses^{120, 121}.

This discrepancy might be due to the degree of hypoxia and pre-stimulation. The first phase of the constriction might not be limited to pulmonary arteries, because it was also observed in a variety of isolated systemic arteries^{22, 122, 123}. Thus the second phase of the vasoconstriction which is restricted to arteries of pulmonary origin¹²⁴ had been suggested to be the physiologically more important process for HPV^{125, 126}. Whereas acute HPV is thought to be mediated by a calcium increase in PASM, sustained HPV has been shown to rely on a calcium sensitization of the myofilaments, possibly via phosphorylation by Rho-kinase^{25, 28, 29}.

Although there is no complete consensus, if the sensitization mechanism is mediated by the endothelium, it was shown in most, but not all studies, that the full expression of sustained HPV requires an intact endothelium^{22, 27, 127-129}. DDAH1 overexpression in the DDAH1^{tg} mice used in this study is driven by a human β -actin promoter and thus occurs in a tissue- and cell type-unspecific manner¹³⁰. However, as DDAH1 promotes NO production (see below) and main NO production in the lung occurs in the endothelium¹³¹, the finding of this thesis, that the second phase of sustained HPV is completely abolished in isolated lungs of DDAH1^{tg} mice, supports the important role of the endothelium for sustained HPV.

As possible mediators, the increased production of NO in DDAH1^{tg} mice may play a role, as DDAH1 inhibits ADMA which is an endogenous NOS inhibitor. Thus the net result of overexpression of DDAH1 would be an increased production of NO. From this study, this hypothesis is supported by the fact that 1) the difference of the second phase in DDAH1^{tg} mice was reversed after the application of the NOS inhibitor L-NNA in WT and DDAH1^{tg} mice and 2) the level of NO metabolites in perfusate was increased in DDAH1^{tg} mice compared to WT mice. NO is considered as the major endothelium-derived vasoactive factor and is synthesized from oxygen and L-arginine by a family of three NO synthases, all of which are expressed in the lung¹³². Endothelial NOS plays an important role in maintaining low pulmonary vascular tone⁷⁶. NO activates sGC which results in activation and synthesis of the second messenger cGMP which in turn activates cGMP-dependent protein kinases (protein kinases G) leading to reduction in cytosolic Ca²⁺ concentration and inhibition of the actin-myosin contractile system. This leads to vascular smooth muscle relaxation, inhibition of thrombocyte activity and decreased cell proliferation⁷⁷. The action of NO can be inhibited by 1) NOS inhibition either endogenously by ADMA and L-NMMA or pharmacologically by

L-NNA 2) sGC inhibitors such as ODQ and 3) PDE enzymes, which can exist in several isoforms and metabolize cGMP¹³³.

Lung NO is the most important vasodilator and contributes to the amelioration of PH¹²⁸. It has been reported, that inhibition of EDRF-NO synthesis potentiates HPV both in vivo and in perfused lungs¹²⁹. This fits to the findings of this thesis, that the pulmonary vasoconstriction was increased during sustained hypoxic ventilation in presence of L-NNA in both, WT and DDAH1^{tg} mice, even though in WT mice only significantly between minutes 15 to 85 of the hypoxic ventilation period. Moreover, in presence of L-NNA, overexpression of DDAH1 resulted no longer in decreased HPV compared to WT mice. Therefore the difference in both mouse strains can be explained by an increased NOS activity in DDAH1^{tg} mice. Furthermore, the application of the sGC inhibitor ODQ resulted in a similar increase of PAP in DDAH1^{tg} mice as observed with L-NNA treatment. Therefore it can be proposed, that the increased levels of NO in DDAH1^{tg} mice caused vasodilation via cGMP-dependent pathways. The relevance for cGMP-dependent pathways is emphasized by the finding that the level of cGMP in lung perfusate was strongly increased at the time point of sustained hypoxic ventilation in isolated lungs of DDAH1^{tg} mice, being in line with the inhibition of vasoconstriction. Concentration of cGMP was more than 2-fold higher in DDAH1^{tg} than in WT mice similar to the concentration of NO, a finding that again fits to activation of the NO-cGMP pathway as an underlying mechanism for the decreased HPV in DDAH1^{tg} mice. However, DDAH1^{tg} mice showed significantly lower PAP at late time points of hypoxic ventilation than WT mice in presence of ODQ.

One explanation for this effect might be an incomplete inhibition of sGC in DDAH1^{tg} mice based on the fact, that sGC is highly activated in DDAH1^{tg} mice due to high NO concentration. On the other hand sGC could be activated in WT mice by NO-independent mechanisms to a higher degree than in DDAH1^{tg} mice which would result in stronger relief of the vasodilative action of sGC during inhibition. However, activation of cGMP-independent pathways by NO in DDAH1^{tg} mice, which may involve nitrite or reactions of NO with protein thiols to form S-nitrosothiols¹³⁴, as well as interaction of NO with mitochondria resulting in vasoactive effects¹³⁵, can not be excluded. When comparing the effects of L-NNA and ODQ in WT mice, it becomes evident that ODQ only enhances late time points of HPV, in contrast to L-NNA that significantly enhances early time points. This supports the conclusion that sGC could be activated by NO-independent mechanisms in WT mice¹³⁶ and NO may have a cGMP-independent vasodilative effect in WT mice as suggest in the DDAH1^{tg} mice.

In contrast to NO and cGMP, the level of ADMA was highly decreased at all time points of sustained hypoxia in DDAH1^{tg} compared to WT mice. At the end of the 3 hours hypoxic ventilation period, the level of ADMA was approximately lowered by about 65% in DDAH1^{tg} compared to WT mice. The inverse correlation between ADMA levels and DDAH1 overexpression is confirmed by a lot of studies such as the study of Dayoub et al. who have generated transgenic mice that overexpress the human isoform of DDAH1. These mice exhibited greater tissue DDAH activity and reduced plasma ADMA levels¹³⁰. The discrepancy between the decreased level of ADMA and unchanged NO, as well as cGMP levels in normoxia and acute hypoxia could be explained by compensatory downregulation of NO production in DDAH1^{tg} mice, as discussed above. It should be pointed out as well that cGMP and NO levels show the tendency to be increased in acute hypoxia, but may not have accumulated enough in the measurement period to be significantly changed or cause vasodilatation. This may be different in the vivo situations.

Interestingly, ADMA was increased in WT mice after 3 hours of hypoxic ventilation, in contrast to NO and cGMP. It remains to be elucidated, how the unchanged levels of NO and cGMP can be achieved in face of increased ADMA levels. Possibly, after 3 hours hypoxic ventilation, pathways that increase NO and cGMP levels were activated, but compensatory increase of ADMA kept NO and cGMP concentrations at the same level as during normoxic ventilation. However, it has to be kept in mind, that ADMA also could exert vasoconstrictive properties via NO-cGMP-independent mechanisms, that might be responsible specifically for sustained HPV. Moreover, perfusate levels of ADMA, NO and cGMP may only partially reflect cellularly active levels of these substances. As a future perspective, the mechanism of the increase in ADMA should be investigated, as possible connections to the suggested ROS pathway of HPV might exist^{117, 137-139}.

Finally, the differences in sustained HPV in the described groups could not be attributed to variations in lung weight. Although there was a tendency to a decrease in lung weight changes in experiments with inhibited NO-cGMP pathway compared to non-treated groups, these alterations did not correlate to differences in sustained HPV. Moreover, the effects of DDAH1 overexpression, L-NNA and ODQ were specific for hypoxia, as no differences in normoxic PAP recordings could be detected between these experimental groups and untreated controls.

In summary this study revealed that the overexpression of DDAH1 results in the decrease of the sustained phase of HPV via NO-cGMP-dependent pathways. Increased ADMA levels might play a role in the regulation of sustained HPV in WT mice.

6.3 Chronic hypoxic exposure

Exposure to chronic hypoxia induces structural and functional changes in the pulmonary arterial bed^{84, 140}. These changes include proliferation and migration of smooth muscle cells, as well as an increased accumulation of extracellular matrix.

In the present study after exposure of mice to 3 weeks of chronic hypoxia, there was development of PH as specified by significantly increased right ventricular pressure, right heart hypertrophy and vascular remodelling in WT mice and DDAH1^{tg} mice. However, there were no significant differences detected between WT mice and DDAH1^{tg} mice. This would have been anticipated, as ADMA and NO which are both regulated by DDAH play an important role in PH.

Hypoxia can inhibit the uptake of the NO precursor L-arginine by pulmonary arterial endothelial cells within 4 hours and may suppress the expression of NO synthase and activity^{79, 141, 142}. NO, synthesized by endothelial NO synthase, is a potent vasodilator and is considered to play an important role in regulating pulmonary vascular tone^{79, 84}. NO is the only known dilator that specifically suppresses HPV⁸¹ and to which the vascular responses to chronic hypoxia have partially been attributed⁸³. Therefore, reduced production of NO in endothelial cells of the pulmonary arteries contributes to the progression of PH. The promotion of endogenous NO production in endothelial cells of the pulmonary arteries could be used as a therapeutic strategy in PH¹⁴³.

NO production is regulated by endogenous NOS inhibitor ADMA. It was found that a marked increase in plasma ADMA levels accompanied hypoxia-induced experimental PH¹⁴⁴. The role of ADMA in PH of other etiologies has also been investigated, and patients with idiopathic PH were found to have higher plasma ADMA levels than healthy controls¹⁴⁵. Most importantly, the expression of PRMT, which synthesizes ADMA, was found to be upregulated in mice exposed to chronic hypoxia, resulting in increased ADMA tissue levels and a decreased L-arginine/ADMA ratio, thereby supporting an important role of PRMT-mediated ADMA generation in hypoxia-induced PH¹⁴⁶. Furthermore, it has been reported that the levels of ADMA were highly increased in monocrotaline-induced PH in rats¹⁴⁷. ADMA is degraded by DDAH which therefore might also play a role in development of hypoxia-induced PH. The activity of DDAH enzyme in the lungs was decreased in chronic hypoxia-induced PH. This might be a result of the corresponding decrease in the protein expression of the DDAH1 isoform. Furthermore, the expression of the DDAH1 isoform was inhibited upon exposure to hypoxia, thus increasing ADMA levels¹⁰¹.

However, we could find no significant difference in development of PH induced by hypoxia in DDAH1^{tg} mice compared to WT mice. Overexpression of DDAH1 enzyme resulted only in the small tendency to decreased RVSP in hypoxic DDAH1^{tg} mice by 5% compared to WT mice exposed to chronic hypoxia. In parallel, RV/(LV+S) ratio had the tendency to be decreased in DDAH1^{tg} mice compared to WT mice exposed to chronic hypoxia.

The most common feature of all forms of PH is the increase in the thickness of the medial layer of the normal muscular arteries and an extension of muscle into smaller and more peripheral vessels. In hypoxic WT and DDAH1^{tg} mice, the portion of fully muscularized pulmonary arteries was significantly increased compared to their respective normoxic groups. Furthermore, the portion of non-muscularized pulmonary arteries was significantly decreased compared to their respective normoxic groups. Although the total percentage of fully muscularized pulmonary arteries in DDAH1^{tg} mice exposed to 3 weeks hypoxia had the tendency to be decreased by 8% compared to hypoxic WT mice, there was also no significant difference in vascular remodelling quantified by morphometry between both mouse strains.

The failure of DDAH1^{tg} to inhibit development of hypoxia-induced PH, although it inhibits sustained HPV, might be due to the fact that different mechanisms may regulate HPV and pulmonary vasculature responses to chronic hypoxia¹⁴⁸. Specifically DDAH2 might be more important in the development of PH than DDAH1¹⁴⁷. In the DDAH1^{tg} mice increased levels of DDAH1 activity might be opposed by counterregulation of vasoconstrictive pathways, as observed in normoxia in DDAH1^{tg} mice, in which decreased ADMA levels were not reflected by increased NO or cGMP concentrations. Furthermore, the NO-cGMP pathway is already compensatory activated in chronic hypoxia¹⁴⁹, so that further activation by DDAH1 overexpression might not be possible.

In conclusion, the data of the present study provide evidence for the conclusion, that DDAH1 specifically regulates sustained HPV via ADMA signalling. DDAH1 overexpression specifically inhibits sustained HPV through ADMA/NO-dependent pathways. This conclusion is supported by the finding that 1) DDAH1 overexpression decreased levels of ADMA compared to WT mice, increased NO concentration compared to WT mice in hypoxia and completely inhibited sustained HPV and 2) 3 hours exposure to hypoxia increased ADMA levels in WT mice, but not in DDAH1 overexpressing mice.

Getting insight into DDAH1-dependent mechanisms may help finding new strategies for therapeutic intervention in HPV via controlling the NO pathway which plays an important role in the regulation of sustained HPV and PH. Possible cGMP-independent signalling of

DDAH1, counterregulatory mechanisms existing in the DDAH1 overexpressing mouse strain and upstream pathways of DDAH1/ADMA regulation should be addressed in further studies.

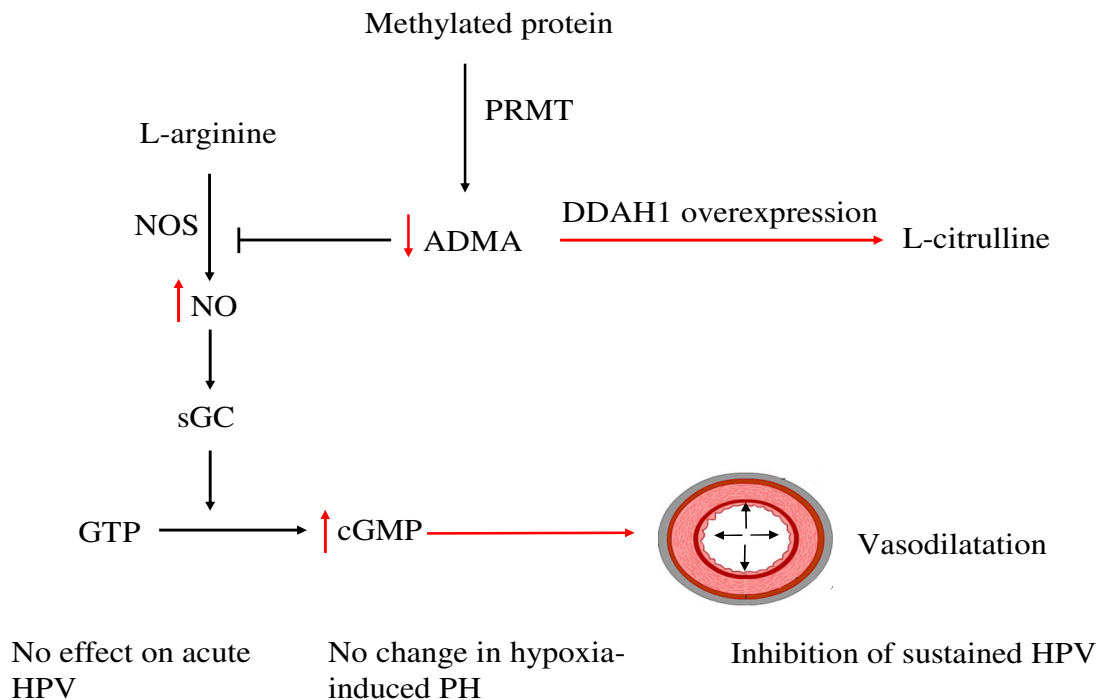


Figure 30: Effects of DDAH1 overexpression on alterations of the pulmonary vasculature induced by acute, sustained and chronic hypoxia. Overexpression of DDAH1 results in a complete inhibition of sustained hypoxia-induced pulmonary vasoconstriction, however, it has no effect on acute HPV or chronic hypoxia-induced PH. PRMT: protein arginine methyltransferase; DDAH1: dimethylarginine dimethylaminohydrolase 1; ADMA: asymmetric ω - N^G , N^G -dimethylarginine; NOS: nitric oxide synthase; NO: nitric oxide; sGC: soluble guanylyl cyclase; GTP: guanosine triphosphate; cGMP: cyclic 3', 5'-guanosine monophosphate; PH: pulmonary hypertension; HPV: hypoxic pulmonary vasoconstriction.

7. SUMMARY

Hypoxia is a prominent factor for induction of pulmonary vasoconstriction and pulmonary hypertension (PH). Hypoxic pulmonary vasoconstriction (HPV) can be induced by alveolar hypoxia lasting seconds to minutes (= acute HPV) or minutes to hours (= sustained HPV). Both phases of HPV play an important role in matching local perfusion to ventilation, thus optimizing pulmonary gas exchange. However, the irreversible increase of pulmonary arterial pressure (PAP) induced by sustained HPV might also facilitate development of PH. PH is a fatal disease characterized by increased pulmonary vascular resistance. The pathophysiology of PH can include endothelial dysfunction and pulmonary arterial smooth muscle cell hypertrophy and proliferation. Nitric oxide (NO) is a well-known vasodilator controlling a diverse range of pulmonary functions such as regulation of PAP. Asymmetric ω -N^G, N^G-dimethylarginine (ADMA) is a potent inhibitor of all three nitric oxide synthase (NOS) isoforms, resulting in impaired NO production. ADMA is degraded by dimethylarginine dimethylaminohydrolase (DDAH) 1 and 2, both expressed in the lung.

Therefore, the current study investigated the effects of DDAH1 on acute and sustained HPV as well as on hypoxia-induced PH in isolated, ventilated and perfused mouse lungs, and in a whole animal model. PH was quantified by measurement of right ventricular systolic pressure, right-to-left heart ratio and vascular morphometry. Concentration of ADMA and cyclic 3', 5'-guanosine monophosphate (cGMP) was determined by enzyme linked immunosorbent assay (ELISA). NO was measured by a chemiluminescence analyzer.

DDAH1 overexpression had no effects on acute HPV. However, in sustained HPV (3 hours of hypoxia), DDAH1 overexpression abolished the increase in PAP almost completely and concomitantly decreased levels of ADMA, and significantly increased levels of NO and cGMP compared to wild-type (WT) mice. Sustained HPV could be restored by application of the NOS inhibitor N^ω-Nitro-L-arginine (L-NNA), and the soluble guanylyl cyclase (sGC) inhibitor 1H-[1, 2, 4]oxadiazolo-[4, 3-a]quinoxalin-1-one (ODQ). Chronic hypoxic exposure (10% O₂, 3 weeks) induced PH in WT and DDAH1^{tg} mice without a difference in the degree of PH in both mouse strains.

This study revealed, that DDAH1 regulates ADMA concentration, NO bioavailability and vessel tone specifically in sustained HPV. Therefore, getting insight into DDAH1-dependent mechanisms may help find new strategies for treatment of diseases with impaired ventilation-perfusion matching due to decreased sustained HPV.

8. ZUSAMMENFASSUNG

Hypoxie ist einer der häufigsten Faktoren, die zu pulmonaler Vasokonstriktion und pulmonaler Hypertonie (PH) führen. Die hypoxische pulmonale Vasokonstriktion (HPV) wird durch alveoläre Hypoxie induziert, die einige Sekunden bis Minuten (= akute HPV) oder Minuten bis Stunden (= prolongierte HPV) dauern kann. Beide Phasen der HPV spielen eine wichtige Rolle für die Anpassung der lokalen Perfusion an die alveoläre Ventilation und optimieren somit den pulmonalen Gasaustausch. Der Anstieg des pulmonalarteriellen Druckes (PAP), der durch die prolongierte HPV induziert wird, steht jedoch in der Diskussion, auch die Entwicklung von chronischer PH zu fördern. PH ist eine häufig tödlich verlaufende Erkrankung, die durch einen permanent erhöhten pulmonalvaskulären Widerstand charakterisiert ist. Die Pathophysiologie kann endotheliale Dysfunktion und Hypertrophie und Proliferation von pulmonalarteriellen glatten Muskelzellen umfassen. Stickstoffmonoxid (NO) ist ein bekannter Vasodilatator, der eine Vielzahl pulmonaler Funktionen kontrolliert und unter anderem in die Regulation des PAP involviert ist. Asymmetrisches Dimethylarginin (ADMA) ist ein hochpotenter Inhibitor von allen Isoformen der NO Synthase (NOS), und schränkt somit die NO Produktion ein. ADMA wird von den Dimethylarginin Dimethylaminohydrolasen (DDAH) 1 und 2 abgebaut, die beide in der Lunge exprimiert werden.

Vor diesem Hintergrund untersuchte die vorliegende Studie die Effekte der DDAH1 auf die akute und prolongierte HPV und hypoxie-induzierte PH in der isolierten, ventilerten und perfundierten Mäuselunge, bzw. im intakten Tier. Die PH wurde mittels Messung des rechtsventrikulären systolischen Druckes, des Gewichtsverhältnisses von rechtem zum linkem Ventrikel und der vaskulären Morphometrie quantifiziert. Die Konzentration von ADMA und zyklischem Guanosinmonophosphat (cGMP) wurde mittels enzymgekoppeltem Immunadsorptionstest (EIA) bestimmt. NO wurde mit einem Chemilumineszenz-Analysator gemessen.

DDAH1-Überexpression hatte keine Effekte auf die akute HPV. Allerdings war in prolongierter HPV nach 3 Stunden Hypoxie die Erhöhung des PAP bei DDAH1 Überexpression komplett aufgehoben und gleichzeitig waren die Perfusatspiegel von ADMA erniedrigt und von NO und cGMP signifikant erhöht. Die prolongierte HPV konnte durch die Applikation des NOS Inhibitors N_ω-Nitro-L-arginine (L-NNA), und den Inhibitor der löslichen Guanylatcyclase (sGC), 1H-[1, 2, 4]oxadiazolo-[4, 3-a]quinoxalin-1-one (ODQ), wiederhergestellt werden. Exposition chronischer Hypoxie (10% O₂, 3 Wochen) führte zur

Entwicklung von PH in WT und DDAH1^{tg} Mäusen, ohne einen Unterschied in der Ausprägung der PH in beiden Mauslinien.

Die Studie zeigte, dass die DDAH1 die ADMA Konzentration, die NO Bioverfügbarkeit und den Gefäßtonus spezifisch während der prolongierten HPV reguliert.

Ein besseres Verständnis des DDAH1 Stoffwechselweges könnte dabei helfen, neue therapeutische Möglichkeiten bei Erkrankungen mit eingeschränkter Ventilations-Perfusions-Anpassung aufgrund erniedrigter prolongierter HPV zu finden.

9. REFERENCES

1. Gordon, E.J. William Harvey and the circulation of the blood. *South. Med. J.* **84**, 1493-1498 (1991).
2. Haddad, S.I. & Khairallah, A.A. A forgotten chapter in the history of the circulation of the blood. *Ann. Surg.* **104**, 1-8 (1936).
3. Coppola, E.D. The discovery of the pulmonary circulation: a new approach. *Bull. Hist. Med.* **31**, 44-77 (1957).
4. Bradford, J.R. & Dean, H.P. The Pulmonary Circulation. *J. Physiol.* **16**, 34-158 (1894).
5. Motley, H.L. & Cournand, A. The influence of short periods of induced acute anoxia upon pulmonary artery pressures in man. *Am. J. Physiol.* **150**, 315-320 (1947).
6. Weissmann, N., Grimminger, F., Walmrath, D. & Seeger, W. Hypoxic vasoconstriction in buffer-perfused rabbit lungs. *Respir. Physiol.* **100**, 159-169 (1995).
7. Marshall, B.E., Marshall, C., Benumof, J. & Saidman, L.J. Hypoxic pulmonary vasoconstriction in dogs: effects of lung segment size and oxygen tension. *J. Appl. Physiol.* **51**, 1543-1551 (1981).
8. Hirschman, J.C. & Boucek, R.J. Angiographic evidence of pulmonary vasomotion in the dog. *Br. Heart J.* **25**, 375-381 (1963).
9. Kato, M. & Staub, N.C. Response of small pulmonary arteries to unilobar hypoxia and hypercapnia. *Circ. Res.* **19**, 426-440 (1966).
10. Nagasaka, Y., Bhattacharya, J., Nanjo, S., Gropper, M.A. & Staub, N.C. Micropuncture measurement of lung microvascular pressure profile during hypoxia in cats. *Circ. Res.* **54**, 90-95 (1984).
11. Hauge, A. Conditions governing the pressor response to ventilation hypoxia in isolated perfused rat lungs. *Acta Physiol. Scand.* **72**, 33-44 (1968).
12. Nossaman, B.D. & Kadowitz, P.J. The role of the RhoA/Rho kinase-pathway in pulmonary hypertension. *Curr. Drug Discov. Technol.* **6**, 59-71 (2009).
13. Ward, J.P., Knock, G.A., Snetkov, V.A. & Aaronson, P.I. Protein kinases in vascular smooth muscle tone: role in the pulmonary vasculature and hypoxic pulmonary vasoconstriction. *Pharmacol. Ther.* **104**, 207-231 (2004).
14. Inazu, M., Zhang, H. & Daniel, E.E. Different mechanisms can activate Ca²⁺ entrance via cation currents in endothelial cells. *Life Sci.* **56**, 11-17 (1995).
15. Sweeney, M. & Yuan, J.X. Hypoxic pulmonary vasoconstriction: role of voltage-gated potassium channels. *Respir. Res.* **1**, 40-48 (2000).

16. Karaki, H., Ozaki, H., Hori, M., Mitsui-Saito, M., Amano, K., Harada, K., Miyamoto, S., Nakazawa, H., Won, K. & Sato, A. Calcium movements, distribution, and functions in smooth muscle. *Pharmacol. Rev.* **49**, 157-230 (1997).
17. Resta, T.C., Broughton, B.R. & Jernigan, N.L. Reactive oxygen species and RhoA signaling in vascular smooth muscle: role in chronic hypoxia-induced pulmonary hypertension. *Adv. Exp. Med. Biol.* **661**, 355-373 (2010).
18. McMurtry, I.F., Abe, K., Ota, H., Fagan, K.A. & Oka, M. Rho kinase-mediated vasoconstriction in pulmonary hypertension. *Adv. Exp. Med. Biol.* **661**, 299-308 (2010).
19. Madden, J.A., Vadula, M.S. & Kurup, V.P. Effects of hypoxia and other vasoactive agents on pulmonary and cerebral artery smooth muscle cells. *Am. J. Physiol.* **263**, L384-L393 (1992).
20. Ogata, M., Ohe, M., Katayose, D. & Takishima, T. Modulatory role of EDRF in hypoxic contraction of isolated porcine pulmonary arteries. *Am. J. Physiol.* **262**, H691-H697 (1992).
21. Demiryurek, A.T., Wadsworth, R.M., Kane, K.A. & Peacock, A.J. The role of endothelium in hypoxic constriction of human pulmonary artery rings. *Am. Rev. Respir. Dis.* **147**, 283-290 (1993).
22. Leach, R.M., Robertson, T.P., Twort, C.H. & Ward, J.P. Hypoxic vasoconstriction in rat pulmonary and mesenteric arteries. *Am. J. Physiol.* **266**, L223-L231 (1994).
23. Zhang, F. & Morice, A.H. Effect of levromakalim on hypoxia-, KCl- and prostaglandin F₂ alpha-induced contractions in isolated rat pulmonary artery. *J. Pharmacol. Exp. Ther.* **271**, 326-333 (1994).
24. Bennie, R.E., Packer, C.S., Powell, D.R., Jin, N. & Rhoades, R.A. Biphasic contractile response of pulmonary artery to hypoxia. *Am. J. Physiol.* **261**, L156-L163 (1991).
25. Robertson, T.P., Aaronson, P.I. & Ward, J.P. Hypoxic vasoconstriction and intracellular Ca²⁺ in pulmonary arteries: evidence for PKC-independent Ca²⁺ sensitization. *Am. J. Physiol.* **268**, H301-H307 (1995).
26. Robertson, T.P., Ward, J.P. & Aaronson, P.I. Hypoxia induces the release of a pulmonary-selective, Ca²⁺-sensitising, vasoconstrictor from the perfused rat lung. *Cardiovasc. Res.* **50**, 145-150 (2001).
27. Hoshino, Y., Morrison, K.J. & Vanhoutte, P.M. Mechanisms of hypoxic vasoconstriction in the canine isolated pulmonary artery: role of endothelium and sodium pump. *Am. J. Physiol.* **267**, L120-L127 (1994).
28. Robertson, T.P., Dipp, M., Ward, J.P., Aaronson, P.I. & Evans, A.M. Inhibition of sustained hypoxic vasoconstriction by Y-27632 in isolated intrapulmonary arteries and perfused lung of the rat. *Br. J. Pharmacol.* **131**, 5-9 (2000).

29. Fagan, K.A., Oka, M., Bauer, N.R., Gebb, A.S., Ivy, D.D., Morris, G.K. & McMurtry, F.I. Attenuation of acute hypoxic pulmonary vasoconstriction and hypoxic pulmonary hypertension in mice by inhibition of Rho-kinase. *Am. J. Physiol. Lung Cell Mol. Physiol.* **287**, L656-L664 (2004).
30. Heath, D., Edwards, C., Winson, M. & Smith, P. Effects on the right ventricle, pulmonary vasculature, and carotid bodies of the rat of exposure to, and recovery from, simulated high altitude. *Thorax* **28**, 24-28 (1973).
31. Barer, G.R., Bee, D. & Wach, R.A. Contribution of polycythaemia to pulmonary hypertension in simulated high altitude in rats. *J. Physiol.* **336**, 27-38 (1983).
32. Wach, R., Emery, C.J., Bee, D. & Barer, G.R. Effect of alveolar pressure on pulmonary artery pressure in chronically hypoxic rats. *Cardiovasc. Res.* **21**, 140-150 (1987).
33. Broughton, B.R., Walker, B.R. & Resta, T.C. Chronic hypoxia induces Rho kinase-dependent myogenic tone in small pulmonary arteries. *Am. J. Physiol. Lung Cell Mol. Physiol.* **294**, L797-L806 (2008).
34. Nagaoka, T., Fagan, K.A. & Gebb, S.A. Inhaled Rho-kinase inhibitors are potent and selective vasodilators in rat pulmonary hypertension. *Am. J. Respir. Crit. Care Med.* **171**, 494-499 (2005).
35. Killilea, D.W., Hester, R., Balczon, R., Babal, P. & Gillespie, M.N. Free radical production in hypoxic pulmonary artery smooth muscle cells. *Am. J. Physiol. Lung Cell Mol. Physiol.* **279**, L408-L412 (2000).
36. Wang, X., Tong, M., Chinta, S., Raj, J.U. & Gao, Y. Hypoxia-induced reactive oxygen species downregulate ET_B receptor-mediated contraction of rat pulmonary arteries. *Am. J. Physiol. Lung Cell Mol. Physiol.* **290**, L570-L578 (2006).
37. Grishko, V., Solomon, M., Breit, J.F., Killilea, D.W., Ledoux, S.P., Wilson, G.L. & Gillespie, M.N. Hypoxia promotes oxidative base modifications in the pulmonary artery endothelial cell VEGF gene. *FASEB J.* **15**, 1267-1269 (2001).
38. Jin, L., Ying, Z. & Webb, R.C. Activation of Rho/Rho kinase signaling pathway by reactive oxygen species in rat aorta. *Am. J. Physiol. Heart Circ. Physiol.* **287**, H1495-H1500 (2004).
39. Braunwald, E. On future directions for cardiology. The Paul D. White lecture. *Circulation* **77**, 13-32 (1988).
40. Humbert, M., Khaltaev, N., Bousquet, J. & Souza, R. Risk factors for pulmonary arterial hypertension. *Clin. Chest Med.* **22**, 459-475 (2001).
41. Fishman, A.P. Clinical classification of pulmonary hypertension. *Clin. Chest Med.* **22**, 385-91, vii (2001).

42. Simonneau, G., Galie, N., Rubin, L.J., Langleben, D., Seeger, W., Domenighetti, G., Gibbs, S., Lebrec, D., Speich, R., Beghetti, M., Rich, S. & Fishman, A. Clinical classification of pulmonary hypertension. *J. Am. Coll. Cardiol.* **43**, 5S-12S (2004).
43. Simonneau, G., Robbins, I.M., Beghetti, M., Channick, R.N., Jing, G.Z., Krowka, M.J., Langleben, D., Delcroix, N.M., Christopher P. Elliott, C.D., Gaine, S.P., Nakanishi, M.T. & Souza, R. Updated clinical classification of pulmonary hypertension. *J. Am. Coll. Cardiol.* **54**, S43-S54 (2009).
44. Rich, S., Dantzker, D.R., Ayres, S.M., Bergofsky, E.H., Brundage, B.H., Detre, K.M., Fishman, A.P., Goldring, R.M., Groves, B.M. & Koerner, S.K. Primary pulmonary hypertension. A national prospective study. *Ann. Intern. Med.* **107**, 216-223 (1987).
45. Loyd, J.E., Primm, R.K. & Newman, J.H. Familial primary pulmonary hypertension: clinical patterns. *Am. Rev. Respir. Dis.* **129**, 194-197 (1984).
46. Loyd, J.E., Butler, M.G. & Foround T.M. Genetic anticipation and abnormal gender ratio at birth in familial primary pulmonary hypertension. *Am. J. Respir. Crit. Care Med.* **152**, 93-97 (1995).
47. Elliott, G., Alexander, G., Leppert, M., Yeates, S. & Kerber, R. Coancestry in apparently sporadic primary pulmonary hypertension. *Chest* **108**, 973-977 (1995).
48. Newman, J.H., Wheeler, L., Lane, K.B., Loyd, E., Gaddipati, R., Phillips, J.A. & Loyd, J.E. Mutation in the gene for bone morphogenetic protein receptor II as a cause of primary pulmonary hypertension in a large kindred. *N. Engl. J. Med.* **345**, 319-324 (2001).
49. McGoon, M., Gutterman, D., Steen, V., Barst, R., McCrory, D.C., Fortin, T.A. & Loyd, J.E. Screening, early detection, and diagnosis of pulmonary arterial hypertension: ACCP evidence-based clinical practice guidelines. *Chest* **126**, 14S-34S (2004).
50. Falk, J.A., Philip, K.J. & Schwarz, E.R. The emergence of oral tadalafil as a once-daily treatment for pulmonary arterial hypertension. *Vasc. Health Risk Manag.* **6**, 273-280 (2010).
51. Barst, R.J., Rubin, L.J., Long, W.A., McGoon, M.D., Rich, S., Badesch, D.B., Groves, B.M., Tapson, V.F., Bourge, R.C. & Brundage, B.H. A comparison of continuous intravenous epoprostenol (prostacyclin) with conventional therapy for primary pulmonary hypertension. The Primary Pulmonary Hypertension Study Group. *N. Engl. J. Med.* **334**, 296-302 (1996).
52. Channick, R.N., Simonneau, G., Sitbon, O., Robbins, I.M., Frost, A., Tapson, V.F., Badesch, D.B., Roux, S., Rainsio, M., Bodin, F. & Rubin, L.J. Effects of the dual endothelin-receptor antagonist bosentan in patients with pulmonary hypertension: a randomised placebo-controlled study. *Lancet* **358**, 1119-1123 (2001).

53. Rubin, L.J., Badesch, D.B., Barst, R.J., Galie, N., Black, C.M., Keogh, A., Pulido, T., Frost, A., Roux, S., Leconte, I., Landzberg, M. & Simonneau, G. Bosentan therapy for pulmonary arterial hypertension. *N. Engl. J. Med.* **346**, 896-903 (2002).
54. Ghofrani, H.A., Wiedemann, R., Rose, F., Olschewski, H., Schermuly, R.T., Weissmann, N., Seeger, W. & Grimminger, F. Combination therapy with oral sildenafil and inhaled iloprost for severe pulmonary hypertension. *Ann. Intern. Med.* **136**, 515-522 (2002).
55. Bharani, A., Mathew, V., Sahu, A. & Lunia, B. The efficacy and tolerability of sildenafil in patients with moderate-to-severe pulmonary hypertension. *Indian Heart J.* **55**, 55-59 (2003).
56. Sastry, B.K., Narasimhan, C., Reddy, N.K., Anand, B., Prakash, G.S., Raju, P.R. & Kumar, D.N. A study of clinical efficacy of sildenafil in patients with primary pulmonary hypertension. *Indian Heart J.* **54**, 410-414 (2002).
57. Ghofrani, H.A., Schermuly, R.T., Rose, F., Wiedemann, R., Kohstall, M.G., Kreckel, A., Olschewski, H., Weissmann, N., Enke, B., Ghofrani, S., Seeger, W. & Grimminger, F. Sildenafil for long-term treatment of nonoperable chronic thromboembolic pulmonary hypertension. *Am. J. Respir. Crit. Care Med.* **167**, 1139-1141 (2003).
58. Tapson, V. Atrial septostomy: why we still need it. *Chest* **131**, 947-948 (2007).
59. Galley, H.F. & Webster, N.R. Physiology of the endothelium. *Br. J. Anesth.* **93**, 105-113 (2004).
60. Lopes, A.A., Maeda, N.Y., Goncalves, R.C. & Bydlowski, S.P. Endothelial cell dysfunction correlates differentially with survival in primary and secondary pulmonary hypertension. *Am. Heart J.* **139**, 618-623 (2000).
61. Inoue, A., Yanagisawa, M., Kimura, S., Kasuya, Y., Miyachi, T., Goto, K. & Masaki, T. The human endothelin family: three structurally and pharmacologically distinct isopeptides predicted by three separate genes. *Proc. Natl. Acad. Sci. U. S. A* **86**, 2863-2867 (1989).
62. Naruse, M., Naruse, K., Kurimoto, F., Horiuchi, J., Tsuchiya, K., Kawana, M., Kato, Y., Zeng, Z.P., Sakurai, H. & Demura, H. Radioimmunoassay for endothelin and immunoreactive endothelin in culture medium of bovine endothelial cells. *Biochem. Biophys. Res. Commun.* **160**, 662-668 (1989).
63. Lipton, H.L., Hauth, T.A., Summer, W.R. & Hyman, A.L. Endothelin produces pulmonary vasoconstriction and systemic vasodilation. *J. Appl. Physiol.* **66**, 1008-1012 (1989).
64. Kourembanas, S., Marsden, P.A., McQuillan, L.P. & Faller, D.V. Hypoxia induces endothelin gene expression and secretion in cultured human endothelium. *J. Clin. Invest.* **88**, 1054-1057 (1991).

65. Gardiner, S.M., Kemp, P.A., March, J.E., Bennett, T., Davenport, A.P. & Edvinsson, L. Effects of an ET-1 receptor antagonist, FR139317, on regional hemodynamic responses to endothelin-1 and [Ala^{11,15}]Ac-endothelin-1 (6-21) in conscious rats. *Br. J. Pharmacol.* **112**, 477-486 (1994).
66. Teerlink, J.R., Breu, V., Sprecher, U., Clozel, M. & Clozel, J.P. Potent vasoconstriction mediated by endothelin ET_B receptors in canine coronary arteries. *Circ. Res.* **74**, 105-114 (1994).
67. Giaid, A., Yanagisawa, M., Langleben, D., Michel, R.P., Levy, R., Shennib, H., Kimura, S., Masaki, T., Duguid, W.P. & Stewart, D.J. Expression of endothelin-1 in the lungs of patients with pulmonary hypertension. *N. Engl. J. Med.* **328**, 1732-1739 (1993).
68. Chen, S.J., Chen, Y.F., Opgenorth, T.J., Wessale, J.L., Meng, Q.C., Durand, J., DiCarlo, V.S. & Oparil, S. The orally active nonpeptide endothelin A-receptor antagonist A-127722 prevents and reverses hypoxia-induced pulmonary hypertension and pulmonary vascular remodeling in Sprague-Dawley rats. *J. Cardiovasc. Pharmacol.* **29**, 713-725 (1997).
69. Oparil, S., Chen, S.J., Meng, Q.C., Elton, T.S., Yano, M. & Chen, Y.F. Endothelin A-receptor antagonist prevents acute hypoxia-induced pulmonary hypertension in the rat. *Am. J. Physiol.* **268**, L95-100 (1995).
70. Holm, P. Endothelin in the pulmonary circulation with special reference to hypoxic pulmonary vasoconstriction. *Scand. Cardiovasc. J. Suppl.* **46**, 1-40 (1997).
71. Turner, J.L. & Kozlowski, R.Z. Relationship between membrane potential, delayed rectifier K⁺ currents and hypoxia in rat pulmonary arterial myocytes. *Exp. Physiol.* **82**, 629-645 (1997).
72. Sato, K., Morio, Y., Morris, K.G., Rodman, D.M. & McMurtry, I.F. Mechanism of hypoxic pulmonary vasoconstriction involves ET_A receptor-mediated inhibition of K_{ATP}-channel. *Am. J. Physiol. Lung Cell Mol. Physiol.* **278**, L434-L442 (2000).
73. Delpy, E., Coste, H. & Gouville, A.C. Effects of cyclic GMP elevation on isoprenaline-induced increase in cyclic AMP and relaxation in rat aortic smooth muscle: role of phosphodiesterase 3. *Br. J. Pharmacol.* **119**, 471-478 (1996).
74. Geraci, M.W., Gao, B., Shepherd, D.C., Moore, M.D., Westcott, J.Y., Fagan, K.A., Alger, L.A., Tuder, R.M. & Voelkel, N.F. Pulmonary prostacyclin synthase overexpression in transgenic mice protects against development of hypoxic pulmonary hypertension. *J. Clin. Invest.* **103**, 1509-1515 (1999).
75. Hoshikawa, Y., Voelkel, N.F., Gesell, T.L., Moore, M.D., Morris, K.G., Alger, L.A., Narumiya, S. & Geraci, M.W. Prostacyclin receptor-dependent modulation of pulmonary vascular remodeling. *Am. J. Respir. Crit. Care Med.* **164**, 314-318 (2001).

76. Fagan, K.A., Tyler, R.C., Sato, K., Fouty, B.W., Morris, K.G., Huang, P.L., McMurtry, I.F. & Rodman, D.M. Relative contributions of endothelial, inducible, and neuronal NOS to tone in the murine pulmonary circulation. *Am. J. Physiol.* **277**, L472-L478 (1999).
77. Boger, R.H. & Bode-Boger, S.M. Asymmetric dimethylarginine, derangements of the endothelial nitric oxide synthase pathway, and cardiovascular diseases. *Semin. Thromb. Hemost.* **26**, 539-545 (2000).
78. Nathan, C. & Xie, Q.W. Regulation of biosynthesis of nitric oxide. *J. Biol. Chem.* **269**, 13725-13728 (1994).
79. Durmowicz, A.G. & Stenmark, K.R. Mechanisms of structural remodeling in chronic pulmonary hypertension. *Pediatr. Rev.* **20**, e91-e102 (1999).
80. Ogawa, Y., Kawabe, J., Onodera, S., Tobise, K., Morita, K., Harada, T., Hirayama, T. & Takeda, A. Role of endothelium in biphasic hypoxic response of the isolated pulmonary artery in the rat. *Jpn. Circ. J.* **57**, 228-236 (1993).
81. Grimminger, F., Spriestersbach, R., Weissmann, N., Walmrath, D. & Seeger, W. Nitric oxide generation and hypoxic vasoconstriction in buffer-perfused rabbit lungs. *J. Appl. Physiol.* **78**, 1509-1515 (1995).
82. Weissmann, N., Voswinckel, R., Tadic, A., Hardebusch, T., Ghofrani, H.A., Schermuly, R.T., Seeger, W. & Grimminger, F. Nitric oxide (NO)-dependent but not NO-independent guanylate cyclase activation attenuates hypoxic vasoconstriction in rabbit lungs. *Am. J. Respir. Cell Mol. Biol.* **23**, 222-227 (2000).
83. Karamsetty, V.S., Kane, K.A. & Wadsworth, R.M. The effects of chronic hypoxia on the pharmacological responsiveness of the pulmonary artery. *Pharmacol. Ther.* **68**, 233-246 (1995).
84. Jeffery, T.K. & Wanstall, J.C. Pulmonary vascular remodeling: a target for therapeutic intervention in pulmonary hypertension. *Pharmacol. Ther.* **92**, 1-20 (2001).
85. Le Cras, T.D., Xue, C., Rengasamy, A. & Johns, R.A. Chronic hypoxia upregulates endothelial and inducible NO synthase gene and protein expression in rat lung. *Am. J. Physiol.* **270**, L164-L170 (1996).
86. Shaul, P.W., North, A.J., Brannon, T.S., Ujiie, K., Wells, L.B., Nisen, P.A., Lowenstein, C.J., Snyder, S.H. & Star, R.A. Prolonged in vivo hypoxia enhances nitric oxide synthase type I and type III gene expression in adult rat lung. *Am. J. Respir. Cell Mol. Biol.* **13**, 167-174 (1995).
87. Tyler, R.C., Muramatsu, M., Abman, S.H., Stelzner, T.J., Rodman, D.M., Bloch, K.D. & McMurtry, I.F. Variable expression of endothelial NO synthase in three forms of rat pulmonary hypertension. *Am. J. Physiol.* **276**, L297-L303 (1999).

88. Dubbin, P.N., Zambetis, M. & Dusting, G.J. Inhibition of endothelial nitric oxide biosynthesis by N-nitro-L-arginine. *Clin. Exp. Pharmacol. Physiol.* **17**, 281-286 (1990).
89. Woodman, O.L. & Dusting, G.J. N-nitro-L-arginine causes coronary vasoconstriction and inhibits endothelium-dependent vasodilatation in anesthetized greyhounds. *Br. J. Pharmacol.* **103**, 1407-1410 (1991).
90. Emil, S., Kanno, S., Berkeland, J., Kosi, M. & Atkinson, J. Sustained pulmonary vasodilation after inhaled nitric oxide for hypoxic pulmonary hypertension in swine. *J. Pediatr. Surg.* **31**, 389-393 (1996).
91. Russell, P., Wright, C., Kapeller, K., Barer, G. & Howard, P. Attenuation of chronic hypoxic pulmonary hypertension in rats by cyclooxygenase products and by nitric oxide. *Eur. Respir. J.* **6**, 1501-1506 (1993).
92. Oka, M., Hasunuma, K., Webb, S.A., Stelzner, T.J., Rodman, D.M. & McMurtry, I.F. EDRF suppresses an unidentified vasoconstrictor mechanism in hypertensive rat lungs. *Am. J. Physiol.* **264**, L587-L597 (1993).
93. Bedford, M.T. & Richard, S. Arginine methylation an emerging regulator of protein function. *Mol. Cell* **18**, 263-272 (2005).
94. Closs, E.I., Basha, F.Z., Habermeier, A. & Forstermann, U. Interference of L-arginine analogues with L-arginine transport mediated by the y⁺ carrier hCAT-2B. *Nitric Oxide* **1**, 65-73 (1997).
95. Teerlink, T., Nijveldt, R.J., de, J.S. & van Leeuwen, P.A. Determination of arginine, asymmetric dimethylarginine, and symmetric dimethylarginine in human plasma and other biological samples by high-performance liquid chromatography. *Anal. Biochem.* **303**, 131-137 (2002).
96. Bulau, P., Zakrzewicz, D., Kitowska, K., Leiper, J., Gunther, A., Grimminger, F. & Eickelberg, O. Analysis of methylarginine metabolism in the cardiovascular system identifies the lung as a major source of ADMA. *Am. J. Physiol. Lung Cell Mol. Physiol.* **292**, L18-L24 (2007).
97. Vallance, P., Leone, A., Calver, A., Collier, J. & Moncada, S. Accumulation of an endogenous inhibitor of nitric oxide synthesis in chronic renal failure. *Lancet* **339**, 572-575 (1992).
98. Matsuoka, H., Itoh, S., Kimoto, M., Kohno, K., Tamai, O., Wada, Y., Yasukawa, H., Iwami, G., Okuda, S. & Imaizumi, T. Asymmetrical dimethylarginine, an endogenous nitric oxide synthase inhibitor, in experimental hypertension. *Hypertension* **29**, 242-247 (1997).
99. Boger, R.H., Bode-Boger, S.M., Sydow, K., Heistad, D.D. & Lentz, S.R. Plasma concentration of asymmetric dimethylarginine, an endogenous inhibitor of nitric oxide synthase, is elevated in monkeys with hyperhomocyst(e)inemia or hypercholesterolemia. *Arterioscler. Thromb. Vasc. Biol.* **20**, 1557-1564 (2000).

100. Gorenflo, M., Zheng, C., Werle, E., Fiehn, W. & Ulmer, H.E. Plasma levels of asymmetrical dimethyl-L-arginine in patients with congenital heart disease and pulmonary hypertension. *J. Cardiovasc. Pharmacol.* **37**, 489-492 (2001).
101. Millatt, L.J., Whitley, G.S., Li, D., Leiper, J.M., Siragy, H.M., Carey, R.M. & Johns, R.A. Evidence for dysregulation of dimethylarginine dimethylaminohydrolase 1 in chronic hypoxia-induced pulmonary hypertension. *Circulation* **108**, 1493-1498 (2003).
102. Vallance, P. & Leiper, J. Cardiovascular biology of the asymmetric dimethylarginine: dimethylarginine dimethylaminohydrolase pathway. *Arterioscler. Thromb. Vasc. Biol.* **24**, 1023-1030 (2004).
103. Tran, C.T., Fox, M.F., Vallance, P. & Leiper, J.M. Chromosomal localization, gene structure, and expression pattern of DDAH1: comparison with DDAH2 and implications for evolutionary origins. *Genomics* **68**, 101-105 (2000).
104. Chen, Y., Li, Y., Zhang, P., Traverse, J.H., Hou, M., Xu, X., Kimoto, M. & Bache, R.J. Dimethylarginine dimethylaminohydrolase and endothelial dysfunction in failing hearts. *Am. J. Physiol. Heart Circ. Physiol.* **289**, H2212-H2219 (2005).
105. Tojo, A., Welch, W.J., Bremer, V., Kimoto, M., Kimura, K., Omata, M., Ogawa, T., Vallance, P. & Wilcox, C.S. Colocalization of demethylating enzymes and NOS and functional effects of methylarginines in rat kidney. *Kidney Int.* **52**, 1593-1601 (1997).
106. Russwurm, M. & Koesling, D. Guanylyl cyclase: NO hits its target. *Biochem. Soc. Symp.* 51-63 (2004).
107. Russwurm, M., Wittau, N. & Koesling, D. Guanylyl cyclase/PSD-95 interaction: targeting of the nitric oxide-sensitive alpha2beta1 guanylyl cyclase to synaptic membranes. *J. Biol. Chem.* **276**, 44647-44652 (2001).
108. Collier, J. & Vallance, P. Second messenger role for NO widens to nervous and immune systems. *Trends Pharmacol. Sci.* **10**, 427-431 (1989).
109. Vermeersch, P., Buys, E., Pokreisz, P., Marsboom, G., Ichinose, F., Sips, P., Pellens, M., Gillijns, H., Swinnen, M., Graveline, A., Collen, D., Dewerchin, M., Brouckaert, P., Bloch, K.D. & Janssens, S. Soluble guanylate cyclase-alpha deficiency selectively inhibits the pulmonary vasodilator response to nitric oxide and increases the pulmonary vascular remodeling response to chronic hypoxia. *Circulation* **116**, 936-943 (2007).
110. Omar, H.A. & Wolin, M.S. Endothelium-dependent and independent cGMP mechanisms appear to mediate O₂ responses in calf pulmonary resistance arteries. *Am. J. Physiol.* **262**, L560-L565 (1992).
111. Stasch, J.P., Becker, E.M., Alonso-Alija, C., Apeler, H., Dembowski, K., Feurer, A., Gerzer, R., Minuth, T., Perzborn, E., Pleiss, U., Schröder, H.,

- Schroeder, W., Stahl, E., Steinke, W., Straub, A. & Schramm, M. NO-independent regulatory site on soluble guanylate cyclase. *Nature* **410**, 212-215 (2001).
112. Dumitrascu, R., Weissmann, N., Ghofrani, H.A., Dony, E., Beuerlein, K., Schmidt, H., Stasch, J.P., Gnoth, M.J., Seeger, W., Grimminger, F. & Schermuly R.T. Activation of soluble guanylate cyclase reverses experimental pulmonary hypertension and vascular remodeling. *Circulation* **113**, 286-295 (2006).
113. Brunner, F., Schmidt, K., Nielsen, E.B. & Mayer, B. Novel guanylyl cyclase inhibitor potently inhibits cyclic GMP accumulation in endothelial cells and relaxation of bovine pulmonary artery. *J. Pharmacol. Exp. Ther.* **277**, 48-53 (1996).
114. Seeger, W., Walmrath, D., Grimminger, F., Rosseau, S., Schütte, H., Krämer, H.J., Ermert, L. & Kiss, L. Adult respiratory distress syndrome: model systems using isolated perfused rabbit lungs. *Methods Enzymol.* **233**, 549-584 (1994).
115. Weissmann, N., Akkayagil, E., Quanz, K., Schermuly, R.T., Ghofrani, H.A., Fink, L., Hänze, J., Rose, F., Seeger, W. & Grimminger, F. Basic features of hypoxic pulmonary vasoconstriction in mice. *Respir. Physiol. Neurobiol.* **139**, 191-202 (2004).
116. Schermuly, R.T., Dony, E., Ghofrani, H.A., Pullamsetti, S., Savai, R., Roth, M., Sydykov, A., Lai, Y.J., Weissmann, N., Seeger, W. & Grimminger, F. Reversal of experimental pulmonary hypertension by PDGF inhibition. *J. Clin. Invest.* **115**, 2811-2821 (2005).
117. Weissmann, N., Winterhalder, S., Nollen, M., Voswinckel, R., Quanz, K., Ghofrani, H.A., Schermuly, R.T., Seeger, W. & Grimminger, F. NO and reactive oxygen species are involved in biphasic hypoxic vasoconstriction of isolated rabbit lungs. *Am. J. Physiol. Lung Cell Mol. Physiol.* **280**, L638-L645 (2001).
118. Zhang, F., Woodmansey, P.A. & Morice, A.H. Acute hypoxic vasoconstriction in isolated rat small and large pulmonary arteries. *Physiol. Res.* **44**, 7-18 (1995).
119. Zhang, F., Carson, R.C., Zhang, H., Gibson, G. & Thomas, H.M. III. Pulmonary artery smooth muscle cell $[Ca^{2+}]_i$ and contraction: responses to diphenyleneiodonium and hypoxia. *Am. J. Physiol.* **273**, L603-L611 (1997).
120. Jabr, R.I., Toland, H., Gelband, C.H., Wang, X.X. & Hume, J.R. Prominent role of intracellular Ca^{2+} release in hypoxic vasoconstriction of canine pulmonary artery. *Br. J. Pharmacol.* **122**, 21-30 (1997).
121. Paddenberg, R., König, P., Faulhammer, P., Goldenberg, A., Pfeil, U. & Kummer, W. Hypoxic vasoconstriction of partial muscular intra-acinar pulmonary arteries in murine precision cut lung slices. *Respir. Res.* **7**, 93 (2006).
122. De Mey, J.G. & Vanhoutte, P.M. Heterogeneous behavior of the canine arterial and venous wall. Importance of the endothelium. *Circ. Res.* **51**, 439-447 (1982).

123. Yang, B.C., Nichols, W.W., Lawson, D.L. & Mehta, J.L. Agonist-induced tension determines vascular reactivity during anoxia and reoxygenation. *Life Sci.* **50**, 1805-1812 (1992).
124. Leach, R.M., Robertson, T.P., Twort, C.H. & Ward, J.P. Hypoxic vasoconstriction in rat pulmonary and mesenteric arteries. *Am. J. Physiol.* **266**, L223-L231 (1994).
125. Aaronson, P.I., Robertson, T.P. & Ward, J.P. Endothelium-derived mediators and hypoxic pulmonary vasoconstriction. *Respir. Physiol. Neurobiol.* **132**, 107-120 (2002).
126. Ward, J.P. & Robertson, T.P. The role of the endothelium in hypoxic pulmonary vasoconstriction. *Exp. Physiol.* **80**, 793-801 (1995).
127. Robertson, T.P., Aaronson, P.I. & Ward, J.P. Ca²⁺ sensitization during sustained hypoxic pulmonary vasoconstriction is endothelium dependent. *Am. J. Physiol. Lung Cell Mol. Physiol.* **284**, L1121-L1126 (2003).
128. Sasaki, S., Asano, M., Ukai, T., Nomura, N., Maruyama, K., Manabe, T. & Mishima, A. Nitric oxide formation and plasma L-arginine levels in pulmonary hypertensive rats. *Respir. Med.* **98**, 205-212 (2004).
129. Sprague, R.S., Thiemermann, C. & Vane, J.R. Endogenous endothelium-derived relaxing factor opposes hypoxic pulmonary vasoconstriction and supports blood flow to hypoxic alveoli in anesthetized rabbits. *Proc. Natl. Acad. Sci. USA* **89**, 8711-8715 (1992).
130. Dayoub, H., Achan, V., Adimoolam, S., Jacobi, J., Stuehlinger, M.C., Wang, B.Y., Tsao, P.S., Kimoto, M., Vallance, P., Patterson, A.J. & Cooke, J.P. Dimethylarginine dimethylaminohydrolase regulates nitric oxide synthesis: genetic and physiological evidence. *Circulation* **108**, 3042-3047 (2003).
131. Cremona, G., Dinh Xuan, A.T. & Higenbottam, T.W. Endothelium-derived relaxing factor and the pulmonary circulation. *Lung* **169**, 185-202 (1991).
132. Sherman, T.S., Chen, Z., Yuhanna, I.S., Lau, K.S., Margraf, L.R. & Shaul, P.W. Nitric oxide synthase isoform expression in the developing lung epithelium. *Am. J. Physiol.* **276**, L383-L390 (1999).
133. Beavo, J.A. & Brunton, L.L. Cyclic nucleotide research-still expanding after half a century. *Nat. Rev. Mol. Cell Biol.* **3**, 710-718 (2002).
134. Coggins, M.P. & Bloch, K.D. Nitric oxide in the pulmonary vasculature. *Arterioscler. Thromb. Vasc. Biol.* **27**, 1877-1885 (2007).
135. Taylor, C.T. & Moncada, S. Nitric oxide, cytochrome C oxidase, and the cellular response to hypoxia. *Arterioscler. Thromb. Vasc. Biol.* **30**, 643-647 (2010).

136. Wolin, M.S., Gupte, S.A., Mingone, C.J., Neo, B.H., Gao, Q. & Ahmad, M. Redox regulation of responses to hypoxia and NO-cGMP signaling in pulmonary vascular pathophysiology. *Ann. N. Y. Acad. Sci.* **1203**, 126-132 (2010).
137. Weissmann, N., Tadic, A., Hänze, J., Rose, F., Winterhalder, S., Nollen, M., Schermuly, R.T., Ghofrani, H.A., Seeger, W. & Grimminger, F. Hypoxic vasoconstriction in intact lungs: a role for NADPH oxidase-derived H₂O₂? *Am. J. Physiol. Lung Cell Mol. Physiol.* **279**, L683-L690 (2000).
138. Sommer, N., Pak, O., Schörner, S., Derfuss, T., Krug, A., Gnaiger, E., Ghofrani, H.A., Schermuly, R.T., Huckstorf, C., Seeger, W., Grimminger, F. & Weissmann, N. Mitochondrial cytochrome redox states and respiration in acute pulmonary oxygen sensing. *Eur. Respir. J.* **36**, 1056-1066 (2010).
139. Weir, E.K., Hong, Z. & Chen, Y. Superoxide dismutase: master and commander? *Eur. Respir. J.* **36**, 234-236 (2010).
140. Humbert, M., Morrell, N.W., Archer, S.L., Stenmark, K.R., MacLean, M.R., Lang, I.M., Christman, B.W., Weir, E.K., Eickelberg, O., Voelkel, N.F. & Rabinovitch, M. Cellular and molecular pathobiology of pulmonary arterial hypertension. *J. Am. Coll. Cardiol.* **43**, 13S-24S (2004).
141. Su, Y. & Block, E.R. Hypoxia inhibits L-arginine synthesis from L-citrulline in porcine pulmonary artery endothelial cells. *Am. J. Physiol.* **269**, L581-L587 (1995).
142. Zharikov, S.I. & Block, E.R. Association of L-arginine transporters with fodrin: implications for hypoxic inhibition of arginine uptake. *Am. J. Physiol. Lung Cell Mol. Physiol.* **278**, L111-L117 (2000).
143. Mitani, Y., Maruyama, K. & Sakurai, M. Prolonged administration of L-arginine ameliorates chronic pulmonary hypertension and pulmonary vascular remodeling in rats. *Circulation* **96**, 689-697 (1997).
144. Arrigoni, F.I., Vallance, P., Haworth, S.G. & Leiper, J.M. Metabolism of asymmetric dimethylarginines is regulated in the lung developmentally and with pulmonary hypertension induced by hypobaric hypoxia. *Circulation* **107**, 1195-1201 (2003).
145. Kielstein, J.T., Bode-Böger, S.M., Hesse, G., Martens-Lobenhoffer, J., Takacs, A., Fliser, D. & Hoepfer, M.M. Asymmetrical dimethylarginine in idiopathic pulmonary arterial hypertension. *Arterioscler. Thromb. Vasc. Biol.* **25**, 1414-1418 (2005).
146. Yildirim, A.O., Bulau, P., Zakrzewicz, D., Kitowska, K.E., Weissmann, N., Grimminger, F., Morty, R.E. & Eickelberg, O. Increased protein arginine methylation in chronic hypoxia: role of protein arginine methyltransferases. *Am. J. Respir. Cell Mol. Biol.* **35**, 436-443 (2006).
147. Pullamsetti, S., Kiss, L., Ghofrani, H.A., Voswinckel, R., Haredza, P., Klepetko, W., Aigner, C., Fink, L., Muiyal, J.P., Weissmann, N., Grimminger, F.,

- Seeger, W. & Schermuly, R.T. Increased levels and reduced catabolism of asymmetric and symmetric dimethylarginines in pulmonary hypertension. *FASEB J.* **19**, 1175-1177 (2005).
148. Shaul, P.W., Wells, L.B. & Horning, K.M. Acute and prolonged hypoxia attenuate endothelial nitric oxide production in rat pulmonary arteries by different mechanisms. *J. Cardiovasc. Pharmacol.* **22**, 819-827 (1993).
149. Kirsch, M., Kemp-Harper, B., Weissmann, N., Grimminger, F. & Schmidt, H.H. Sildenafil in hypoxic pulmonary hypertension potentiates a compensatory up-regulation of NO-cGMP signaling. *FASEB J.* **22**, 30-40 (2008).

10. APPENDIX

10.1 Statement/Erklärung an Eides Statt

Hereby, I declare on oath, that the thesis “Hypoxia-dependent mechanisms in the pulmonary circulation - Role of dimethylarginine dimethylaminohydrolase 1 (DDAH-1) in acute, sustained and chronic hypoxia” is the product of my original research, and I did not use other sources or methods than those I have cited. In addition, I declare that this thesis is not submitted to any another evaluation, neither in this form nor in another.

I have not acquired or tried to acquire any other academic degree than that documented in the application.

“Ich erkläre: Ich habe die vorgelegte Dissertation selbständig, ohne unerlaubte fremde Hilfe und nur mit den Hilfen angefertigt, die ich in der Dissertation angegeben habe. Alle Textstellen, die wörtlich oder sinngemäß aus veröffentlichten oder nicht veröffentlichten Schriften entnommen sind, und alle Angaben, die auf mündlichen Auskünften beruhen, sind als solche kenntlich gemacht. Bei den von mir durchgeführten und in der Dissertation erwähnten Untersuchungen habe ich die Grundsätze guter wissenschaftlicher Praxis, wie sie in der ”Satzung der Justus Liebig Universität Gießen zur Sicherung guter wissenschaftlicher Praxis” niedergelegt sind, eingehalten“.

10.2 Acknowledgments

It is my pleasure to express my deepest gratitude and respect to Prof. Dr. Werner Seeger, University of Giessen Lung Center for providing me this opportunity to do this work in this excellent, very advanced and highly qualified environment for lung and heart research.

I owe heavy debt of gratitude to Prof. Dr. Norbert Weissmann, Chair for Molecular Mechanisms of Emphysema, Hypoxia and Lung Aging “Excellence Cluster Cardio Pulmonary System”, Justus Liebig University Giessen, University of Giessen Lung Center, for suggesting the protocol, valuable suggestions, kind supervision, psychological support and final revision of the text.

Very special thanks is heartily paid to Dr. Natascha Sommer, for her kind cooperation, inspiring ideas, management of difficulties I faced, supportive attitudes, revision of the text, and sincere help along the time period of work.

I would like to send my thanks to the respectful Egyptian Professors: Farid M. A. Hamada and Ramadan A.M. Hemeida and Dr. Ashraf M. A. Taye for their support of the work and for giving me the opportunity to come to Giessen.

I want to express many thanks for the very fruitful collaboration with Dr. John P. Cooke, Professor of Cardiovascular Medicine, Stanford University School of Medicine, Stanford, CA, USA, including the generation of DDAH1^{tg} mice.

My sincere gratitude goes to Karin Quanz for her excellent technical assistance, teaching me most of techniques I learned.

I am also grateful to Lisa Fröhlich for her effort, and generous support to complete this work by learning histological techniques.

My sincere thanks go to my colleagues, Oleg Pak, Dr. B. Egemnazarov for help in some technical and computer skills.

I would also like to express my thanks to all technical staffs Alice Vohmann, Ingrid Breitenborn-Müller, Carmen Homberger, Miriam Schmidt, and Elena Schumacher for help in need.

I am very thankful to my wife Dr. Safaa, and kids, Mohammed, Mennh, and Ahmed for their patience, support and motivation to accomplish this work.

Finally, I can not forget the Government of Arab Republic of Egypt & Al-Azhar University (Egypt) for the financial support to achieve this work, thanks a lot.

**Der Lebenslauf wurde aus der elektronischen
Version der Arbeit entfernt.**

**The curriculum vitae was removed from the
electronic version of the paper.**



Publication

Ramadan A.M. Hemeida, Gouda K.A. Helal, Mohammed H. Abd El-Wahab, Osama A. Badary and **Adel G.M. Bakr. (2008):** Neuroprotective effect of melatonin against ethanol-induced damage in rat brain stem. Assiut Med. J. 32:2: 121-128.